Novel Organosilicone Materials and Patterning Techniques for Nanoimprint Lithography

by

Carlos Alberto Pina

A dissertation submitted in partial fulfillment
of the requirements for the degree of
Doctor of Philosophy
(Macromolecular Science and Engineering)
in The University of Michigan
2009

Doctoral Committee:

Associate Professor L. Jay Guo, Co-Chair
Peng-Fei Fu, Dow Corporation, Co-Chair
Professor Richard M. Laine
Associate Professor Jinsang Kim

2009

Dedication

This dissertation is dedicated to my parents, sisters, nephews and especially little Jorge Alejandro for their support, understanding and encouragement.

Acknowledgements

Prof. L. Jay Guo, my Ph.D. co-chair, gave me the great opportunity to become a member of his research group. During my doctoral studies I discovered that Prof. Guo, an expert in nanoimprinting, is a great scientist with an extraordinary vision to pursue front edge research; most important, he is an excellent and kind person. The time I have been under his mentorship has being highly significant for my professional development. I have learnt not only to do science but to be a better person. He has taught me to never give up and confront the scientific challenges encountered through my research life with courage and passion. The time I spent in his group was highly valuable and fertile.

My most sincere acknowledgement to Dr. Peng-Fei Fu, my other co-chair, for all of the precious time spent advising and teaching me during this journey. I will always keep in mind his valuable suggestions and comments. This dissertation would not be accomplished without his extraordinary technical and scientific knowledge in the silicon polymer field.

I would also like to thank my Committee members for their invaluable time spent on my thesis committee. Prof. Jinsang Kim kindly provided enormous help to develop my projects. Also, I really appreciate Prof. Stella Pang for accepting to become a part of my Committee at the last moment. Her intelligent comments are a big contribution to this dissertation.

Prof. Richard M. Laine always showed his disposition to provide guidance at all times. I really appreciate his valuable contributions to this dissertation. In addition, his advice, deep knowledge and detailed revisions helped improve this dissertation greatly.

My very deep and sincere acknowledgement to Nonna Hamilton, my program coordinator, for her support and help through these 5 years. Nonna was the first person I met in Arbor and she nicely introduced me to the city and to the new culture. Her kindness made this time really enjoyable. I have to say I am really honored for the opportunity to meet such a great human being.

The Nanogroup showed me their support and help at all times. It was really enjoyable to do research in such a nice environment. I spent great times with Larry, Wayne, Brandon, Phil, Sting, Myung-Gyu, Se Hyun, Hui-Joon, Tao, Abram, Yi-Kuei, Yi-Hao, and Sung-Lian and Jinsung Kim. I also acquire very valuable technical and scientific knowledge from all of them.

The Macromolecular Science and Engineering Program gave me the big opportunity to pursue my doctoral studies in this prestigious institution. Pleasant time was shared with the other students from this program; particularly Santy, Sarah and Anne. Furthermore, Santy nicely helped me use the gel permeation chromatography (GPC) instrument and vacuum oven in her lab; and Anne Jurggenauth provided important advices during my GSI appointment in the Chemistry Department.

Abraham, Hyun Joon and Jenny from Prof. Peter Green’s group kindly allowed me use the ellipsometer, vacuum oven and rheometer in their lab. Many of my projects were accomplished with their help.

I would like to thank the LNF staff for all the expertise and technical support; especially to Sandrine, Dennis, Russ and Phil. I also want to thank Jim Windak from the Chemistry department for his help with the Fourier transformed infrared (FTIR) and GPC instruments.

EMAL staff members have been doing an excellent job in maintaining the facilities in optimal conditions. EMAL instruments such as the XL30-FEG and the nanoindenter played a key role for the development of this dissertation.

My gratitude to the Mexican National Council of Science and Technology (CONACYT) for providing me the fellowship 166049 to pursue my doctoral studies.

Table of Contents

List of Figures

List of Tables

Chapter 1

Introduction

Nanotechnology, the control of matter at the nano- and molecular level, is making a profound impact on several fields from communications, electronics and energy to medicine. Lithography and other patterning techniques are exceptional tools for nanofabrication technologies.[1] In fact, photolithography has made it possible for the current tendency pursued by the semiconductor industry (SI) manufacture high performance chips by following the strategy of a constant feature size reduction in complementary metal-oxide semiconductor (CMOS) integrated circuit fabrication. However the tools that can allow such nanoscale patterning and the fabrication facilities in general have become prohibitively expensive since a single photolithography tool. Additionally, in photolithography, the resolution depends on the wavelength of the light used. However, due to the difficulty of exploiting shorter wavelengths in photolithgraphy, the resolution of photolithography is reaching its physical limit; features smaller than 45 nm are difficult to resolve with photolithography.[2] With consideration of other physical barriers, it has become extremely challenging to stay on the curve of the Moore's law, which aims at doubling the number of transistors on a IC chip every 18 months.[3]

Therefore, the development of new affordable and scalable nanoscale fabrication techniques is of primary importance for the future progress of the semiconductor industry. In fact, new lithographic techniques, also known as next generation lithography techniques (NGL's), are being developed and improved.[4,5] These technologies possess the great potential to benefit other technological fields and research areas such as optics, cell biology and tissue engineering.

NGL's include extreme-ultraviolet (EUV) lithography, x-ray lithography, electron beam lithography (EBL), focused ion beam (FIB) lithography and nanoimprint lithography (NIL).[5]

EUV-lithography is the natural extension of photolithography. Due to the shorter wave length 13nm, has a higher resolution (structures as small as 12nm have been patterned)[6] than pholithography and it is currently being developed for the 32 and 22nm node processes.[7] However, EUV patterning must performed under vacuum conditions which reduce the throughput and increase the equipment and processing costs.[8] A higher resolution NGL optical technique is X-ray lithography which has patterned 20 nm size structures.[9,10] Unfortunately, similarly to EUV, this lithography also requires expensive equipment.

Electron beam lithography and focused ion beam lithography are writing approaches with impressive resolutions since sub-5nm structures have been patterned.[11,12] However, as they are serial approaches, the processing times to pattern regular size wafers are very long, from days to weeks, and these techniques can also be expensive.

A NGL with a higher throughput is Nanoimprinting lithography, an inexpensive patterning massive parallel approach.[13-15] Interestingly, molecular scale resolutions down to 2nm have been demonstrated with this simple molding approach.[16] NIL was mentioned in the Massachusetts Institute of Technology's "Technology Review" as one of 10 emerging technologies that will strongly impact the world. [17] In addition, the International Technology Roadmap for Semiconductors (ITRS) included NIL in the 2003 report as a candidate technology for future generation Si chip manufacturing.[18] The beauty of NIL is its simplicity; here, the nanoscale features from a mold are transferred into a polymeric thin film called the resist with the aid of pressure and temperature or UV light during the imprinting step. Then, during the mold releasing process, the mold is detached from the resist to expose the transferred patterned structures (figure 1). The resist is normally coated on a thick layer (few mm) of material named the substrate.

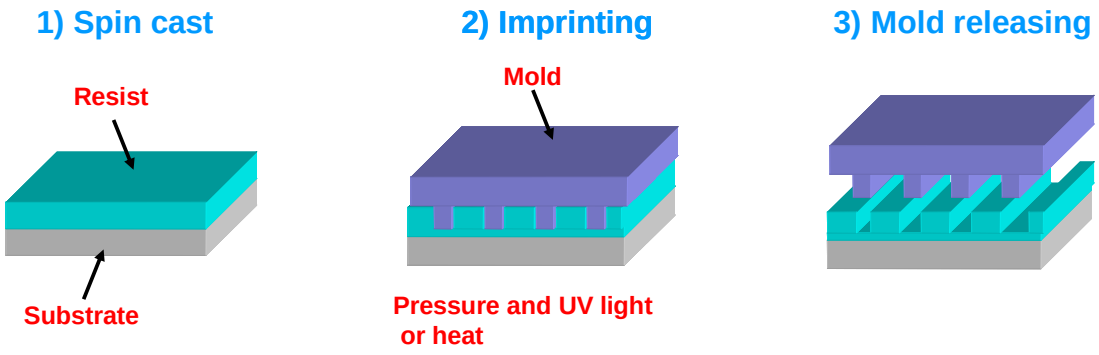

Figure 1.1 Schematics of the general NIL process.

Large areas can be patterned in a matter of minutes using NIL derivatives such as roll to roll imprinting.[19] Therefore, these characteristics have made nanoimprint lithography excelled as one of the most promising NGL's to become an alternative patterning tool to replace photolithography.

However, NIL still faces challenges which prevented to be implemented in the SI sector such as the high defect densities normally obtained during the replication process and overlay difficulties. The large presence of defects is mainly related to the mechanical stability of the resist material and the roles played by the mold-resist and resist-substrate interfaces. In fact, the following problems can be related to the observed defect densities: resist breaking, pattern collapse (lateral bending of imprinted structures), resist sticking to the mold, and resist detaching from the substrate.

A resist material with high modulus (larger than 100 MPa) is required to achieve nanoscale resolution and avoid pattern collapse (figure 2).[20] Apparently, a material with a high tensile strength is needed to avoid the breaking of the material during the mold releasing step. Furthermore, during the mold releasing process, the material can stick to the mold instead of remaining on the substrate surface. Thus, a resist material with low affinity to the mold is required. Finally, another issue encountered during the mold releasing process is the resist detachment from the substrate which can be avoided with a good substrate-resist adhesion. Thus, the resist must gather a number of properties to serve as a suitable patternable layer for an accurate and high resolution nanoscale replication.

The development of an appropriate resist material is of fundamental importance for the successful implementation of NIL in the semiconductor industry as well as in several other nanotechnological fields. In addition, the engineering of advanced functional resist materials with suitable imprinting properties can have important implications in several areas such as cell and protein arrays to study biological systems,

scaffolds for tissue engineering, nanowire fabrication for optoelectronics, fabrication of flexible and transparent solar cells.

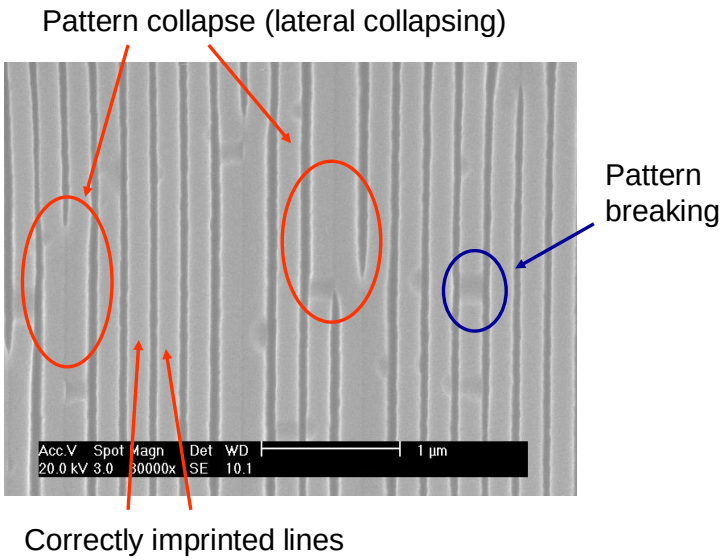

Figure 1.2 SEM picture showing an imprinted pattern with several pattern collapse and breaking.

Thus, given the role nanoimprint lithography can play as a potential mass production nanotechnology, and the importance of the resist for its future advancement, this dissertation focuses on the development of new patterning polymer materials for NIL. The capabilities of the developed polymers were investigated for a range of NIL applications such as their use as flexible, UV-transparent stamps and silicon compatible etching layers. Furthermore, new strategies were created to enhance the resolution and patterning capabilities of nanoimprint lithography for a variety of additional important applications.

1.1 Summary of lithographic techniques

Next, a brief review of the most important nanofabrication techniques including photolithography and next generation lithography's, with an emphasis on nanoimprint lithography (materials and approaches) is presented.

1.1.1 Photolithography

Here a photoresist (UV-curable polymer precursor) is spin coated onto a silicon (Si) wafer substrate. Then, the resist layer is exposed to ultraviolet radiation using an exposure tool or mask. The patterns in the resist are formed when the "development" step is performed. In the development step, the exposed or unexposed regions, depending if a positive or a negative resist is used, are selectively removed by a compatible solvent. The areas of the wafer where the resist was removed can be useful for a number of subsequent processes such as etching or lift-off.[21]

A variation of photolithography is immersion lithography which is now used for the 45nm process. This method uses ultrapure water as the immersion medium instead of air which is normally used in photolithography. This way, a larger numerical aperture can be achieved due to the higher index of refraction of water; a lager numerical aperture provides a higher resolution according to this equation,

Equation 1.1 $$R \propto \lambda/NA$$

where R is the resolution, λ is the wavelength of the light used and NA is the numerical aperture.

The patterns fabricated with immersion lithography can present some defects, mainly related to the presence of water as the immersion fluid. The photoresist can absorb water modifying both the resist characteristics and patterning sizes. In addition, many defects can be caused by the generation of bubbles in the immersion fluid.

Another derivation of photolithography is double patterning. In this technique, the photoresist is exposed to a series of consecutive patterning steps to create smaller structures (<45nm) than normally achieved with photolithography. It has shown resolutions down to 20nm. Unfortunately, the need of consecutive steps reduces the processing throughput and has a negative impact on the alignment.

1.1.2 Next generation lithography

As previously mentioned, several types of alternative lithographic techniques, or next generation lithography, are currently being developed to overcome the resolution limitations encountered in photolithography such as extreme-ultraviolet lithography (EUV-lithography), electron beam lithography, focus ion beam lithography (FIB), X-ray lithography and Nanoimprint lithography (NIL). However, NIL is presented with more detail in a separate section.

1.1.2.1 Extreme-ultraviolet lithography

Is a natural extension of optical lithography where the wavelength of the exposure light ranges between 50 and 5nm. An advantage over other next generation lithography's is that it uses masks with 4 or 5 fold reduction while the others require 1X membrane masks. In EUV the stage is used under high vacuum conditions which makes it an

expensive technology. It also uses reflective optics rather than diffractive optics as all of the available materials are strong EUV light absorbers and there are not materials transparent enough.[22] The highest resolution EUV-lithography has achieved is the patterning of 12nm structures.[6,7] Unfortunately, this technology performs the patterning under vacuum environment so it is a low throughput and expensive process.

1.1.2.2 Electron-beam lithography (EBL)

In electron-beam lithography (EBL), a high energy (>25KeV) electron beam is scanned on a substrate to expose a radiation-sensitive material. This technique has the advantage that produces structures of few nanometers in size (sub-5 nm) directly on a resist without the use of a mask.[11] However, EBL is a serial approach so the processing times are long (it can several days to pattern a single 4in wafer) if compared to optical projection. Moreover, EBL equipment can be more expensive than the photolithography counterpart.[23]

1.1.2.3 X-ray lithography

In x-ray lithography, a mask is imaged onto a wafer by using x-rays of very short wavelength (4-50Å). The short wavelengths eliminate the diffraction effects that limit the resolution of photolithography. The major advantage of x-ray lithography is its potential for attaining high resolutions; currently down to 20nm.[9,10] On the other hand, a major drawback is the need to develop an effective mask fabrication technology. In addition, X-ray lithography unfortunately requires expensive equipment and the high accuracy alignment required is still a limitation.[21]

1.1.2.4 Focused ion beam lithography

In focused ion beam lithography, a source of ions is sputtered onto a resist material. The advantage of FIB compared to electron beams is that since ions are more massive, they suffer less scattering (lees deviation from the original trajectory) and they can also be more sensitive than e-beam resists. A high resolution has been demonstrated since 3nm size holes structures have been fabricated with this technique.[12,24] The most common ion source is a tungsten (W) tip covered by a liquid metal such as gallium. However, more reliable ion sources must be developed in the future; the life time of ion sources must be larger than 1000 hours As EBL, FIB is also a serial approach with long processing times; the writing speed in FIB is lower than EBL.[25-27]

1.1.2.5 Other nanofabrication techniques

Several micro- and nanopatterning techniques are currently being developed for research purposes such as micro-contact printing,[23] scanning tunneling microscopy,[28] inkjet printing[29] and robotic deposition;[30]. The current development stage of these methods is still far from reaching industrial settings so a more detailed explanation is beyond the scope of this summary.

1.1.3 Nanoimprint lithography

Nanoimprint lithography (NIL) is at this time one of the most competitive and promising NGLs.[15] This patterning technique allows a high-throughput fabrication of nanostructures with great precision. Imprint lithography makes a conformal replica of surface relief patterns of a master mold by mechanically embossing softened materials

called resists (Figure 1.1).[13,14] The resist used in imprinting should be easily deformed under an applied pressure. The materials to be imprinted are deposited on top of the substrate by spin cast, dispensed as droplets or filled the space between the mold and substrate by capillary forces. Initially, the substrates used can be either rigid substrates or flexible plastic substrates. Materials such as Si, glass and metals are appropriate as substrates. The Si master mold made on SiO_2 layers is coated with a self-assembled monolayer of a releasing material (normally a fluorinated silane) to facilitate its releasing from the resist. The success of NIL as a nanotechnology tool for industrial production relies heavily on the capability of fabricating nanostructures on different types of materials.

1.1.3.1 Types of nanoimprint lithography

Imprinting techniques can be divided into two main methods depending on the conditions used, hot embossing and UV-nanoimprinting.[15]

In hot embossing, a thermoplastic such as poly (methyl methacrylate) (PMMA) is heated above its glass transition temperature. Then, high pressure is applied to fill a silicon dioxide master mold cavities with the melted polymer. A step is required to cool the system close to room temperature and release the mold. Plenty of research has been performed with hot embossing. If adhered to master mold during the mold releasing process, thermoplastics can be easily removed with a fast solvent cleaning step using acetone, for example. However, the long heating and cooling cycles makes it not ideal for a high throughput industrial process, the patterning of a 4in wafer a minute can be considered a high throughput process. In addition, the high pressure (>400psi) employed

that allows the long chains of the polymer flow into the mold cavities can easily break the expensive SiO_2 master mold.[15] Thermoset precursors, materials that are solidified with a heat treatment, are also employed in hot embossing. These materials can be processed at lower temperatures with a shorter cycle time.

UV imprinting, another variation of nanoimprinting, is performed at room temperature avoiding the long thermal cycles of hot embossing.[31] In this technique, a photocurable monomer or oligomer is imprinted at room temperature. As the molecular weight of the photocurable material is low, it only requires low pressures (<50psi) to achieve a complete filling of the mold cavities. The monomer is normally formulated along several other additives such as photoinitiators, diluents, and sufactants. The photoinitiators is used to initiate the polymerization process; diluents are used to adjust the material viscosity; and surfactants are used to decrease the adhesion to the mold.

1.1.3.2 Applications of nanoimprint lithography

Many applications in electronics, photonics, magnetic devices and the biological field have been developed using this simple, low cost, and high resolution (2 nm) technique. In the biological field DNA,[32] proteins[33-35] and guiding tracks for molecular motors have been patterned;[36] nanowire arrays have been fabricated for electronic applications[37]; new magnetic devices have been engineered such as patterned magnetic media[38,39] and high density quantized magnetic disc;[40] wire grid polarizers,[41] light emiting diodes[42,43] and diffractive optical elements[44] were developed for photonics.

1.1.3.3 Materials for nanoimprint lithography

The development of an appropriate resist is one of the most important tasks to implement NIL for industrial applications. In fact, the success of NIL as a next generation lithographic technique strongly depends on the research for new materials that are better suited as the nanoimprint resist.[30] Practically any material that can be molded can be used for nanoimprinting such metals and polymers. However, polymers are preferred due to the low temperatures required for their processing. In addition, the majority of them are relatively inexpensive and a potentially infinite variety of different polymers with specific functionalities can be synthesized. Once the polymers are synthesized, their surface can be modified (with the exception of few such as TEFLON) to achieve specific purposes. In addition, the bulk properties of polymers can be tailored with the addition of various additives such as plasticizers.

An appropriate resist must fulfill several requirements. It should possess good mechanical integrity, high modulus (>100MPa), and high tensile strength to avoid breaking during the mold release process. A low molecular weight is preferable to allow an imprinting with low pressure (<50psi).[45] Strong adhesion to the substrate is required so the resist remains on the surface after the mold is released. On the other hand, the resist should also present low adhesion to the mold. A low shrinking during the imprinting is preferable to faithfully replicate the mold nanostructures. In addition, a fast curing material that allows a high throughput process is required to compete with well established lithographic techniques such as photolithography. A material which is resistant to etching processes is desirable. A nanoimprint resist system with a combined

mold release and etch resistance properties that allows a fast and precise nanopatterning is highly desired.

Thermoplastics

Several polymers have been employed as resists for nanoimprint lithography. The most commonly used materials in the original NIL scheme are thermoplastic polymers such as PMMA and polystyrene (PS), which become viscous fluids when heated above their glass transition temperatures (T_g). However, typically the viscosity of the heated polymers remains high (several thousands of Pa.s) and thus the imprinting process requires significant pressure (>400psi). In addition, these thermal plastic resists normally have a high tendency to stick to the mold, which seriously affects the fidelity and quality of the pattern definition. Furthermore they do not offer the necessary etch resistance. As mentioned PMMA, PS as well as other thermoplastics have been employed as resists. Several materials are now commercially available.

Thermosets

Thermosets are low viscosity monomers or oligomers which solidify upon heat exposure acquiring the shape of the mold. They can be imprinted at moderate temperatures and the formulation can be adjusted to achieve fast cures. Several thermoset materials have been used for nanopatterning.[46,47]

UV-Curable precursors

Photocurable materials require ultraviolet light irradiation to solidify. These materials as well as thermosets do not change their shape after being cured. In addition, they can only be dissolved or destroyed under very harsh conditions. On the other hand, thermoplastics can easily modify their shape upon heating above their glass transition temperatures or melting points. Methyl methacrylate and epoxypropoxy based precursors are the most common materials used as resists for UV-nanoimprinting[48]. Methacrylate based materials crosslink through a free radical process. However free radical polymerizations are inhibited by the presence of oxygen. Thus, an inert atmosphere such as nitrogen in which the polymerization occurs is preferred.

Crosslinking by a cationic polymerization is a process leading to the solidifying of epoxy materials among others. This process is advantageous because it is not inhibited by oxygen and can be performed in air.

In addition, several functional resists with purpose-specific properties have been developed. For example, patternable materials with dielectric properties have been used.[49] Biodegradable materials have been patterned. Materials for tissue engineering and cell alignment have been previously used.[45] Vinyl ether[31] and thiol-based polymers precursors[50] have also being extensively used in UV-nanoimprinting.

1.1.3.4 Mold materials for nanoimprint lithography

Nanoimprint lithography was initially possible with a hard silicon oxide master mold. A releasing self-assembled monolayer, normally a fluorosilane, is coated on top of the mold to attain an easy mold releasing and avoid resist sticking to the mold or resist

breaking.[51] Common methods to fabricate the original master mold are e-beam lithography or interference lithography. A disadvantage of e-beam lithography is the long processing times required for the mold fabrication (it can take days or weeks). On the other hand, with interference lithography structures smaller than 100nm are not really fabricated. In addition, nanoimprinting, followed by some etching steps such O_2 plasma and CHF_3 plasma etching, can be used to fabricate the SiO_2 mold. Unfortunately, the master mold can easily be broken or damaged during the replication process. In order to avoid damages to the original silicon master, relatively inexpensive polymeric stamps have recently been developed.[52-56] Such polymeric stamps can be used a number of times with minimal damage.[56] Thermoplastics as well as curable materials are appropriate for the fabrication of polymeric stamps. For instance, PDMS was one of the first and most common materials used as a stamp for nanoscale replication.[15,57-61] However, it swells when exposed to common organic solvents and easily deforms under high pressures.

Fluoropolymers have also been used to fabricate stamps such as ETFE[56] and modified PTFE.[53] These materials possess low surface energy (<20mN/m), and do not require further surface treatments for mold releasing. However, their processing requires high pressures and temperatures which can damage the SiO_2 mold. Curalbe polymers such as perfluoroethers and sol-gel materials have also been developed.[54,55,62] Unfortunately, they have shown poor mechanical properties (modulus lower than 50MPa) for high resolution nanoimprinting.

Additionally, any thermoplastic with imprinting capabilities, such as PMMA, PS or poly (vinyl alcohol) (PVA), can also act as a mold if a surface treatment, O_2 plasma

followed by a fluorosilane coating is performed onto their surface. However, these type of molds can only be employed at temperatures lower than their glass transition temperatures (<150ºC for most common polymers). The same principle can be applied to thermosetting material, with the advantage that these polymers maintain their mechanical properties at higher temperatures than thermoplastics.

1.2 Outline

This dissertation research is divided into two main categories. The purpose is to develop thermally and UV curable polymer precursors for NIL applications. Chapter 2 describes the formulation and implementation of polydimethylsiloxane (PDMS) as a suitable resist and stamp for nanoimprint lithography. The mechanical and thermal properties of PDMS were measured with dynamical mechanical analysis and differential scanning calorimetry (DSC), respectively. Chapter 3 focuses on the synthesis of a wide range of silicone resins with different types of building units to achieve nanoscale resolution imprinting. Silicone resins with different compositions were synthesized and their imprinting capabilities were evaluated using micro- and nanoscale size molds. In addition, a new imprinting approach which combines UV and thermal curing is introduced. Chapter 4 details the synthesis, characterization and imprinting properties of different types of silsesquioxane (SSQ) materials. The moduli of these materials measured with nanoindentation is presented. In addition, viscosity and degree of shrinkage results evaluated with a rheometer and with an ellipsometer, respectively, are discussed. Finally, a two layer approach to enhance imprinting and mold releasing is introduced in this chapter. The improvement of the releasing properties of SSQ resists for

an easy mold demolding by adding proper fluorosurfactants is reviewed in chapter 5. Chapter 6 discusses the development of a low surface energy fluorinated SSQ stamp. The experimental procedure to fabricate the fluorinated SSQ stamp is described along with its patterning capabilities.

The second goal of this dissertation is to investigate and create new patterning tools to broad and enhance NIL capabilities. Chapter 7 explores the imprinting of nanostructures with no residual layer. Two different approaches involving the developed thermal and UV curable materials are introduced. Finally, the size reduction of patterned structures on multifunctional photocurable polymer resists systems is covered in chapter 8. Three new methods to modify and control the size and shape of fabricated nanostructures are depicted.

References

[1] Bratton, D.; Yang, D.; Dai, J. Y.; Ober, C. K. *Polym. Adv. Technol.* **2006**, *2*, 94-103.

[2] Peercy, P. S. *Nature* **2000**, *6799,* 1023-1026.

[3] Moore, G. E. **1965**, *8,* 114-114-116.

[4] Ito, T.; Okazaki, S. *Nature* **2000**, *6799,* 1027-1031.

[5] Mailly, D. *Eur. Phys. J. -Spec. Top.* **2009**, 333-342.

[6] Naulleau, P. P.; Anderson, C. N.; Chiu, J.; Denham, P.; George, S.; Goldberg, K. A.; Goldstein, M.; Hoef, B.; Hudyma, R.; Jones, G.; Koh, C.; La Fontaine, B.; Ma, A.; Montgomery, W.; Niakoula, D.; Park, J.; Wallow, T.; Wurm, S. Microelectronic Engineering; 2009; Vol. 86, pp 448-455.

[7] Naulleau, P. P.; Anderson, C. N.; Chiu, J.; Dean, K.; Denham, P.; George, S.; Goldberg, K. A.; Hoef, B.; Jones, G.; Koh, C.; La Fontaine, B.; Ma, A.; Montgomery, W.; Niakoula, D.; Park, J.; Wallow, T.; Wurm, S. *J. Vac. Sci. Technol. B* **2009**, *1*, 66-70.

[8] Wua, B.; Kumar, A. *J. Vac. Sci. Technol. B* **2007**, *6*, 1743-1761.

[9] Smith, H. I.; Schattenburg, M. L.; Hector, S. D.; Ferrera, J.; Moon, E. E.; Yang, I. Y.; Burkhardt, M. *Microelectron. Eng.* **1996**, *1-4*, 143-158.

[10] Chen, Y.; Simon, G.; Haghiri-Gosnet, A. M.; Carcenac, F.; Decanini, D.; Rousseaux, F.; Launois, H. *Journal of Vacuum Science & Technology B*; 1998; Vol. 16, pp 3521-3525.

[11] Arjmandi, N.; Lagae, L.; Borghs, G. *J. Vac. Sci. Technol. B* **2009**, *4*, 1915-1918.

[12] Gierak, J.; Madouri, A.; Biance, A. L.; Bourhis, E.; Patriarche, G.; Ulysse, C.; Lucot, D.; Lafosse, X.; Auvray, L.; Bruchhaus, L.; Jede, R. Microelectronic Engineering; 2007; Vol. 84, pp 779-783.

[13] CHOU, S. Y.; KRAUSS, P. R.; RENSTROM, P. J. *Appl. Phys. Lett.* **1995**, *21*, 3114-3116.

[14] Chou, S. Y.; Krauss, P. R.; Renstrom, P. J. *Science* **1996**, *5258*, 85-87.

[15] Guo, L. J. *Adv Mater* **2007**, *4*, 495-513.

[16] Hua, F.; Sun, Y. G.; Gaur, A.; Meitl, M. A.; Bilhaut, L.; Rotkina, L.; Wang, J. F.; Geil, P.; Shim, M.; Rogers, J. A.; Shim, A. *Nano Lett.* **2004**, *12*, 2467-2471.

[17] Special Report, *Technol. Rev.* **2003**, *106*, 36.

[18] http://www.itrs.net/reports.html.

[19] Ahn, S.; Guo, L. J. *Advanced Materials* **2008**.

[20] Hagberg, E. C.; Malkoch, M.; Ling, Y.; Hawker, C. J.; Carter, K. R. *Nano Lett.* **2007**, *2*, 233-237.

[21] Chen, Y.; Pepin, A. *Electrophoresis* **2001**, *2*, 187-207.

[22] Wua, B.; Kumar, A. *J. Vac. Sci. Technol. B* **2007**, *6*, 1743-1761.

[23] Marrian, C. R. K.; Tennant, D. M. *J. Vac. Sci. Technol. A* **2003**, *5*, S207-S215.

[24] Gierak, J.; Bourhis, E.; Combes, M. N. M.; Chriqui, Y.; Sagnes, I.; Mailly, D.; Hawkes, P.; Jede, R.; Bruchhaus, L.; Bardotti, L.; Prevel, B.; Hannour, A.; Melinon, P.; Perez, A.; Ferre, J.; Jamet, J. P.; Mougin, A.; Chappert, C.; Mathet, V. Microelectronic Engineering; 2005; Vol. 78-79, pp 266-278.

[25] Melngailis, J.; Mondelli, A. A.; Berry, I. L.; Mohondro, R. *J. Vac. Sci. Technol. B* **1998**, *3*, 927-957.

[26] Gamo, K. *Microelectron. Eng.* **1996**, *1-4*, 159-171.

[27] Utke, I.; Hoffmann, P.; Melngailis, J. *J. Vac. Sci. Technol. B* **2008**, *4*, 1197-1276.

[28] Wouters, D.; Schubert, U. S. *Angew. Chem. -Int. Edit.* **2004**, *19*, 2480-2495.

[29] Tekin, E.; Smith, P. J.; Schubert, U. S. *Soft Matter* **2008**, *4*, 703-713.

[30] Nie, Z.; Kumacheva, E. *Nat. Mater.* **2008**, *4*, 277-290.

[31] Kim, E. K.; Stacey, N. A.; Smith, B. J.; Dickey, M. D.; Johnson, S. C.; Trinque, B. C.; Willson, C. G. Journal of Vacuum Science & Technology B; 2004; Vol. 22, pp 131-135.

[32] Pepin, A.; Youinou, P.; Studer, V.; Lebib, A.; Chen, Y. *Microelectronic Engineering* **2002**, 927-932.

[33] Falconnet, D.; Pasqui, D.; Park, S.; Eckert, R.; Schift, H.; Gobrecht, J.; Barbucci, R.; Textor, M. *Nano Letters* **2004**, *10*, 1909-1914.

[34] Hoff, J. D.; Cheng, L. J.; Meyhofer, E.; Guo, L. J.; Hunt, A. J. *Nano Letters* **2004**, *5*, 853-857.

[35] Hoff, J. D.; Hunt, A. *Biophys. J.* **2003**, *2*, 292A-292A.

[36] Bunk, R.; Carlberg, P.; Mansson, A.; Nicholls, I. A.; Omling, P.; Sundberg, M.; Tagerud, S.; Montelius, L. *Japanese Journal of Applied Physics Part 1-Regular Papers Brief Communications & Review Papers* **2005**, *5A*, 3337-3340.

[37] Martensson, T.; Carlberg, P.; Borgstrom, M.; Montelius, L.; Seifert, W.; Samuelson, L. *Nano Letters* **2004**, *4*, 699-702.

[38] McClelland, G. M.; Hart, M. W.; Rettner, C. T.; Best, M. E.; Carter, K. R.; Terris, B. D. *Appl. Phys. Lett.* **2002**, *8*, 1483-1485.

[39] Moritz, J.; Buda, L.; Dieny, B.; Nozieres, J. P.; van de Veerdonk, R. J. M.; Crawford, T. M.; Weller, D. *Appl. Phys. Lett.* **2004**, *9*, 1519-1521.

[40] Wu, W.; Cui, B.; Sun, X. Y.; Zhang, W.; Zhuang, L.; Kong, L. S.; Chou, S. Y. *Journal of Vacuum Science & Technology B* **1998**, *6*, 3825-3829.

[41] Ahn, S. W.; Lee, K. D.; Kim, J. S.; Kim, S. H.; Park, J. D.; Lee, S. H.; Yoon, P. W. *Nanotechnology* **2005**, *9*, 1874-1877.

[42] Cheng, X.; Hong, Y. T.; Kanicki, J.; Guo, L. J. *Journal of Vacuum Science & Technology B* **2002**, *6*, 2877-2880.

[43] Kao, P. C.; Chu, S. Y.; Chen, T. Y.; Zhan, C. Y.; Hong, F. C.; Chang, C. Y.; Hsu, L. C.; Liao, W. C.; Hon, M. H. *IEEE Trans. Electron Devices* **2005**, *8*, 1722-1726.

[44] Wang, J.; Kostal, H. *Laser Focus World* **2005**, *12*, 76-+.

[45] Schift, H. *J. Vac. Sci. Technol. B* **2008**, *2*, 458-480.

[46] Pina-Hernandez, C.; Kim, J. S.; Guo, L. J.; Fu, P. F., *Advanced Materials*, **2007**, *9*, 1222.

[47] Pina-Hernandez, C.; Kim, J.; Fu, P.; Guo, L. J. *Journal of Vacuum Science & Technology B;* 2007, Vol. 25, pp 2402-2406.

[48] Colburn, M. E., *Ph.D. Dissertation*, University of Texas at Austin, 2001.

[49] Ro, H. W.; Jones, R. L.; Peng, H.; Hines, D. R.; Lee, H. J.; Lin, E. K.; Karim, A.; Yoon, D. Y.; Gidley, D. W.; Soles, C. L. *Adv Mater* **2007**, *19*, 2919-+.

[50] Hagberg, E. C.; Malkoch, M.; Ling, Y.; Hawker, C. J.; Carter, K. R. *Nano Lett.* **2007**, *2*, 233-237.

[51] Bailey, T.; Choi, B. J.; Colburn, M.; Meissl, M.; Shaya, S.; Ekerdt, J. G.; Sreenivasan, S. V.; Willson, C. G. *Journal of Vacuum Science & Technology B*; 2000; Vol. 18, pp 3572-3577.

[52] Rolland, J. P.; Van Dam, R. M.; Schorzman, D. A.; Quake, S. R.; DeSimone, J. M. *J. Am. Chem. Soc.* **2004**, *26*, 8349-8349.

[53] Khang, D. Y.; Lee, H. H. *Langmuir* **2004**, *6*, 2445-2448.

[54] Choi, D. G.; Jeong, J. H.; Sim, Y. S.; Lee, E. S.; Kim, W. S.; Bae, B. S. *Langmuir* **2005**, *21*, 9390-9392.

[55] Truong, T. T.; Lin, R. S.; Jeon, S.; Lee, H. H.; Maria, J.; Gaur, A.; Hua, F.; Meinel, I.; Rogers, J. A. *Langmuir* **2007**, *5*, 2898-2905.

[56] Barbero, D. R.; Saifullah, M. S. M.; Hoffmann, P.; Mathieu, H. J.; Anderson, D.; Jones, G. A. C.; Welland, M. E.; Steiner, U. *Advanced Functional Materials* **2007**, *14*, 2419-2425.

[57] Odom, T. W.; Love, J. C.; Wolfe, D. B.; Paul, K. E.; Whitesides, G. M. *Langmuir* **2002**, *13*, 5314-5320.

[58] Kang, H.; Lee, J.; Park, J.; Lee, H. H. *Nanotechnology* **2006**, *1*, 197-200.

[59] Hua, F.; Gaur, A.; Sun, Y. G.; Word, M.; Jin, N.; Adesida, I.; Shim, M.; Shim, A.; Rogers, J. A. *Ieee Transactions on Nanotechnology* **2006**, *3*, 301-308.

[60] Mele, E.; Di Benedetto, F.; Persano, L.; Cingolani, R.; Pisignano, D. *Journal of Vacuum Science & Technology B* **2006**, *2*, 807-812.

[61] Sharpe, R. B. A.; Titulaer, B. J. F.; Peeters, E.; Burdinski, D.; Huskens, J.; Zandvliet, H. J. W.; Reinhoudt, D. N.; Poelsema, B. *Nano Letters* **2006**, *6*, 1235-1239.

[62] Rolland, J. P.; Hagberg, E. C.; Denison, G. M.; Carter, K. R.; De Simone, J. M. *Angewandte Chemie-International Edition* **2004**, *43*, 5796-5799.

Chapter 2

High throughput and etch selective nanoimprinting and stamping based on fast thermal curable polydimethysiloxanes

2.1 Introduction

Thermally curable monomers are very attractive materials for nanoimprint applications since these monomers present in liquid state, making them possible to be imprinted in a short period of time under low pressure and temperature, in sharp contrast to the thermal plastic polymers. As one of these materials, poly(dimethylsiloxane) has previously been used for micro-patterning by several research groups, mainly in the context of soft lithography,[1-5] and found numerous applications in fields as diverse as MEMS, biotechnology, photonics and nanoelectronics. In addition to its well known transparency to UV and visible light along with its high biocompatibility, it has a low surface energy (18-21 mN/m),[6] which allows an easy mold releasing without causing any structural damage to the imprinted structures; moreover, it posses a high resistance to oxygen plasma due to a higher silicon content. However, the PDMS material made from the commercial Sylgard 184 precursor is not suitable for nanoimprint applications due to

two significant drawbacks. Firstly its curing typically requires many hours, which is impractical as a resist material for nanoimprint lithography. Secondly the cured material has a low modulus of ~2 MPa, which not only makes the imprinted pattern prone to lateral collapsing when replicating submicron patterns, but more importantly makes it impossible to replicate features less than hundreds of nm. The latter point can be understood by considering the radius of curvature of a cured PDMS with a modulus E and surface energy (γ), which is $r = \gamma / E$.[7] Well defined and sharp corner structures required for nanometer scale lithography can not be satisfied with a large radius of curvature. As an illustration, an attempt was made to replicate a grating pattern with 350nm linewidth and spacing by using the Sylgard 184 formulation. As shown in the AFM images (Figure 2.1), not only all the lines are rounded at the top, but massive collapasing can be seen everywhere on the sample. As an improvement, a higher modulus (~8 MPa) poly(dimethylsiloxane) (hard PDMS) was developed by Schmid et al.[8] to achieve the patterning of 80nm diameter posts with an aspect ratio 1.25 (depth/width) for soft lithography. Unfortunately, the imprinting cycle (heating-cooling time) for this h-PDMS remained very long (about 2 hrs). Following the same strategy, Viet et al.[9,10] used Sylgard 184 as well as a reformulated polydimethylsiloxane as a thermal-curable resist for Nanoimprinting. However, the improvement was rather limited. The crosslinking time is still too long (5-15 min) and the substrate surface requires tedious treatments,[11,12] both of which seriously prevent it from being practically useful for nanoimprinting. Furthermore, feature size below 200 nm and an aspect ratio structures larger than 1 at the feature size could not be obtained. Recently, Lee et al.[2] were able to obtain 50nm line width patterns with an aspect ratio of 1.3 by modifying the wetting properties of h-PDMS as well as reducing its viscosity for

improving the penetration of the fluid prepolymer into the cavities of the master template. This was achieved by mixing the prepolymer with an adequate solvent and delaying the cross linking reaction by adding an excessive amount of modulator. The imprinting time lasted about 1.5 hours.

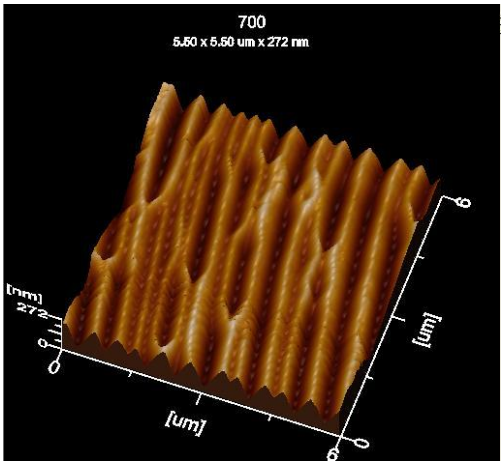

Figure 2.1 Atomic force microscopy (AFM) image of an imprinted 350nm linewidth and spacing grating replicated using Sylgard 184 PDMS. Corner rounding and line collapsing are clearly visible.

Consequently, it was critical to develop a polydimethylsiloxane based nanoimprinting system offering a high throughput and great etch selectivity, so that the nanoimprint technology could be realized in many actual industrial applications. In this context, we have recently investigated a number of polysiloxane based polymer and copolymer systems to simultaneously address the sticking and dry etching resistance issues.[1314] In this project, we report a novel thermal curable polydimethylsiloxane based nanoimprinting resist that allows a successful replication of 70 nm line width structures within a few seconds, a 20-fold reduction in comparing with previously reported PDMS based materials and typical thermoplastic nanoimprint resists. Moreover, the crosslinked

PDMS has sufficient mechanical strength and integrity to be used as a mold for nanoimprint or as stamp for many soft lithography applications.

2.2 Experimental procedure

The thermally curable resist formulation consists of four components: vinyl-terminated (polydimethylsiloxane), a methylhydrosiloxane copolymer which acts as a crosslinker, a Pt catalyst, and an inhibitor. The inhibitor is an unsaturated organic ester that coordinates to the Pt catalyst and keeps it inactive at ambient temperature so the liquid resist can have an extended shelf life required for normal nanoimprint processing. When heated at a higher temperature, such as 80-120 ^{o}C, the inhibitor undergoes either hydrosilyaltion or fast disassociation from the Pt center, releasing the catalyst in its active form.[15] The active species then catalyzes the addition of silyl-hydride (SiH) of the methylhydrosiloxane across the double bond of the vinyl-terminated (polydimethylsiloxane), forming a crosslinked network (figure 2.2). The network provides the mechanical integrity needed for subsequent pattern transfer steps, as well as for the clean separation of the mold after the imprint. Vinyl-terminated pre-polymers with several different degrees of polymerization (DP = 7, 10, 25, 65), and two crosslinkers with SiH weight percent of 1.05 wt% and 1.56 wt%, respectively, were employed in this study. In total, eight different formulations were obtained by combining the four prepolymers and the two crosslinkers.

In nanoimprint experiments, a vinyl prepolymer, a Si-H crosslinker, a Pt catalyst, and an inhibitor were mixed together according to calculated ratios. Once the monomeric liquid precursor was prepared, its concentration was adjusted with low viscous silicone

fluids, such as octamethylcyclotetrasiloxane (D_4) and pentamethylcyclopentasiloxane (D_5) to achieve a desired film thickness after spin coating. The precursor solution was then spun on a silicon substrate and a mold treated with fluorosurfactant was placed on top of it. The imprinting was performed at 80-115°C in less than 10 min with a hydraulic hot press and a Nanonex 2000 nanoimprinter. It is highly recommended that the imprinting be carried out immediately after spin coating the polymer solution so as to avoid the dewetting of the polysiloxane thin film.

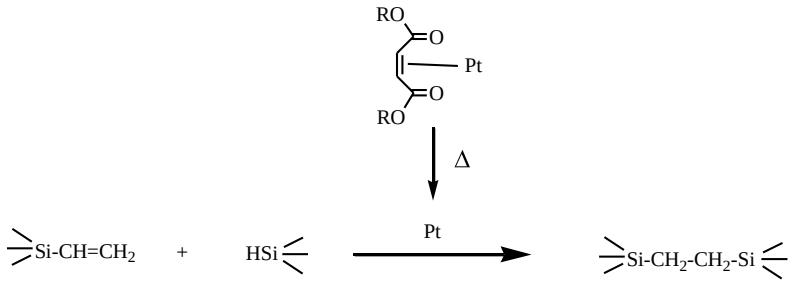

Equation 2.2 Chemistry of the crosslinking reaction of poly(dimethylsiloxane).

Mechanical tests at room temperature were performed with a Dynamical Mechanical Analyzer (DMA) Perkin Elmer 7e. An isothermal scan mode was run during 1 min with the frequency set at 10 Hz. The three point bending probe with rectangular geometry was used. The samples were prepared by pouring the liquid precursor in a metallic mold and then heating at 100^{o} C for 5 min.

The thermal curing of the resist was characterized by using a heat flux differential scanning calorimeter (DSC). Isothermal experiments were carried out between 70^{o}C and 120^{o} C in 10^{o} C intervals. The samples were encapsulated using aluminum pans. The mass

of the samples was kept around 10mg. The sample was heated from 30^{o} C to the curing temperature by using a heating rate of 50^{o} C/min.

In stamp fabrication, a SiO_2 film was thermally grown on a Si wafer, and then chrome (Cr) of 10-nm thickness was deposited on the SiO2 layer by using a radiofrequency (RF) sputter. The Cr layer was used for the improvement of adhesion properties between photoresist (PR) and the SiO_2 layer as well as for an etch mask to the SiO_2 layer.[16] Photoresist (PR) was spin-coated on the Cr layer, and laser interference lithography (LIL) was performed to form a grating pattern on the PR.[17,18] The Cr layer was etched with Cl_2 and O_2 RIE, and then SiO_2 layer with CHF_3 RIE. After etching the SiO_2, the Cr mask was removed by Cr wet etchant. The He-Cd Laser used has a wavelength of 325 nm and a power of 50 mW. The patterns were obtained through the laser interference between the direct beam and the reflected beam from the mirror.

Nanoimprint was also used to fabricate the replicated stamp from the original one produced by ILL. For the replication, again a substrate with a SiO_2 film on Si was used. Before imprinting, the fabricated stamp was pretreated by an anti-sticking layer (1H, 1H, 2H, 2H Perfluorodecyl trichlorosilane) to prevent the stamp from adhering to the imprint pattern for the demolding step. A thin 10nm film of Cr was also used as mask layer and was deposited in an electron beam evaporation system. The nanoimprint resist was spincoated, baked on hotplate to remove residual solvent and imprinted using a Nanonex 2000 nanoimprinter. RIE was used to first remove the residual polymer layer and then pattern the Cr masking layer. The nanoimprint resist was then dissolved in acetone and the sample was rinsed using methanol and IPA and dried in N_2. The SiO_2 was reactive-ion etched to its full depth and then the Cr was removed using a wet etchant.

2.3 Results

The low viscosity of the precursor liquid allows very quick filling of trench structures on the mold.[19] A pressure of 20 psi to 100 psi is sufficient for the imprinting process which is carried out at room temperature. Moreover, the improved formulation utilized in this work allows an extremely fast curing (10 sec) at moderate temperature (80-120 ^{o}C). The rise time of the heating process is ~ 2 sec by IR lamp in Nanonex imprinter. These mild conditions help increase greatly the process throughput over that permitted by most thermoplastics. The liquid resist precursor was applied by spin-coating, which ensures its suitability for high-throughput nanolithography processes, in sharp contrast with the liquid droplet dispensing method used in Step-and-Flash-Imprint Lithography (SFIL).[20,21] Importantly, the application of low viscous silicone fluids, such as D_4 or D_5, as the diluent for the polydimethylsiloxane based resist, completely eliminates the tedious substrate surface treatment step. Typically shrinkage occurs when materials crosslink on curing. The shrinkage for our system is about 3-5% (close to epoxy), which is also lower than the acrylate-based systems used in SFIL. A lower shrinkage can allows faithful pattern replication during NIL process.

The modulus of a crosslinked material is a critical factor for nanoimprint lithography. Ideal imprinting requires a careful balance between the ease of mold separation and the mechanical integrity of the imprinted structures, especially those with high aspect ratios. A resist with a high modulus allows tall structures to be replicated without lateral collapsing due to capillary force, but they are typically brittle and may crack and break during mold separation. A resist with a low modulus allows for a clean mold separation, but the replicated structures may suffer from collapsing (an example is

shown in Fig 2.3. In general the modulus of a cured polymer material depends on the crosslinking density. In our material formulation, the modulus of the cured PDMS can be adjusted by tuning the molecular mass as well as the SiH concentration of the crosslinker (Figure 2). As presented in Figure 2.3 (data obtained by Dynamical Mechanical Analysis, DMA), we show that a high modulus material can be achieved by either employing a shorter DP prepolymer (e.g. DP 10 vs. 25) or a crosslinker with a high amount of SiH functional groups (e.g. 1.56% vs. 1.05%). Both strategies will increase the crosslinking density per unit volume of cured material.

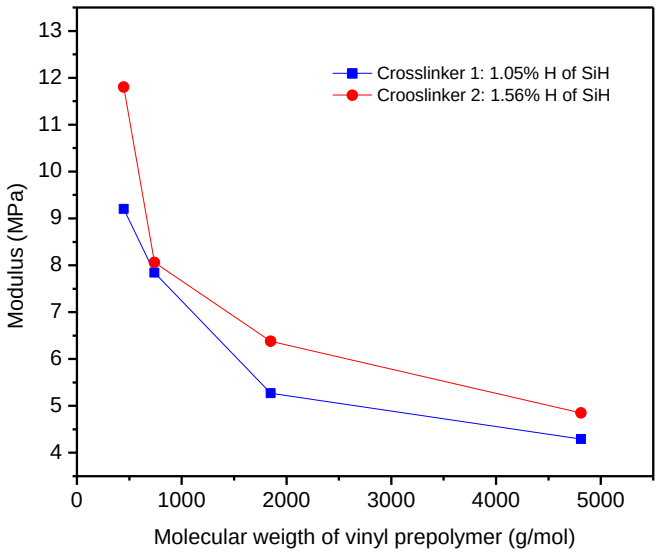

Figure 2.3 Modulus of the cured material as a function of molecular weight of vinyl terminated polydimethylsiloxane polymers.

DSC Isothermal scans were performed to obtain the time required to cure the resist formulation at different temperatures. For these experiments, a prepolymer with a DP of 25 and a crosslinker with 1.56 wt% of SiH groups were utilized. Three different catalyst concentrations (Pt%) in the formulated resists were tested: 120ppm, 230ppm and 340ppm.

At a temperature higher than 120°C, the resists cure almost instantly, even before reaching the set temperature for the isothermal scan due to the relatively slow rise time of the instrument. For this reason, the data reported here corresponds to the total time required from the start to the end of the curing process below 120°C. It should be pointed out that fast curing at elevated temperature is a desirable property for high throughput applications, while the imprinting step itself is carried out at ambient or relatively low temperature. Fast heat rising time is also necessary for high-throughput imprinting, which can be provided by high-power IR lamp heating (as in Nanonex tool) or other suitable mechanisms. Figure 2.4 shows the time to complete curing as a function of temperature. The results indicate that the curing kinetics is strongly temperature dependent. For example, when the curing temperature for PDMS with 120ppm of catalyst is increased from 70°C to 90°C, the crosslinking is completed in less than 4 min instead of 14 min. This is due to more efficient deactivation of the inhibitors at higher temperatures that releases catalyst faster. As expected, increasing the amount of catalyst also significantly reduces the curing time, especially at low temperatures. By increasing three times the amount of catalyst, the curing time was reduced from 14 min to 2.7 min. at 70°C. This effect is less evident at temperatures above 110°C since the curing time becomes extremely short (less than 1 min) and difficult to measure with the current instrument. In actual nanoimprint experiment, a 700nm period grating was replicated at 115°C in less than 10 sec (see below), a curing speed that is over two orders of magnitude faster than that of the previously reported PMDS materials.

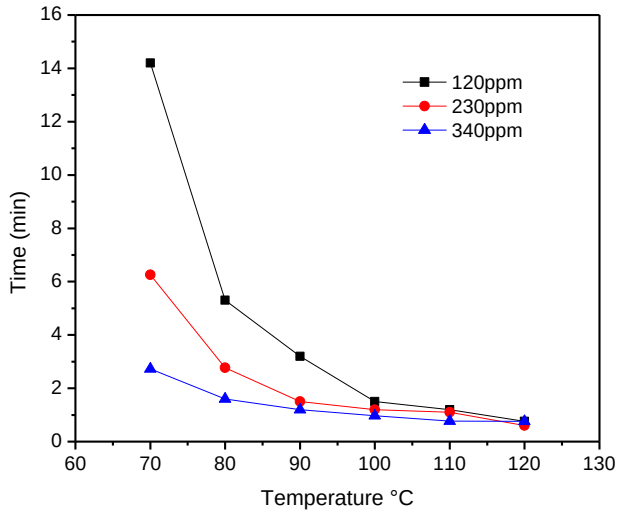

Figure 2.4 Curing time vs. temperatures for different catalysts concentrations.

Next we present results that correlate the dimension of the replicated PDMS resist structures with the modulus of the cured materials. Figure 2.5 shows the replicated microscale structures by using a low modulus resist formulated with a prepolymer of DP 65. As the structures are of a relatively large size, a modulus of 4.3 MPa was sufficient. For this case, the silicon oxide mold was employed without any type of the fluorosurfactant monolayer coatings normally used to prevent the adhesion of the imprinted pattern to the mold. The 1.56% SiH crosslinker was used to ensure fast curing for the thick resist used in this experiment.

For patterning structures in the sub-micron regime, a higher modulus elastomer was required. For that purpose, a pre-polymer with a lower degree of polymerization as well as the crosslinker with 1.56% wt. of SiH groups was used. As can be seen in Figure 2.5(c), the vinyl poly(dimethylsiloxane) with a DP of 25 presented good properties for generating 350 nm line width patterns after curing for 5 minutes at 80°C. By increasing both the amount of catalyst from 120ppm to 340ppm and the temperature up to 115° C, we were able to replicate the same sub-micron features within only 10 seconds. In comparison

with h-PDMS (viscosity of 362cP) reported previously, the present resist shows a very low viscosity (22cP), which facilitates the flow of the liquid into the mold holes. This value is even lower than the viscosity reported by Lee et al.[2] (50cP) after mixing PDMS with a compatible solvent to increase wettability. As a consequence, for the sub-micron and nanoscale replication reported here, resist flow is not a concern.

When small dimension gratings are replicated, the capillary forces between the structures significantly increase. As a consequence, the resist requires increased stiffness to avoid the structures from collapsing after mold releasing. To satisfy this requirement, a DP 10 prepolymer along with the higher SiH crosslinker was used, providing the structural integrity required to imprint sub-200 nm dense line gratings [Figure 2.5(d)]. The higher crosslink density achieved with this formulation resulted in a resist with a modulus of 8 MPa.

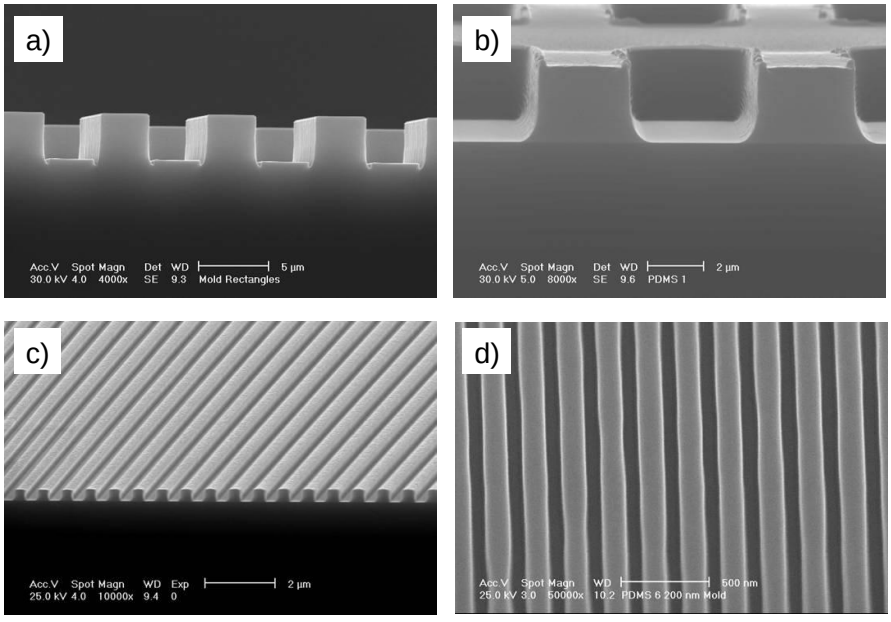

Figure 2.5 SEM micrographs of thermal-curable silicon resist formulations: a) imprinted microstructures (DP 65), and b) its corresponding silicon oxide mold; c) patterns with a 350 nm line width and spacing, using a resist with DP 25, d) 120 nm line width patterns, using a resist with DP 10.

For sub-100nm scale features, we found that 70 nm line width structures could be patterned using the same DP 10 prepolymer along with the higher SiH crosslinker. However, as the grating replicated was not completely uniform (collapsing can be observed through several areas), a DP 7 prepolymer was utilized instead (the crosslinker remained the same) to achieve the desired results [Figure 2.6(a)]. The higher modulus of this formulation provided sufficient structural integrity to withstand the high capillary forces acting at the nanometer level.

In addition to fast curing and easy mold releasing due to the low surface energy presented by the PDMS material, the high silicon content of the polymer also makes it highly resistant to reactive ion etching (RIE). The oxygen plasma etch rate of this crosslinked poly(dimethylsiloxane) resist is 1 nm per minute, which is two orders of magnitude lower than that of commonly used thermal plastic imprinting resist PMMA (etch rate of 100 nm per minute), making the former material an excellent etch mask for pattern transfer. A 70 nm line width pattern, [Figure 2.6(a)], was etched using O_2 plasma and CHF_3 plasma As can be seen in the SEM picture [Figure 2.6(b)] after the residual layer was removed by RIE, the poly(dimethylsiloxane) structures present no roughness from oxygen plasma etching, in contrast to the results obtained before with PDMS copolymers.[30] Finally, the patterned PDMS was used as a etch mask to transfer the pattern into a SiO_2 layer by using CF_4/O_2 plasma. As presented in Figures 2.6(c) and (d), the SiO_2 pattern remained smooth. This illustrates excellent pattern transfer by using the imprinted PDMS directly without the use of any additional hard etching mask.

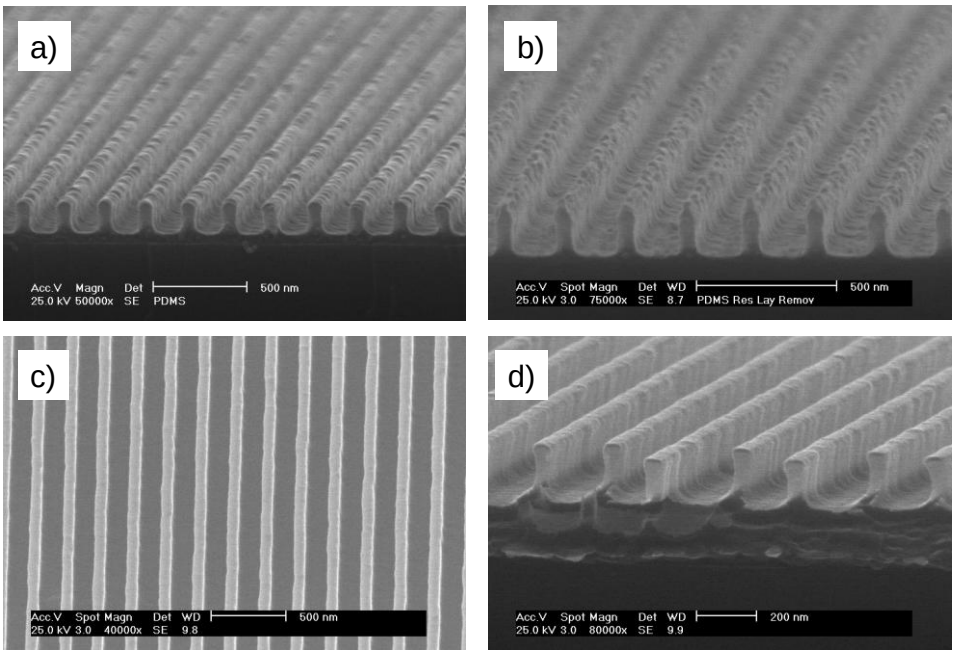

Figure 2.6 SEM images of 70 nm line width structures etched in SiO_2; a) thermal-curable polysiloxane pattern, b) pattern after O_2 plasma and residual later removal; c), d) SiO_2 structure obtained by CHF_3/O_2 Etching.

PDMS elastomers have found wide range of applications in the context of soft-lithography and micro-stamping,[1-5] however as noted earlier commercial PDMS materials are not suitable to produce sub-500nm scale features due to its low modulus. Since the material formulation presented in this paper works very effective as a nanoimprint resist, capable of sub-100nm resolutions, we anticipate that it will find a range of applications if a thick-layer of imprinted PDMS is used directly as an elastomeric stamp. As a demonstration, we were able to use the replicated 700nm period grating sample (structures similar to that shown in Fig. 2.5(c) as a stamp to print submicron scale conductive polymer PEDOT patterns using a polymer inking and stamping technique (Figure 2.7).[22] In additional, the imprinted 350 nm linewidth grating structures has also recently been used to successfully replicate agarose stamps for reactive wet stamping[23] on various substrates to produce deep submicron features.[24]

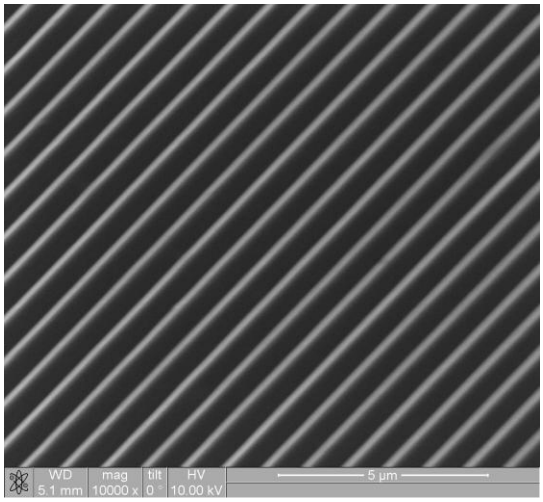

Figure 2.7 Patterned 700 nm period grating structures in conductive polymer PEDOT with a cured PDMS stamp by using the polymer inking and stamping technique.[22]

2.4 Conclusions

In summary, a low pressure and fast thermal-curable system based on the hydrosilylation chemistry of siloxane polymers was developed. A thermal curing time less than 10 seconds was obtained, in strong contrast to previously demonstrated PDMS type resist requiring tens of min to hours to be fully cured. The fast crosslinking time ensures the high-throughput needed in nanoimprint lithography. The application of low viscous silicone fluids, such as D_4 or D_5, as the diluent for the polydimethylsiloxane based resist, completely eliminates the tedious substrate surface treatment step, and further increases the efficiency of the nanoimprinting process. The ability to tune the modulus imparts flexibility to the resist in meeting different process conditions. This property allowed the replication of nanometric structures with satisfactory results. The high silicon content of the cured material leads to low surface energy, which eases mold releasing, and high etching resistance. The replicated PDMS material can also be used as a stamp directly in

many soft lithography and micro-stamping applications to produce deep submicron structures.

References

[1] T. W. Odom, J. C. Love, D. B. Wolfe, K. E. Paul, G. M. Whitesides, *Langmuir* **2002**, *13*, 5314.

[2] H. Kang, J. Lee, J. Park, H. H. Lee, *Nanotechnology* **2006**, *1*, 197.

[3] F. Hua, A. Gaur, Y. G. Sun, M. Word, N. Jin, I. Adesida, M. Shim, A. Shim, J. A. Rogers, *IEEE Transactions on Nanotechnology* **2006**, *3*, 301.

[4] E. Mele, F. Di Benedetto, L. Persano, R. Cingolani, D. Pisignano, *Journal of Vacuum Science & Technology B* **2006**, *2*, 807.

[5] R. B. A. Sharpe, B. J. F. Titulaer, E. Peeters, D. Burdinski, J. Huskens, H. J. W. Zandvliet, D. N. Reinhoudt, B. Poelsema, *Nano Lett.* **2006**, *6*, 1235.

[6] Y. N. Xia, G. M. Whitesides, *Annual Review of Materials Science* **1998**, 153.

[7] C. Y. Hui, A. Jagota, Y. Y. Lin, E. J. Kramer, *Langmuir* **2002**, *18*, 1394.

[8] H. Schmid, B. Michel, *Macromolecules* **2000**, *8*, 3042.

[9] L. Malaquin, C. Vieu, in *Alternative Lithography* (Ed: C. M. Sotomayor Torres), KLUWER ACADEMIC PUBLISHERS, **2003**, Ch. 8.

[10] L. Malaquin, F. Carcenac, C. Vieu, M. Mauzac, *Microelectronic Engineering* **2002**, 379.

[11] P. AUROY, L. AUVRAY, L. LEGER, *Macromolecules* **1991**, *18*, 5158.

[12] H. Brunner, T. Vallant, U. Mayer, H. Hoffmann, *Langmuir* **1996**, *20*, 4614.

[13] X. Cheng, L. J. Guo, P. F. Fu, *Adv. Mater.* **2005**, *11*, 1419.

[14] P. Choi, P. F. Fu, L. J. Guo *Adv. Funct. Mater.* **2006**.

[15] L. N. Lewis, J. Stein, R. E. Colborn, Y. Gao, J. Dong, *Journal of Organometallic Chemistry* **1996**, *1-2*, 221.

[16] S. Ahn, K. Lee, J. Kim, S. H. Kim, J. Park, S. H. Lee, P. Yoon, *Micro Electronic Engineering , 78-79*, 314.

[17] M. E. Walsh, Nanostructuring Magnetic Thin Films Using Interference Lithography, 2000.

[18] G. B. Onoa, T. B. O'Reilly, M. E. Walsh, H. I. Smith, *Nanotechnology* **2005**, *12*, 2799.

[19] L. J. Guo, *Journal of Physics D-Applied Physics* **2004**, *11*, R123.

[20] P. Ruchhoeft, M. Colburn, B. Choi, H. Nounu, S. Johnson, T. Bailey, S. Damle, M. Stewart, J. Ekerdt, S. V. Sreenivasan, J. C. Wolfe, C. G. Willson, *Journal of Vacuum Science & Technology B* **1999**, *6*, 2965.

[21] M. D. Stewart, S. C. Johnson, S. V. Sreenivasan, D. J. Resnick, C. G. Willson, C. G. *Journal of Microlithography Microfabrication and Microsystems* **2005**, *1*, 011002.

[22] D. W. Li, L. J. Guo, *Appl. Phys. Lett.* **2006**, *6*, 063513.

[23] C. J. Campbell, S. K. Smoukov, K. J. M. Bishop, B. A. Grzybowski, *Langmuir* **2005**, *7*, 2637.

[24] S. K. Smoukov, *private communications*

Chapter 3

Silicone Resin Copolymers

3.1 Introduction

Silicone resins (SSQ's) are a type of hybrid organic-inorganic materials with excellent properties such as good thermal stability, low dielectric constant (<3) and good mechanical properties. The first silicone resins $(CH_3SiO_{1.5})_n$ were isolated by Scott in 1946 through thermolysis of polymeric products obtained from methyltrichlorosilane and dimethylchlorosilane cohydrolysis.[1] Since then these versatile materials have found widespread applications such as photoresist coatings for electronics and optical devices, interlayer dielectrics and protective coating films for semiconductor devices, liquid crystal display elements, magnetic recording media, optical fiber coatings, gas separation membranes, binders for ceramics.[2]

Silicone resins can be represented according to the number of oxygen atoms bonded to the silicon atom in the oligomeric structure. For example, triorganosiloxane ($R_3SiO_{1/2}$) is referred as M unit; when the silicon is linked to two oxygen atoms it is a D unit and the structure is called diorganosiloxane ($R_2SiO_{2/2}$); when it is bonded to three oxygens it is a T unit or silsesquioxane ($RSiO_{3/2}$). In the case of the silicon atom linked to

four atoms it is a Q unit and it is called silicate ($SiO_{4/2}$) (figure 3.1). The organic group R linked to the silicon atom can be a stable chemical substituent or a reactive substituent.[2]

Resin polymers are normally described by compositional formulas such as $[C_6H_5SiO_{3/2}]_x[(CH_3)_2SiO]_y$ where X and Y are the molar ratios of the components. The molecules can therefore be presented as $T^{Ph}{}_xD_y$ by using the M, D, T and Q expressions.

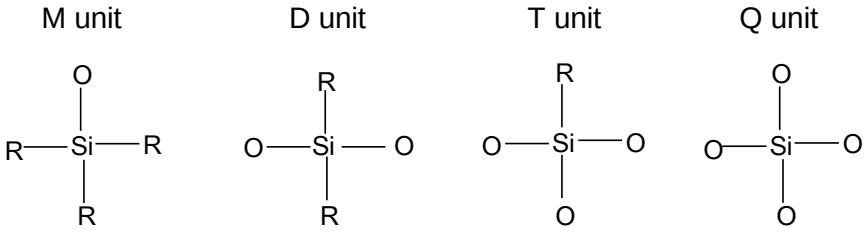

Figure 3.1 Units of silicone resins.

Organosilicone resins can be synthesized through the hydrolytic condensation of chlorosilanes or alkoxysilanes as shown in equation 1,[3] where X can be any organic group and Y presents an alkoxy or fluorine functionality. Silicon resins can present random structures, ladder structures, cage structures and partial cage structures (figure 3.2). The most common silicone resins include phenyl silsesquioxane (PSQ), methyl silsesquioxane (MSQ), and hydridosilsesquioxane (HSQ).[2]

Equation 1 $$n\mathrm{XSiY_3} + 1.5n\mathrm{H2O} \rightarrow (\mathrm{XSiO_{1.5}})_n + 3n\mathrm{HY}$$

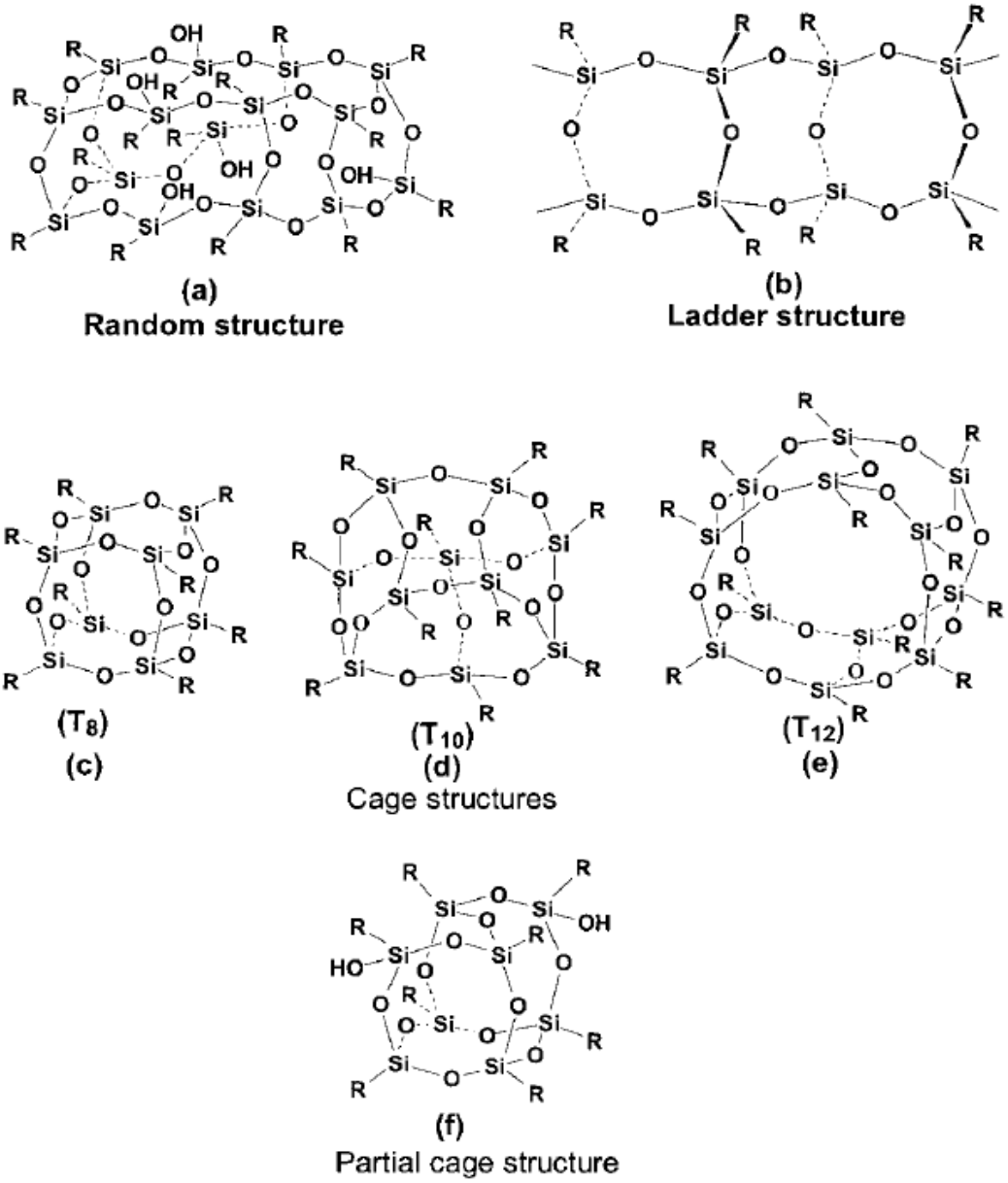

Figure 3.2 Structures of silsesquioxanes[4]

Interestingly, organosilicone materials can be functionalized with several types of organic groups; for instance, they can have photocurable groups to crosslinking the material into a variety of desired physical shape. Another advantage is that these materials can have a broad range of molecular weight and viscosities depending on the

synthesis procedure used. The high silicon and oxygen content makes them have plasma etching properties quite similar to those of amorphous SiO_2. In addition, their mechanical properties can be tailored according to specific needs. Thus, organosilicone materials have excellent properties which make them outstanding candidate materials for to NIL applications.

Therefore, in this project, different types of organosilicone resins with a range of compostions were copolymerized and characterized to find the materials best suited as patterning layers for NIL. Organosilicone copolymers carrying D, T and Q units were synthesized by hydrolytic condensation of alkoxysilanes. T and Q units were chosen because they can provide a suitable modulus (about 1GPa) for nanoimprinting. T and Q units create a network with a high degree of crosslinking which can generate a stiff material. [4] On the other hand, materials with D units were synthesized because they can have a higher flexibility.[4] Materials with different molar ratios of D and T and Q units were prepared to find the more appropriate composition for NIL.

Methyl and phenyl were the substituent groups employed because they generate a more hydrophobic material with a larger oxidative thermal stability and lower shrinking upon heating. On the other hand, phenyl groups improve the material toughness.[4] Finally, the curing was done using epoxypropoxy or methacrylate functional groups.

A typical reaction to synthesize a silicone resin with D and T units, starting from alkoxysilane monomers, is shown in figure 3.3. Silicone resins were synthesized through a hydrolytic in a basic medium. It can be seen in figure 3.3 that the final material contains epoxy moieties which functions as reactive sites for photocuring, phenyl groups which provides toughness and methyl's that reduce the material surface energy.

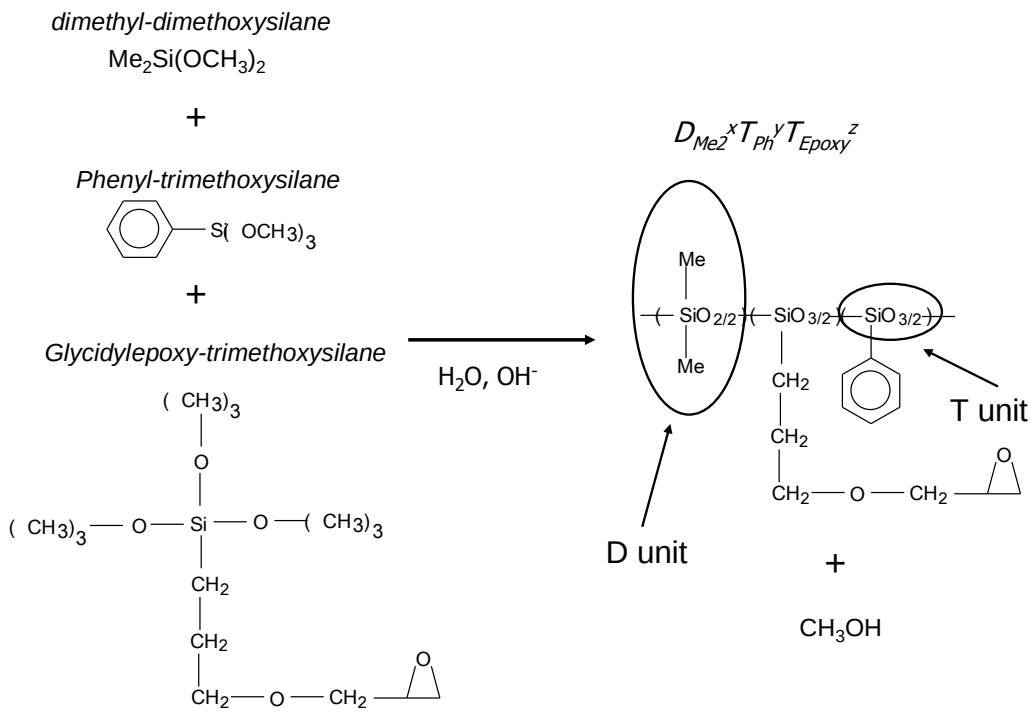

Figure 3.3 Typical synthesis of a silicone resin (this material contains D and T units).

3.2 Synthesis of the silicone materials

The chemical procedure followed to synthesize the silicone resins used in this project is presented below.

3.2.1 Synthesis of poly(phenyl-co-3-glycidoxypropyl)silsesquioxane T(Ph)T(Epoxy)

This is a representative procedure to synthesize silicone resins containing epoxy (3-glycidoxypropyl) groups, $T^{Ph}_{0.20}T^{Epoxy}_{0.80}$.

Phenyltrimethoxysilane and 3-glycidoxypropyltrimethoxysilane were purchased from Gelest; toluene, methanol, cesium hydroxide (CsOH) and acetic acid were purchased from sigma-aldrich; and deionized water was obtained from the clean room facilities. All the chemicals were used as received.

All the reactions were carried out in a nitrogen atmosphere. The alkoxysilanes were cohydrolyzed in a mixing solvent of toluene/methanol/water under basic conditions. O.2 mol of phenyltrimethoxysilane, 0.8 mol of 3-glycidoxypropyl trimethoxysilane, 180 g of methanol, 4mol of water and 0.001mold of CsOh (base) were added to a 1 L 3-neck round-bottomed flask equipped with a magnetic stir bar, a Dean-Stark trap with a condenser, and a nitrogen inlet and outlet. The solution was refluxed at about 66C for 2 h while stirring (about 220g of solvent, mostly methanol, was removed in about 1 h). The temperature was increased to 105ºC while. During this step, more solvent was removed by evaporation so an equal amount of toluene was added to keep a constant resin concentration. It took one hour to increase the temperature to 105º C. The solution was then cooled to 50º C and diluted with 380 g of toluene. Then, the dilute solution was acidified with 6 g of acetic acid and allowed to stir for about 15 min. The solution was washed with 100 ml of deionized water. The mixture was then transferred to a separation funnel and the lower water layer was discarded. The upper layer was further washed 3 times with 100 ml of deionized water, and the slightly cloudy solution was transferred to a wide mouth open vessel. The vessel was placed on a hot plate with a stirrer to remove the toluene at 55ºC during 24 h. Residual toluene was additionally removed using a vacuum oven at 55º C for 5 h. A colorless viscous liquid was obtained and kept for further characterization and evaluation.

3.2.2 Synthesis of poly(methacryloxypropyl)silsesquioxanes T(Ph)T(Methacryloxy)

This is the typical procedure to synthesize a silicone resin with methacryloxy groups, $T^{Ph}_{2/3}T^{Methacryloxy}_{1/3}$. All reactions were carried out in a nitrogen atmosphere.

Phenyltrimethoxysilane and 3-methacryloxypropyltrimethoxysilane were purchased from Gelest; toluene, methanol, cesium hydroxide (CsOH), 2,6-di-terbutyl-4-methylphenol and acetic acid were purchased from sigma-aldrich; deionized water was obtained from the clean room facilities. All the chemicals were used as received without further purification.

Phenyltrimethoxysilane and 3-meacryloxypropyl trimethoxysilane were cohydrolized in a mixture of solvent of toluene/methanol/water under basic condition. 80 g of toluene, 0.20mol of 3-methacryloxypropyltrimethoxysilane, 0.40 mol of phenyltrimethoxysilane, 2.40 mol of water, 1 g of CsOH aqueous solution (50 wt %), 200g of methanol, and 40 g of 2,6-di-terbutyl-4-methylphenol were added to a 1 L 3-neck round-bottomed flask equipped with a mechanical stir shaft, a Dean-Stark trap with a condenser, and a nitrogen inlet and outlet. The solution was refluxed at 66ºC for 1 h and about 250g of solvent (mostly methanol) was removed via the Dean Stark Trap. The solution was refluxed for another hour and more solvent was removed while an equal amount of toluene was added to keep the percentage of the resin concentration constant. After most of the methanol was removed the solution became cloudy. Solvent was continuously removed and the solution became clear again when most of the water was removed through the Dean Stark trap. After 2 h of refluxing at 66ºC, the temperature was slowly raised to 105ºC for 1 h while methanol and water were still being removed. This clear solution was then cooled to 50ºC and diluted to about 15 wt % by adding about 230 g of toluene. The solution was acidified by adding 3 g of acetic acid. It was stirred for 0.5 h. The solution was washed with 100 ml of deionized water 3 times. Then, the solution was transferred to a wide mouth vessel and placed on a hot plate. The solution was heated

at 5ºC for 24 h to evaporate solvent (toluene). Finally, a vacuum oven was used to evaporate residual toluene for 5 h. A colorless viscous liquid was obtained.

3.2.3 Synthesized silicone resins

A list of all the synthesized silicone resins is presented in Table 3.1; they may contain epoxy (Ep, 3-glycidoxypropyl or epoxypropoxy) or methacryloxy (MA, methracrylate or meth) functionalities for photocuring. They can also have phenyl (Ph), methyl (Me) and fluoroalkyl groups. The silicone resins may have D, T or Q units as constitutes.

Table 3.1 List of synthesized silicone materials.

T units (Phenyl)	T units (Methyl)	T units (Fluoroalkyl)	D, T and Q units
$T^{Ph}_{0.20}T^{Epoxy}_{0.80}$	$T^{Me}_{0.20}T^{Epoxy}_{0.80}$	$T^{Ph}_{0.40}T^{Ep}_{0.48}T^{Fluoroalkyl}_{0.02}$	$D^{Me}_{0.50}T^{Ep}_{0.50}$
$T^{Ph}_{0.40}T^{Epoxy}_{0.60}$	$T^{Me}_{0.30}T^{Epoxy}_{0.70}$	$T^{Ph}_{0.40}T^{Ep}_{0.50}T^{Fluoroalkyl}_{0.10}$	$D^{Me}_{0.25}T^{Me}_{0.25}T^{Ep}_{0.50}$
$T^{Ph}_{0.50}T^{Epoxy}_{0.50}$	$T^{Me}_{0.40}T^{Epoxy}_{0.60}$	$T^{Ph}_{0.40}T^{Ep}_{0.50}T^{Fluoroalkyl}_{0.10}$	$D^{Me}_{0.25}T^{Ph}_{0.25}T^{Ep}_{0.50}$
$T^{Ph}_{0.60}T^{Epoxy}_{0.40}$	$T^{Me}_{0.50}T^{Epoxy}_{0.60}$	$T^{Ph}_{0.40}T^{Ep}_{0.50}T^{Fluoroalkyl}_{0.10}$	$D^{Ph}_{0.50}T^{Ep}_{0.50}$
$T^{Ph}_{0.80}T^{Epoxy}_{0.20}$			$D^{Ph}_{0.25}T^{Ph}_{0.25}T^{Ep}_{0.50}$
$T^{Ph}_{0.20}T^{Methacryloxy}_{0.80}$			$T^{Ph}_{0.40}Q_{0.10}T^{Ep}_{0.50}$
$T^{Ph}_{0.30}T^{Methacryloxy}_{0.70}$			$T^{Ph}_{0.30}Q_{0.20}T^{Ep}_{0.50}$
$T^{Ph}_{0.40}T^{Methacryloxy}_{0.60}$			
$T^{Ph}_{0.50}T^{Methacryloxy}_{0.50}$			

3.3 Characterization of the synthesized silicone resins

^{29}Si NMR of a series of synthesized materials is shown in figure 3.4. The material corresponds to a T(Phenyl)T(epoxy) with different molar ratios of the substituent groups. The peak corresponding to T(epoxy) is around 68ppm while the peak corresponding to T(Phenyl) is in 82ppm. Figure 3.4a is the ^{29}Si NMR of a silicone resin with a molar ratio

close to 0.20 of phenyl's and 0.80 of epoxy groups. In the figure, it is evident that the area under the peak is proportional to the molar ratio of phenyl and epoxy functional groups used.

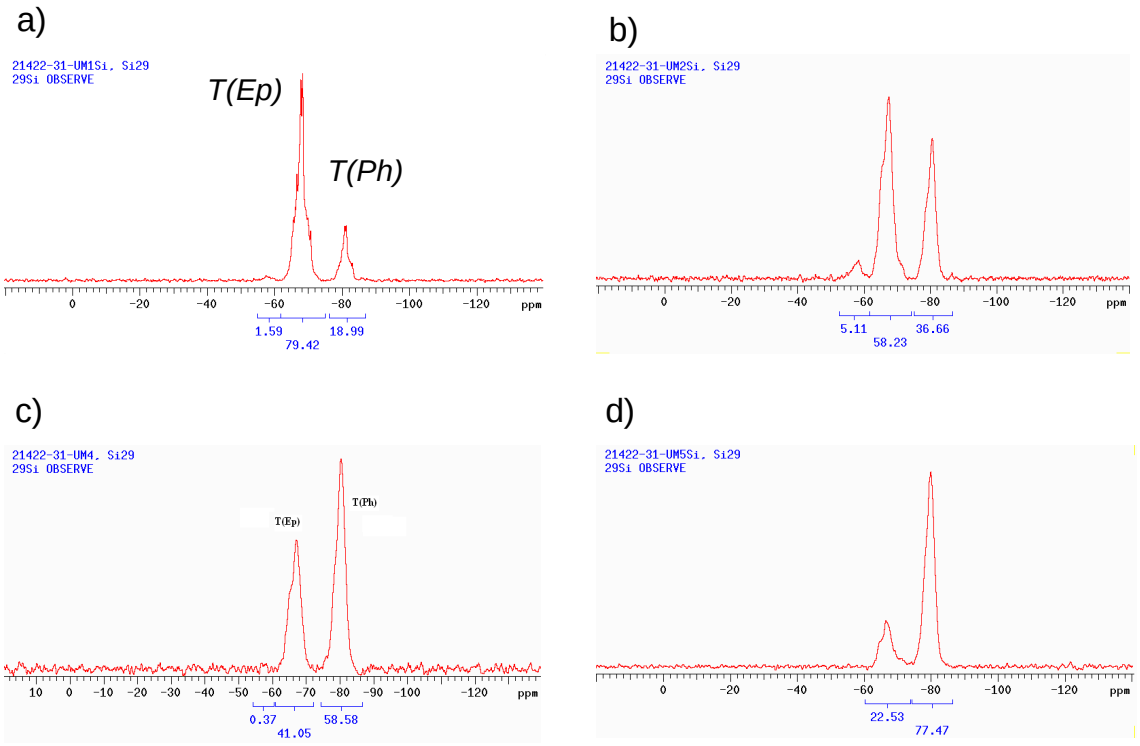

Figure 3.4 ^{29}NMR of a T(Phenyl)T(epoxy) resin with different molar ratios of phenyl and epoxy groups (a) phenyl=20, epoxy=0.80, (b) phenyl=0.40, epoxy=0.60, (c) phenyl=0.60, epoxy=0.40 and (b) phenyl=0.80, epoxy=0.20.

A typical gel permeation chromatography (GPC) to determine the prepolymer molecular weight of the silicone resins is presented in figure 3.5. The number average molecular weight for the $T^{Phenyl}_{0.40}T^{Methacrylate}_{0.60}$ resin is 1966g/mol (retention time of 30min). This relatively low molecular weight (is an important factor to achieve an easy filling of the mold cavities by the patterning material during the imprinting process. The molecular weight of a thermoplastic can be around several thousands g/mol) so they

present viscosities of several hundreds of thousands Pa.s. Similar molecular weights were determined for the rest of the synthesized materials.

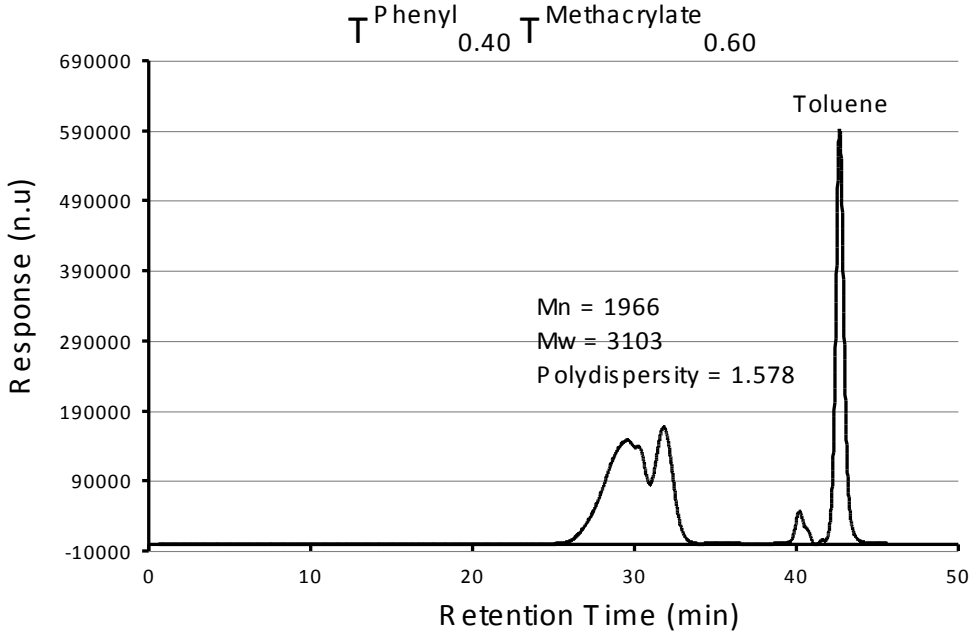

Figure 3.5 GPC obtained to measure the silicone resins molecular weights.

The appropriate selection of photocurable groups allows the SSQ resin to crosslink according to specific needs. Short curing times (few seconds or less) are required to achieve the high throughput process needed for industrial applications of NIL. The versatility in the synthesis of the developed SSQ resins allows a variety of photocurable functionalities. FTIR was used to characterize the synthesized silsesquioxane resin crosslinking dynamics due to UV light exposure under different conditions. A resin with photocurable oxirane (epoxy) rings was used as a model system for these experiments. The crosslinking of the oxirane rings is not oxygen inhibited thus avoids the need for special inert atmospheres. The testing shows that the degree of curing of the epoxy resin increases with the intensity of the irradiated UV light [Figure

3.6(left)]. Higher light intensity activates more epoxy groups at the beginning of the curing reaction, which can overcome the problem of low molecular mobility and diffusion normally induced during the network formation. This leads a higher degree of conversion. The light intensity also increased the curing rate.

In addition, as shown in Figure 3.6(right), higher concentration of photoacid generator (PAG) leads to a higher degree of crosslinking. We would like to point that a faster curing can be achieved utilizing methacrylate functional groups instead of the oxirane rings.

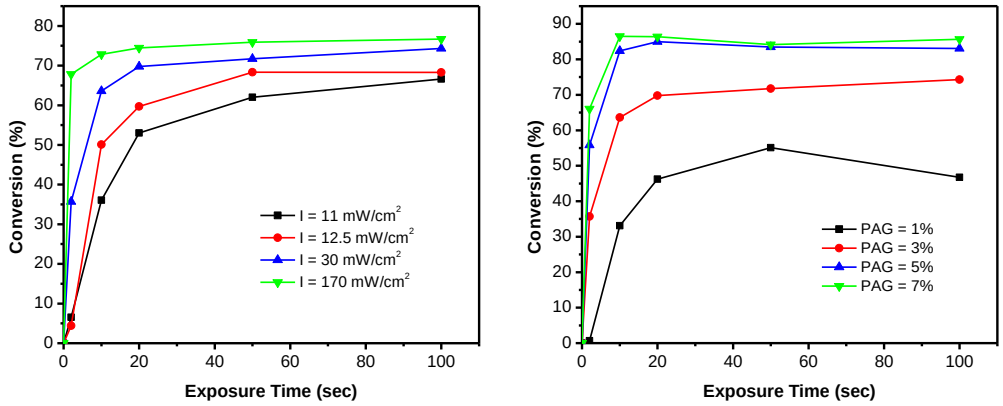

Figure 3.6 IR characterization of Ph-SSQ (epoxy based) material (left) absorbance vs. wavenumber at different UV radiation intensities , (center) Conversion vs. exposure time for different UV light intensities, (right) Effect of the concentration of PAG on the degree of conversion.

3.4. Imprinting tests

All the materials were imprinted using two different types of mold, 700nm (350nm line width) and 220nm (80nm line width) period mold to evaluate their sub-micron and nanopatterning capabilities.

3.4.1 Silicone resins with D and T units

SEM micrographs of imprinted structures on silicone resins containing different percentages of D and T units are shown in figure 3.7; as mentioned grating molds with 700nm (figures at the top row) and 220nm periods (figures at the bottom row) were employed for the imprinting tests. The content (molar percentage) of D units was varied from 0 to 50% while the content of T was changed from 50 to 100%. A silicone resin with methyl and epoxy functionalities was used for this testing and the molar ratio of epoxy groups was always held constant at 0.50 to have fewer variables during the experiments.

It was found that the structures imprinted with the 700nm period mold showed a high amount of breaking when the molar ratio of D units was high (0.50) (figures 3.7b and c). The structures with no D units did not show any breaking (figure 3.7a).

In the same manner, the material with a high amount of D units presented a high degree of breaking when a mold with smaller period size structures (220nm) was used (figures 3.7e and f). The silicone resin with only T units did not present any breaking but it had lateral collapsing (figure 3.7d).

The structures imprinted on resins with a lower degree of crosslinking (resins with D units) tend to present more breaking and pattern collapse because of their inferior mechanical properties. In fact, the materials containing D units have a lower degree of crosslinking than those with T units which gives a lower modulus material.

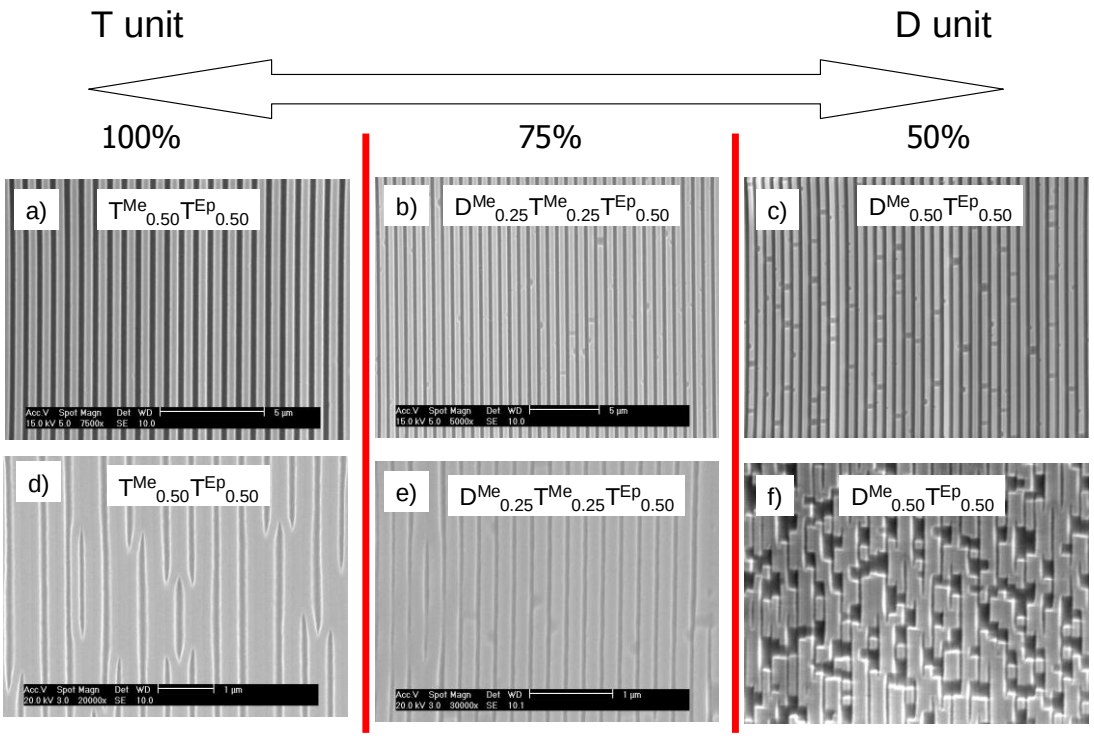

Figure 3.7 SEM pictures of silicone materials gratings imprinted with different contents of D and T units; top row corresponds to 700nm period and bottom row corresponds to 220nm grating mold.

On another set of experiments, the molar ratio of phenyl substituent was varied in silicone resins containing D and T units while the amount of epoxy substituent was maintained constant. Two different materials were used, $D^{Me}_{0.25}T^{Me}_{0.25}T^{Ep}_{0.50}$ and $D^{Me}_{0.25}T^{Ph}_{0.25}T^{Ep}_{0.50}$. The 700nm period pattern was easily imprinted with both resins (figures 3.8a and b). However, the resin with the phenyl moiety gave better results (figure 3.8d) than the material with the methyl moiety (figure 3.8c) when employing the more challenging to replicate 220nm period mold.

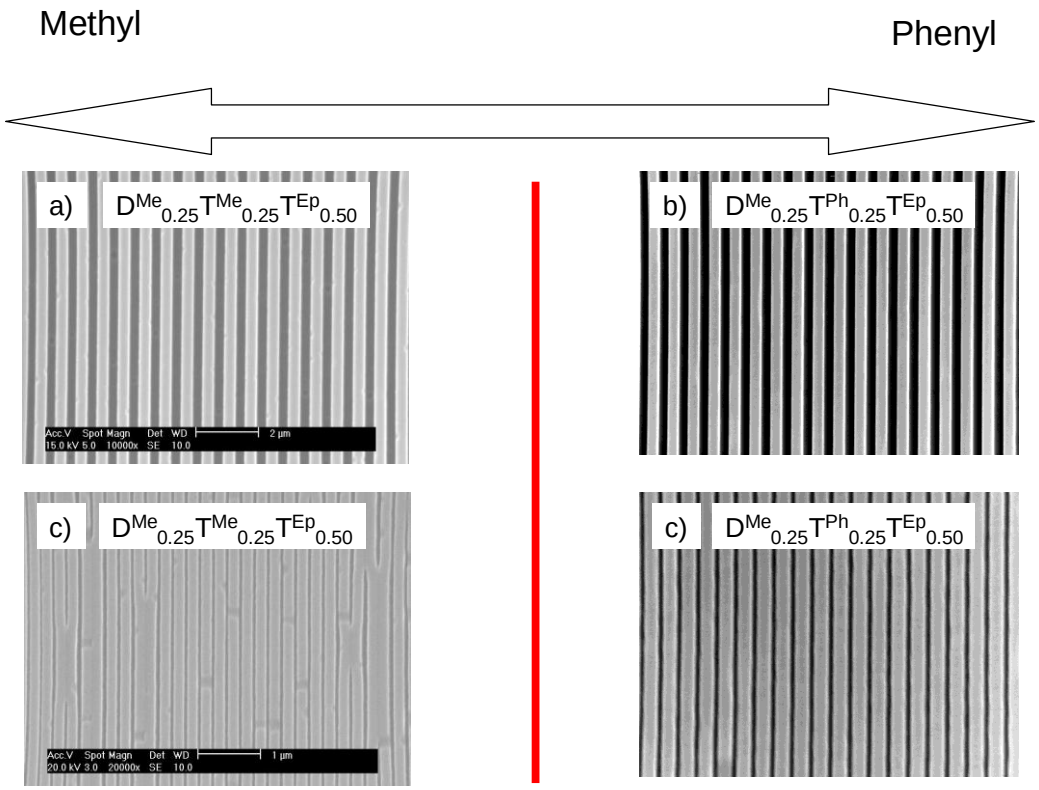

Figure 3.8 SEM pictures of gratings imprinted with D-T materials with different contents of methyl and phenyl groups; top row corresponds to 700nm period and bottom row corresponds to 220nm grating mold.

A stress-strain curve obtained with a tensile test is presented in figure 3.9. This test is useful to understand the effect of using methyl or phenyl functionalities on the silicone resins. The resin which contains phenyl groups has a larger tensile strength than the material with methyl groups. These results can be directly related to the imprinting tests previously shown. A material with a low tensile strength can easily break during the releasing process. That can be the reason why structures imprinted on the resin with methyl groups presents a high degree of breaking. On the other hand, the resin with phenyl groups does not break during demolding process because of its larger tensile strength.

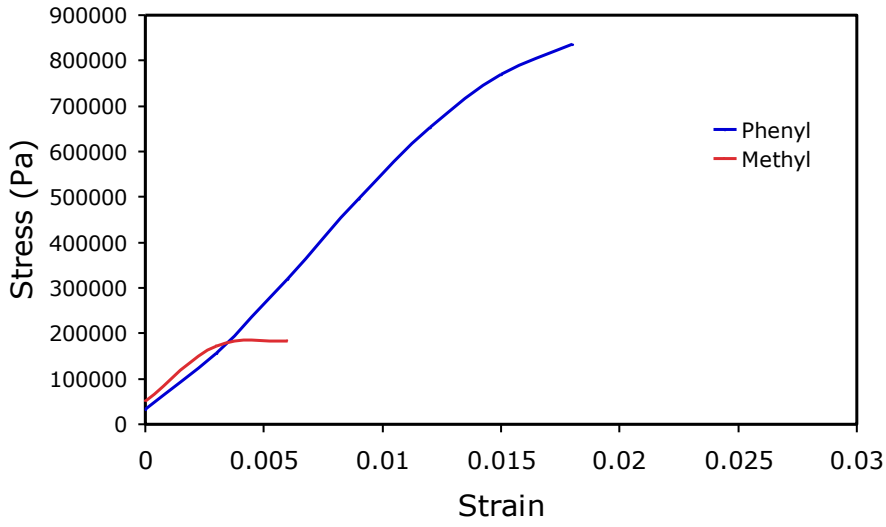

Figure 3.9 Tensile test of SSQ materials which contain phenyl (blue curve) and methyl (red curve) groups in their structure. The SSQ's also have epoxy groups for crosslkinking.

Materials containing phenyl substituent and different amounts of D and T units were also synthesized, $D^{Ph}_{0.25}T^{Ph}_{0.25}T^{Ep}_{0.50}$ and $T^{Ph}_{0.50}T^{Ep}_{0.50}$, to evaluated their imprinting properties. They presented a behavior similar to that of the silicone resins with methyl groups in the sense that the materials with the larger content of T units (lower amount of D units) generated better imprinting results. However, a difference to the methyl substituted resins is that the resin containing both phenyl groups and a 75 percent of T units was enough to imprint the 220nm period mold with no defects (figure 3.10c). Furthermore, the 700nm period mold was accurately replicated by the resin with 50% and 75% of D units (figures 3.10a and b). In addition, it seems that a larger amount of T units prevents the lateral collapsing of the replicated lines.

It can be said that the presence of phenyl groups gives good imprinting results with no apparent lateral collapsing or breaking even if the material has D units. This must

be related to a phenyl induced mechanical properties enhancement as mentioned previously.

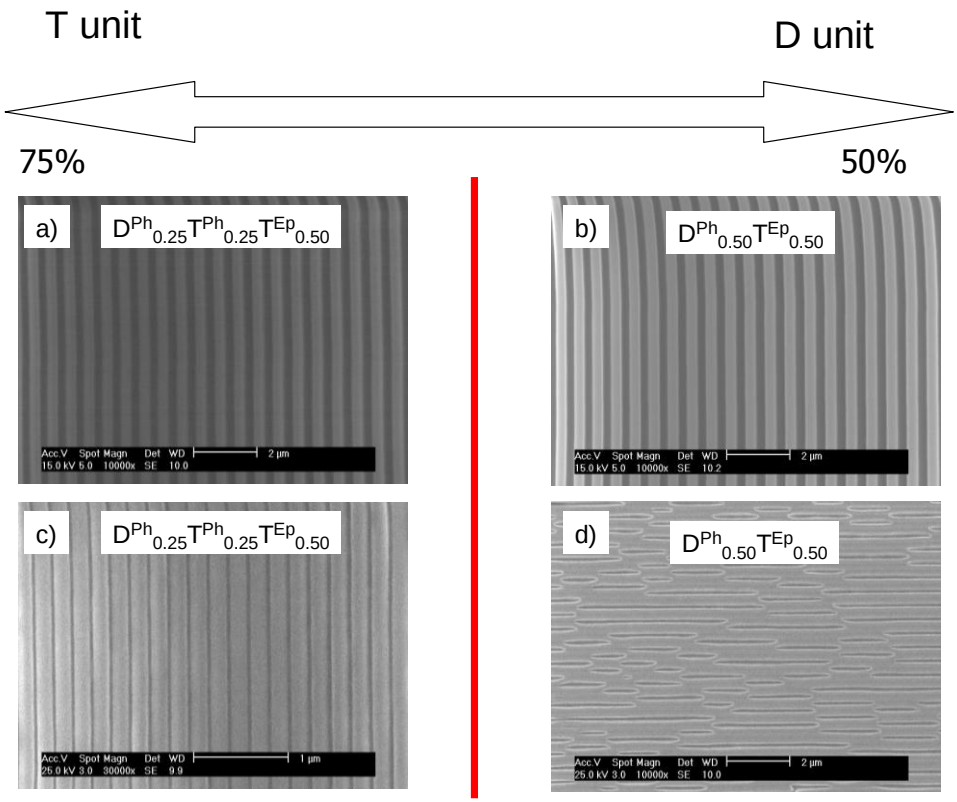

Figure 3.10 SEM pictures of gratings imprinted with D-T materials with different contents of phenyl groups; top row corresponds to 700nm period and bottom row corresponds to 220nm grating mold.

3.4.2 Silicone resins with Q and T units

Silicone resins with Q and T units were also synthesized to test their patterning abilities; the synthesized materials were $T^{Ph}_{0.30}Q_{0.20}T^{Ep}_{0.50}$ and $T^{Ph}_{0.40}Q_{0.10}T^{Ep}_{0.50}$. The Q units provide a higher degree of crosslinking which increases the modulus of the material while decreases its flexibility. It was found that a replication with few defects was achieved (700 and 220nm period mold used) for both materials (figure 3.11). However, in general, the material with the larger content of Q units, $D^{Ph}_{0.30}Q_{0.20}T^{Ep}_{0.50}$, showed more

defects. Resins with a higher amount of Q units were not prepared because small particles tend to be inside the viscous liquid during the resin synthesis.

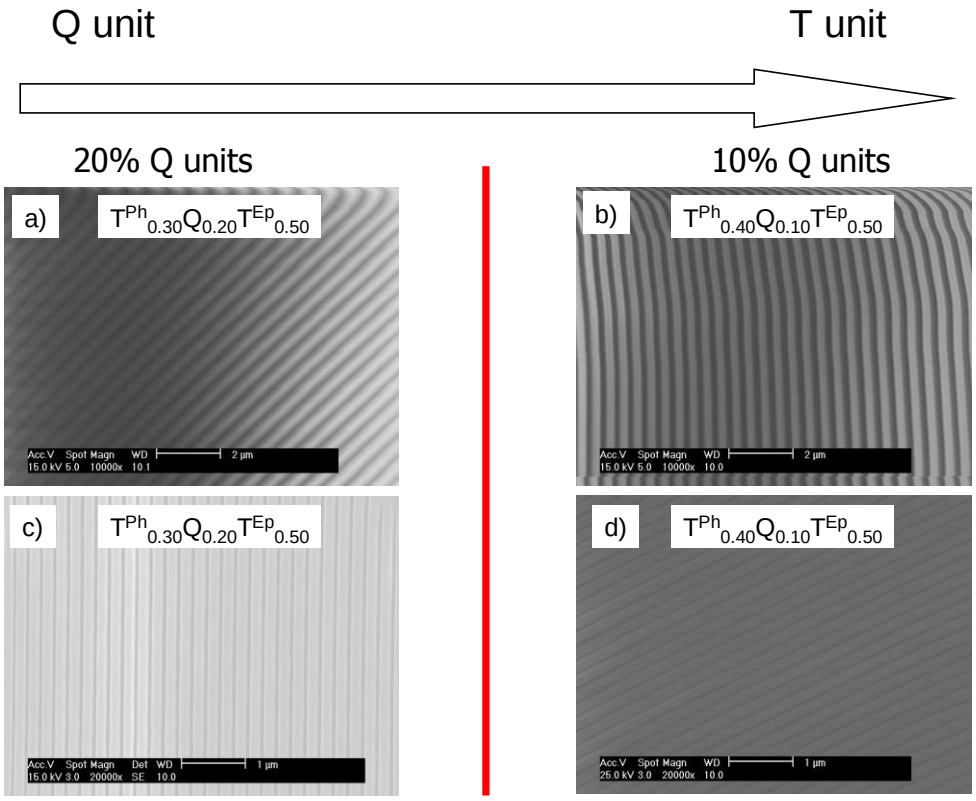

Figure 3.11. SEM pictures of gratings imprinted with Q-T materials; top row corresponds to 700nm period and bottom row corresponds to 220nm grating mold.

3.5 Novel UV + thermal imprinting

The typical UV curing process to imprint the synthesize materials has demonstrated it suitability for the nanoscale replication of a number of materials. However, those silicone resins containing D units and/or methyl groups did not show good results when using this procedure. The importance of imprinting silicone materials with methyl groups is the possibility of directly patterning functional layers for interlayer dielectrics. It has been shown that silsesquioxanes with methyl functionalities have a low

dielectric constant (<3.0) so they could be a replacement of SiO_2 insulating layer in the manufacturing of advanced integrated circuits in the SI industry.

The synthesized silicone resins contain several types of chemical groups to modify the material final properties. Besides methyl and phenyl groups, they contain epoxy substituent which reacts through a cationic polymerization initiated by the exposure of a photoacid generator to UV light. This reaction leads to the crosslinking of the resin to generate a solid material with the appropriate mechanical properties for nanoscale replication. However, not all of the epoxy groups react during the UV exposure step as shown in figure 3.6, where a conversion of about 75% is normally achieved. This means there are additional epoxy groups left unreacted which can crosslink and increase the material modulus.

Therefore, a UV + thermal imprinting process was developed which takes advantage of the unreacted epoxy groups to increase the modulus of the imprinted materials and enhance the material capabilities to imprint smaller size nanostructures with high aspect ratios. The new UV + thermal imprinting is shown in figure 3.12.

To demonstrate the curing of the additional epoxy groups through a thermal process, a series of infrared (IR) spectra were obtained. The infrared spectra for a silicone resin $T^{Ph}_{0.40}Q_{0.10}T^{Ep}_{0.50}$ used a sample model and cured by a UV exposure and a UV + thermal process are presented in figure 3.13. It can be seen that the relative intensity of the 910cm-1 peak corresponding to the C-H stretching vibration of an epoxy groups is smaller for the material cured by the UV + thermal process than that for the material only cured by the UV process; the signal in 700cm-1 was used as the reference peak. This indicates the thermal process induces additional curing into the silicone resin.

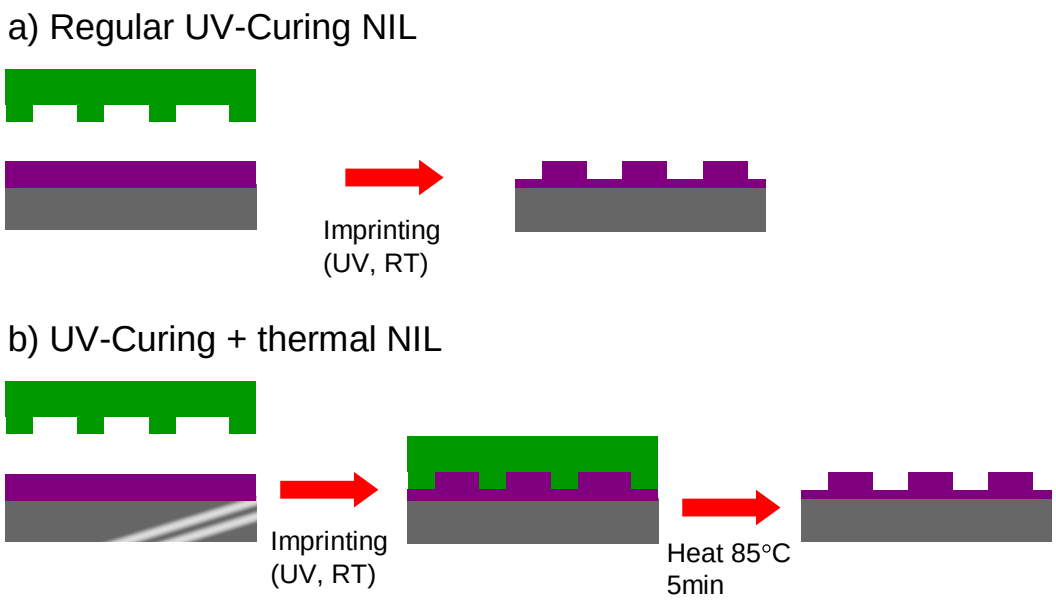

Figure 3.12 Schematics of the (a) regular UV imprinting and (b) the UV + thermal imprinting.

As mentioned, the UV curing of the resin yields only a conversion around 75%. Further crosslinking is not possible because of the low mobility of the polymeric chains in the cured network. However, when the material is heated ~~, the chain mobility increases making it easy for th~~the diffusion of photoacid generator (PAG) tend to increase. Thus, PAG molecules can easily diffuse across the network volume to promote the crosslinking of unreacted epoxy rings. ~~e reactive epoxy rings groups find each other and create additional crosslinking in the material.~~ This higher degree of crosslinking increases the modulus from 0.5MPa to 2MPa which helps prevent pattern collapse as shown later.

For the new imprinting process, the UV-curing was performed as normal (room temperature imprinting for 1 min using pressure); then, a subsequent heating step was done to cure the residual epoxy groups. The additional heating step takes place before the mold releasing step. The temperature used was 80°C for a short period of time (5 min) and not additional pressure was employed.

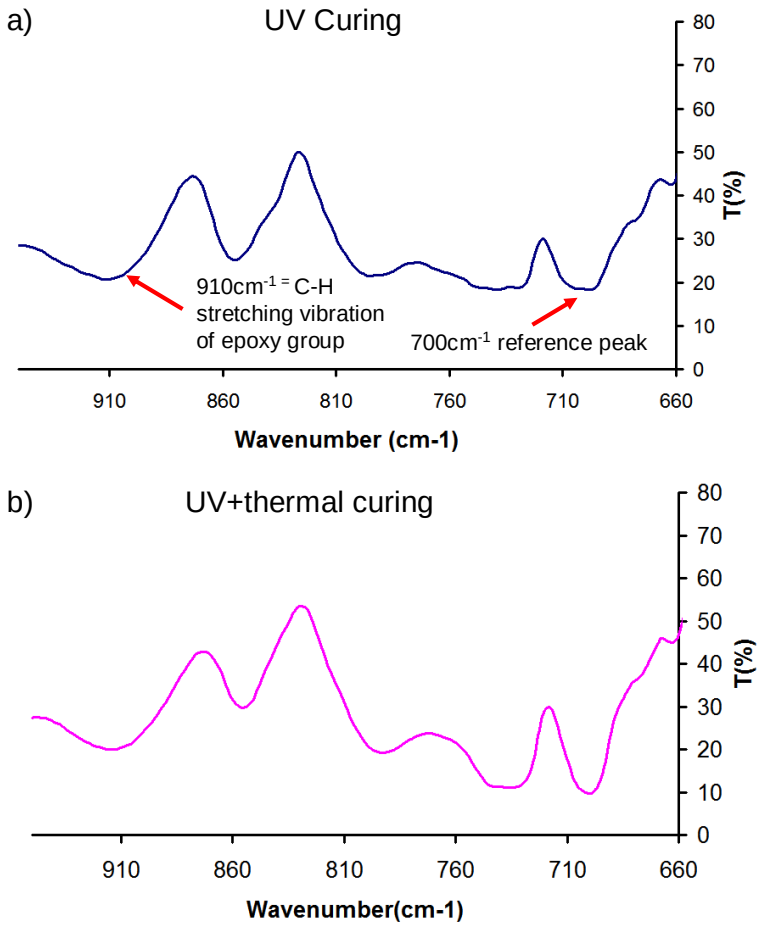

Figure 3.13 Infrared spectrum of a silicone resin cured with (a) UV light and (b) UV light plus thermal heating; $D^{Ph}_{0.40}Q_{0.10}T^{Ep}_{0.50}$ was the material used for the test.

The UV imprinted materials were further tested with the modified UV + thermal imprinting to see if improvements in the replication capabilities could be achieved. Better results were achieved when employing the material with only T units (silsesquioxane) with a methyl substituent ($T^{Me}_{0.50}T^{Ep}_{0.50}$). Although this material showed good results for the UV-imprinting of 700nm period mold, the 220nm period mold presented lateral collapsing. However, the lateral collapsing of the $T^{Me}_{0.50}T^{Ep}_{0.50}$ silsesquioxane was

successfully prevented using the UV + thermal imprinting as presented in figure 3.14. Therefore, the thermal process produces the appropriate degree of crosslinking to achieve the material patterning.

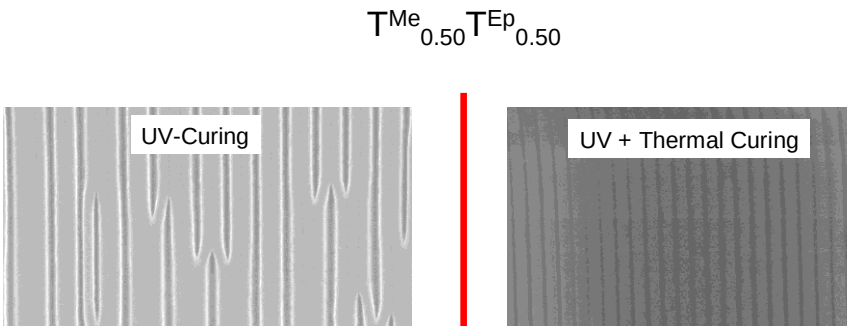

Figure 3.14 SEM pictures of gratings imprinted with T materials by UV and UV + heat curing; 220nm grating mold.

A similar result was obtained for the $D^{Ph}_{0.50}T^{Ep}_{0.50}$ resin. As with the $T^{Me}_{0.50}T^{Ep}_{0.50}$ silsesquioxane, the $D^{Ph}_{0.50}T^{Ep}_{0.50}$ material was perfectly UV-imprinted using a 700nm period mold; but the 220nm period grating induced pattern collapse. However, the lateral collapsing was completely prevented with the UV + thermal imprinting approach (figure 3.15) due to the higher degree of crosslinking of the thermally cured material.

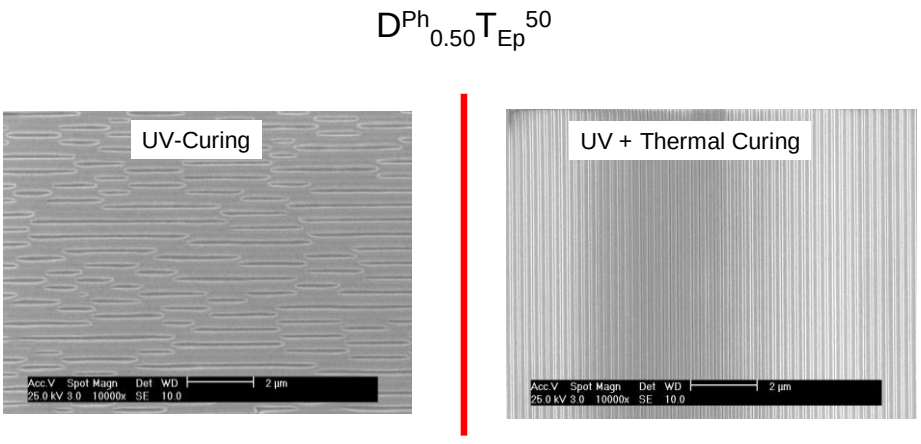

Figure 3.15 SEM pictures of gratings imprinted with D and T materials by UV and UV + heat curing; 220nm grating mold.

The majority of the synthesized silicone resins have shown outstanding properties for the imprinting of small nanogratings such as 220nm period and 140nm line width. However, smaller size patterns (100nm period and 50nm line width) with a large aspect ratio (4:1) are very challenging to replicate because the patterned lines are prone to collapse due to the proximity among them (about 50nm apart).

Fortunately, the UV + thermal imprinting also provided satisfactory results when patterning with the challenging 50nm line width mold. Different types of silicone materials such as $T^{Ph}_{0.20}T^{Ep}_{0.80}$, $T^{Ph}_{0.40}Q_{0.10}T^{Ep}_{0.50}$ and $T^{Ph}_{0.40}T^{Ep}_{0.50}T^{Fluoroalkyl}_{0.10}$ were easily imprinted as shown in figure 3.16.

3.6 Discussion

The materials with T units perform better than those with D units because of the higher degree of crosslinking in the former. Materials with a higher degree of crosslinking present larger modulus so a higher imprinting resolution can be achieved. Silicone resins with Q units also have a higher degree of crosslinking which is helpful for imprinting purposes. On the other hand, the SSQ's with methyl groups have a low tensile strength which leads to an easy breaking of the structures during the demolding process. The phenyl groups provide the high tensile strength the imprinted structures need to withstand the high stresses produced during the demolding step.

The improved UV + thermal patterning provides enhanced resolution (smaller imprinted structures) than the regular UV process because the heating step induces further epoxy crosslinking which generates material with a larger degree of crosslinking.

As mentioned above, a material with a larger degree of crosslinking has a higher modulus and does not collapse laterally during the demolding step. If a material does not have an appropriate modulus, the structures will likely collapse when the demolding is performed.

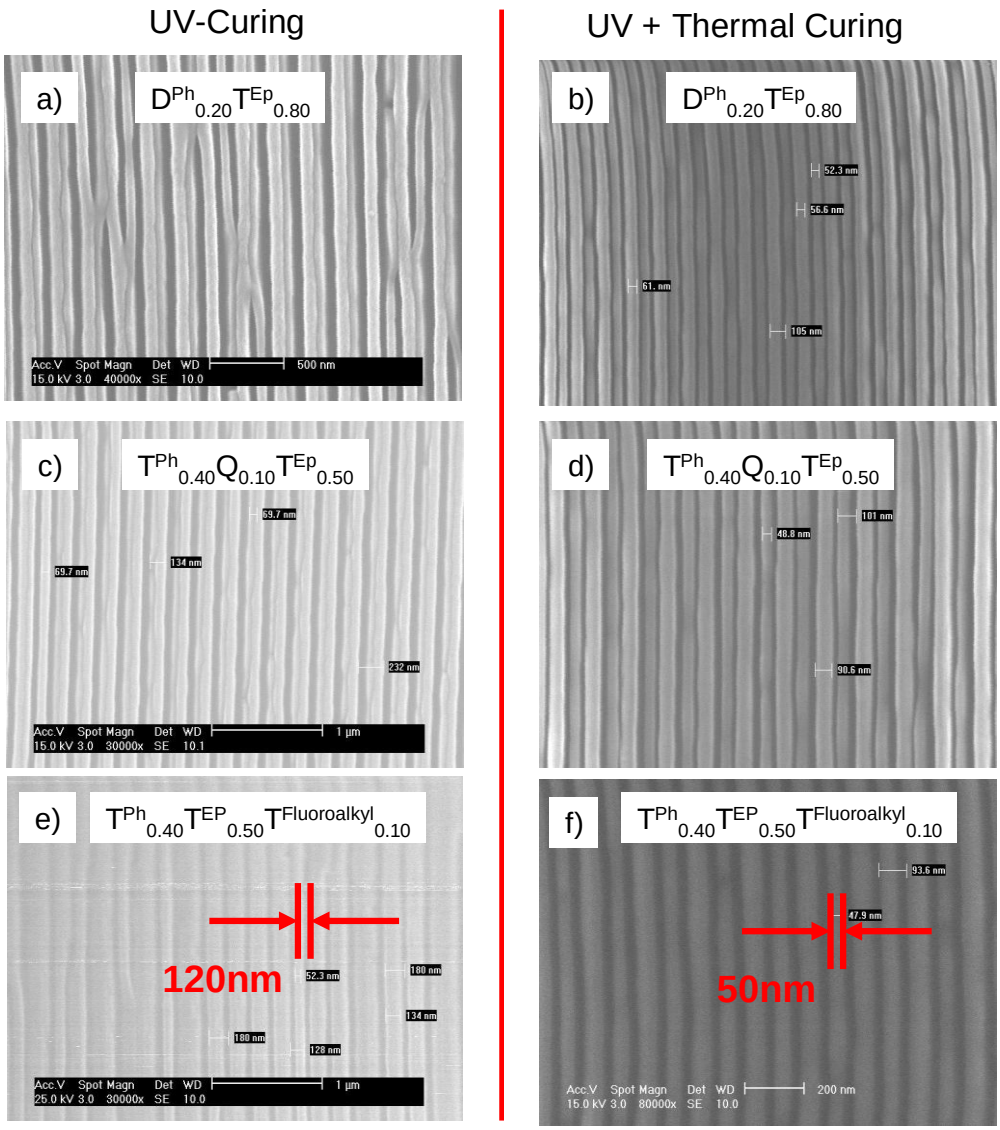

Figure 3.16 SEM pictures of gratings imprinted with silicone resins materials by UV-curing and UV + heat curing with a 100nm grating mold; (a and b) $T^{Ph}_{0.20}T^{Ep}_{0.80}$, (c and d) $T^{Ph}_{0.40}Q_{0.10}T^{Ep}_{0.50}$ and (e and f) $T^{Ph}_{0.40}T^{Ep}_{0.50}T^{Fluoroalkyl}_{0.10}$ (some distortion of the structures can be seen in the SEM pictures which is caused by the SEM e-beam).

3.7 Conclusions

In summary, several types of silicone copolymers with different molar ratios of D, T and Q units were synthesized. They also contained different substituent groups such as methyl and phenyl. It was found that the material with phenyl substituent presented better results than the material with methyl groups. In addition, the resins containing Q and/or T units showed better capabilities for nanoscale patterning than the materials containing D units.

Furthermore, a modified UV + thermal imprinting which takes advantage of the uncured epoxy groups was developed. This process showed greater resolution than the regular UV-imprinting process.

References

[1] Scott, D. W. *J. Am. Chem. Soc.* **1946**, *3*, 356-358.

[2] Baney, R. H.; Itoh, M.; Sakakibara, A.; Suzuki, T. *Chem. Rev.* **1995**, *5*, 1409-1430.

[3] Lu, T. L.; Liang, G. Z.; Kou, K. C.; Guo, Z. A. *J. Mater. Sci.* **2005**, *18*, 4721-4726.

[4] Li, G. Z.; Wang, L. C.; Ni, H. L.; Pittman, C. U. *J. Inorg. Organomet. Polym.* **2001**, *3*, 123-154.

[5] Simpson, T. R. E.; Parbhoo, B.; Keddie, J. L. *Polymer* **2003**, *17*, 4829-4838.

Chapter 4

A versatile photocurable silsesquioxane system for high resolution nanopatterning

4.1. Introduction

In nanoimprint Lithography (NIL) a resist material, e.g. a thermoplastic polymer, is placed in contact with a mold and then mechanically deformed under an applied load to transfer the nanofeatures on the mold surface into the resist (Figure 4.1).[1,2] A key factor for the success of NIL as a nanofabrication technology is the development of advanced materials suitable as the nanoimprint resist.[3]

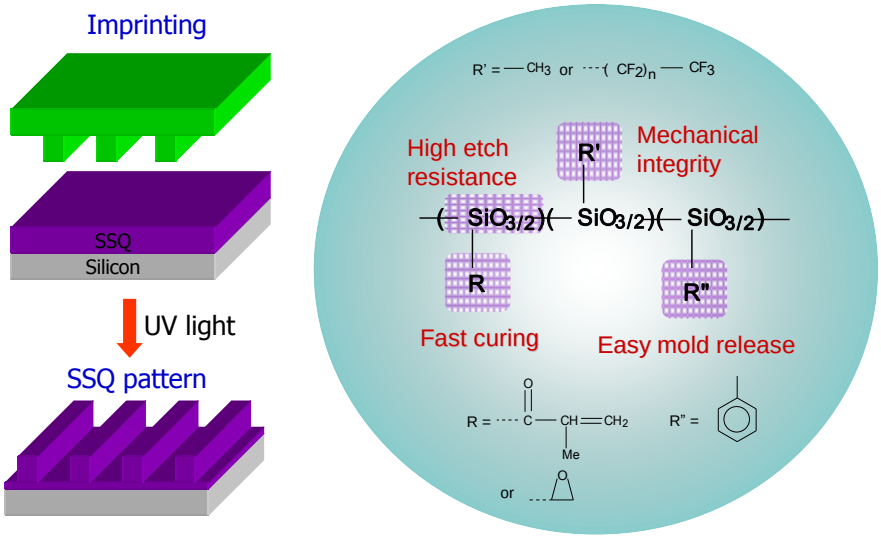

Figure 4.1 (left) Schematics of the NIL process, (right) representative chemical structure of SSQ resins.

Thermoplastic polymers were initially employed as resist layers for NIL. Unfortunately, high pressures and temperatures are required to successfully imprint such materials which besides significantly increasing the processing time can easily damage the expensive SiO_2 mold.[4]

However, for achieving the high throughput required in real industrial operations for high volume production, an imprinting process with no thermal cycles is preferred. For such reason, photocuring materials which can be imprinted at room temperature have been employed in nanopatterning technologies such as in Step and Flash Imprint Lithography, SFIL. In such process, the imprinting pressure is normally very low so the resist has to be a very low viscosity liquid. Therefore, small molecular precursors are used in resist formulation to ensure the low viscosity.[5,6] However there are some drawbacks of using small molecules for nanoimprinting. First the resist shrinkage is very large (~15%) upon curing, which can impact the dimensionality of the replicated patterns. Second, the material may not completely crosslink. E.g. if 90% of the precursor is cured, the remaining 10% monomers, being small molecules, could become a significant outgassing source, creating issues for process integration. Third, such liquid resist is not suitable for spincoating because the film easily dewets due to its low viscosity. Finally, the low molecular weight of commonly used components causes its fast evaporation leading to inhomogeneities in pattern replication.

A resist material that not only presents excellent imprinting capabilities but also shows a high versatility in its chemical design for a range of functionalities and applications is highly desired. Among several types of polymeric systems, silsesquioxanes (SSQ's) materials with a three dimensional organic-inorganic network

structure that combine many desirable properties of conventional organic and inorganic components, provide an exemplary core system for developing versatile functional resist materials.[7] In fact, due to their unique properties, silsesquioxanes have been widely used in applications such as low dielectric constant (k) interlayer materials, photonic waveguide and device materials, protective and insulating coating, to name an important few.

We present the developed photo curable silsesquioxane (SSQ)-based material systems that offer exceptional properties for a range of NIL applications. SSQ's possess several properties desirable for NIL: the flexible siloxane bonds lead to a lower surface energy desirable for demolding process; their high silicon content impart them with a great etch resistance in the pattern transfer process. In addition, many of the electric, optical, and mechanical properties of these SSQ resins can be easily and efficiently tailored according to the specific requirement. For instance, a variety of functional groups can be used such that the resists can be crosslinked via a photo-initiated free radical or cationic polymerization process. Such photo-curable groups can be added to the SSQ backbone to allow the resins to be photochemically solidified within seconds under ambient conditions. Meanwhile, the presence of adhesion and release groups ensures the adequate adhesion of the NIL resist to the substrate and an easy mold release so that the imprinted patterns adhere to the substrate rather than to the mold. This dual function is achieved through molecular design, where the low surface energy group, such as methyl, or fluroalkyl eases the mold releasing process and the high surface energy groups, such as silanol, enhance adhesion to the substrate. Moreover, the presence of phenyl groups enhances the resist material toughness to achieve a high resolution nanopatterning. A

representative multi-functional SSQ structure is shown in figure 4.1, wherein R can be a photocurable organic group and R' and R" can be methyl, fluroalkyl or phenyl. Furthermore, the relatively high molecular weight of the SSQ resin prevents the outgassing issues encountered frequently with low molecular weight silanes and silyl-grafted organic polymers. This is a very attractive feature for achieving high yield in nanolithography for Si chip fabrication.

In addition, the appropriate molecular weight of the engineered SSQ's also allows the formation of highly stable thin films with a good wetting behavior. On the other hand, the viscosity of these SSQ prepolymers, compared to that of heated thermoplastic polymers, is still very low and successful patterning of SSQ resist can be achieved under low pressure (~50psi) conditions.

A range of silsesquioxane resins with different chemical functionalities were synthesized through a hydrolytic condensation of trialkoysilanes ($XSiY_3$). The resins were produced with variable molar ratios of the corresponding silanes. In such manner, it was possible to examine the influence of the substituent group content in the uncured prepolymer as well as on the final crosslinked material.

4.2. Results

SSQ's containing either methyl or phenyl groups were chosen due to their well known superior thermal stability in comparison with other types of moieties such as propyl, butyl, etc. The modulus of such materials was measured with nanoindentation and values larger than 0.5 GPa (figure 4.2) were observed. Several studies have shown that a material with a large modulus is needed to avoid the collapsing of replicated

nanostructures.[8-10] Furthermore, a value close to 0.1GPa is preferred to achieve a good pattern definition and obtain lines with sharp edges.[11] SEM's of 700nm patterns replicated on SSQ resins are shown in figure 4.2.

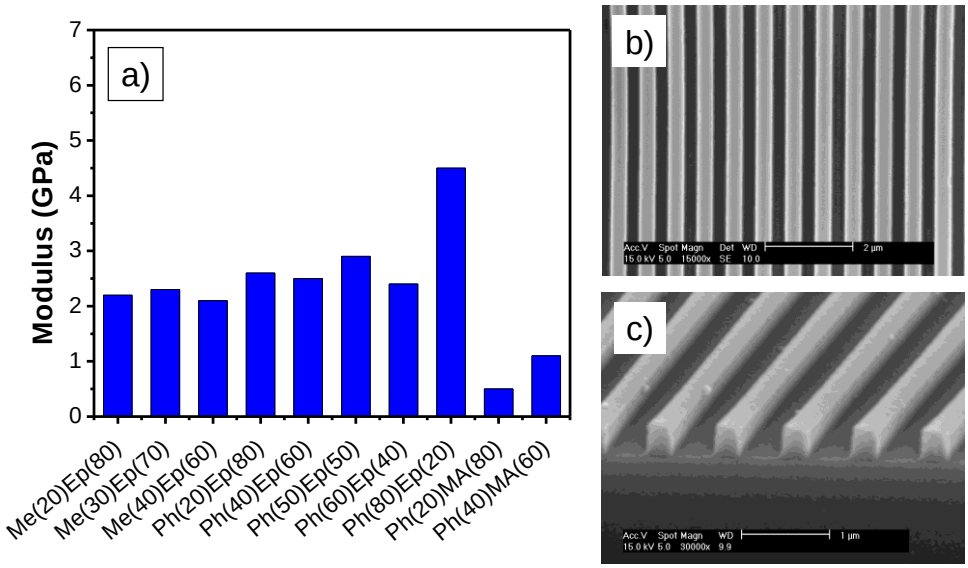

Figure 4.2 (a) Modulus of the UV cured SSQ resins measured by nanoindentation and 700nm grating pattern imprinted in (b) $T_{Me}T_{Ep}$ and (c) $T_{Phe}T_{Ep}$.

Ideally, the shrinking caused by the UV light exposure during the curing process should be minimal to assure an accurate replication of the nanoscale features. As presented in Figure 4.3, the degree of shrinking measured for the SSQ prepolymers was especially low in case of the epoxy based silsesquioxanes (<6%). The low shrinkage found in these epoxy materials is attributed to the conversion of the rigid oxirane ring into a more flexible open-chain segment in the cured material. .

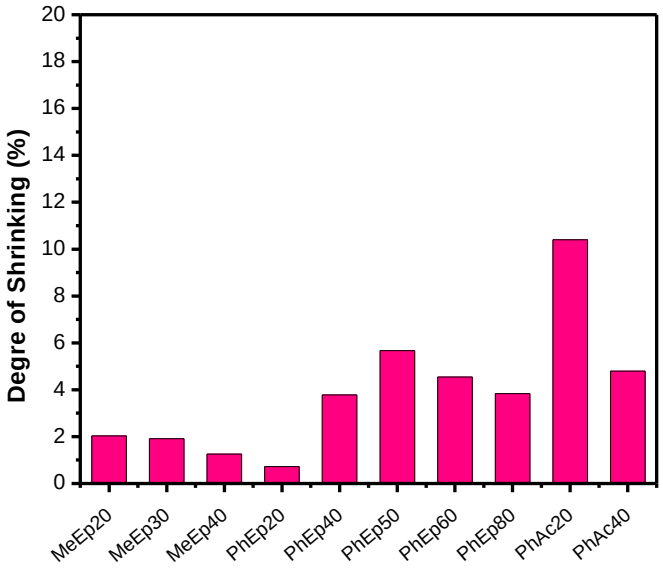

Figure 4.3 Degree of shrinking of the SSQ materials due to UV curing.

According to the equation below, the throughput of the imprinting process depends on the pressure and viscosity of the polymeric precursor. [12]

$$t_f = \frac{\eta_0 s^2}{2p}\left(\frac{1}{h_f^{\,2}} - \frac{1}{h_0^{\,2}}\right)$$

In this equation t_f is the imprinting time, p is the imprinting pressure, η_0 is the viscosity of the resist, h_0 and h_f are the initial and the final resist thickness, respectively, and s is the distance the resist flows. A low viscosity is required to achieve the filling of the mold cavities within few seconds by using low pressure. The low viscosity of UV curable precursors is an advantage over the more viscous thermoplastic polymers such as PMMA (a commonly imprinted thermoplastic) which has a reported viscosity of 4.6 x

10^9Pa.s. (molecular weight of $1.1x10^5$ g mol^{-1}). The time to imprint this material is about 5 min by using 100 bar.[13]

In contrast, 230 Pa.s was the highest viscosity we measured for one of our synthesized SSQ materials ($T^{Ph}_{0.50}T^{Ep}_{0.50}$ or PhEp50), a much lower value than regular thermoplastic polymers at high temperatures (Figure 4.4). Only few seconds and low pressure (50psi) are sufficient to imprint this resin. In addition, a viscosity as low as 1.3 Pa.s was measured for the MeEp30 ($T^{Me}_{0.30}T^{Ep}_{0.70}$) resin. It was also found that the presence of bulky phenyl substituent increased the viscosity of the uncured resin. Finally, the epoxy moiety apparently plays a role in a higher viscosity of the prepolymer. In contrast, the acrylate resins show a lower viscosity.

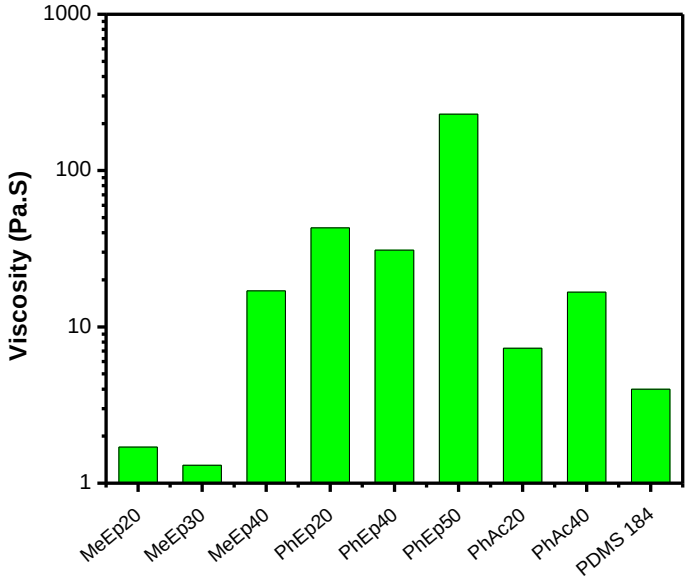

Figure 4.4 Viscosity of SSQ resins.

Imprinted nanoscale structures are exposed to high mechanical stresses during the mold releasing process. These demolding stresses can lead to the breakage or to the deformation of the structures if the resist does not display the appropriate tensile strength. An advantage of silsesquioxane materials is that its chemical structure can be modified to obtain a material with the necessary tensile strength to withstand such high detrimental stresses. SSQ's with either phenyl or methyl groups were synthesized in order to test to the patterns due to mold release.

SSQ's containing methyl groups T(Me)T(Epoxy) displayed appropriate properties for sub-micron size replication. However, when smaller nanosize structures (220nm period) were imprinted with this material, the structures tended to deform and lateral collapsing can be seen as shown in figure 4.5(a). On the other hand, better results (figure 4.5b) were obtained with the silsesquioxane containing phenyl substituents T(Ph)T(Epoxy) as can be seen in figure 4.5b. The phenyl groups are well known for providing an enhanced tensile strength and superior toughness.[14]

Other than methyl or phenyl groups, the developed SSQ's also contain photocurable functionalities, either methacrylate or epoxy, that solidify the initially liquid-like resist by UV exposure to stabilize the imprinted patterns upon demolding.. The correct molar ratio of phenyl's to such crosslinking moieties must be selected to achieve the best desirable mechanical properties. Too high an amount of photocurable groups can lead to a material with poor mechanical properties (high brittleness) for nanoimprinting. For instance, the structures replicated with the SSQ, $T^{Ph}_{0.20}T^{Ep}_{0.80}$, which contains a high amount of epoxy groups can be easily broken during the releasing process generating patterns with a high density defects, as displayed in fig. 4.5c, which is due to

the breakage of the imprinted lines during the demolding step. On the other hand, reducing the number of crosslinking sites, in this case the epoxy groups, and increasing the amount of phenyls significantly diminishes the breaking of the imprinted structures (Figure 4.5d). In general, it was found that a resin synthesized with a molar ratio of a silane containing phenyl groups close to 0.40-0.50 and a molar ratio of a silane containing crosslinking fucntionalities similar to 0.50-0.60 produces the best resist for NIL.

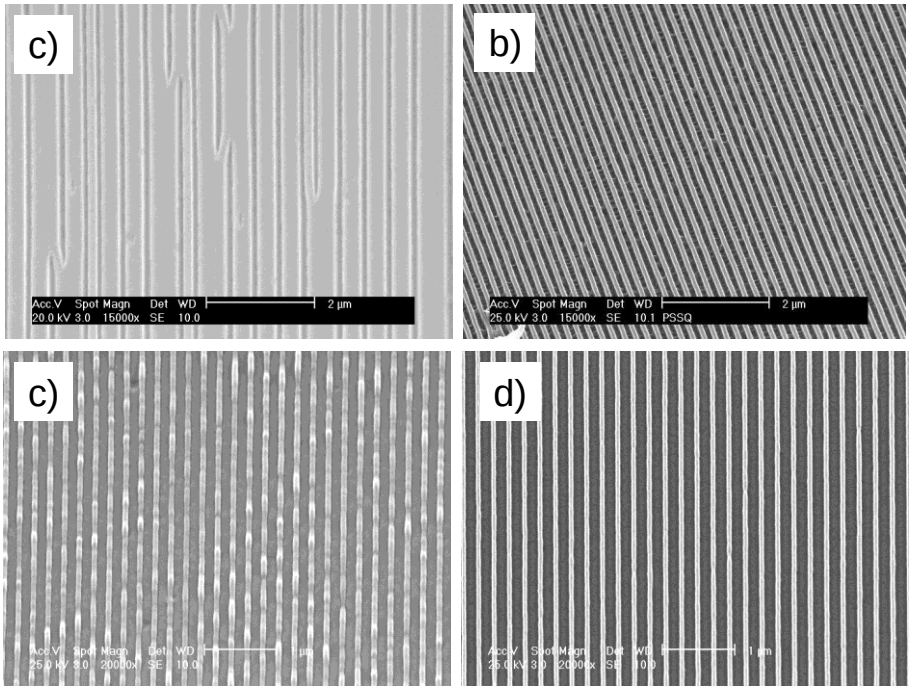

Figure 4.5 220nm period pattern imprinted with (a) T(Me)T(Epoxy) and (b) T(Ph)T(Epoxy). 60 nm line width patterns replicated using SSQ's with (c) high ($T^{Ph}_{0.20}T^{Ep}_{0.80}$) and (d) low ($T^{Ph}_{0.50}T^{Ep}_{0.50}$) ratio of epoxy groups.

The photocurable groups, besides providing crosslinking to produce the mechanical integrity needed for the replication process, can also improve the adhesion between the resist and the substrate, if the later is surface-functionalized with chemically compatible groups. For instance, the substrate surface can be functionalized with an

epoxy based silane when an epoxy-based SSQ is used. In this fashion, the chemical reactive groups from the substrate and the resist react during the crosslinking step leading to a strong resist-substrate adhesion, and hence improved pattern yield.

Another important challenge in nanoimprinting processes is the high adhesion of the resist to the mold during the releasing process, which plays a significant role in the quality and the yield of the imprinted patterns. This issue is normally overcome by treating the SiO_2 mold with perfluorinated monolayers to reduce its surface energy and produce defect free patterns through an easier mold-resist separation.[15] In addition, fluorinated polymeric molds have also been used for such purposes. [16-21]However, as the pattern feature sizes shrink to the nanoscale regime, the contact area between the mold and resist increases dramatically leading to a much stronger mold-resist adhesion.

An effective approach to facilitate mold separation is to reduce the surface energy of the resist. A high surface energy resist generates defects on the imprinted pattern due its strong adhesion to the mold. On the other hand, if the surface energy is too small, the adhesion of the resist to the mold is low too but the sticking of the resist to the substrate is also weak. This will lead to the undesired effect of the resist sticking to the mold during the releasing process.

Perfluoroalkyl substituent's which are well known for providing low surface energy due to the presence of CF_3 groups were used to modify our developed silsesquioxane resists. With this strategy, a material with a lower surface energy for an easy mold release was engineered for applications requiring high yield and high resolution nanopatterning.

In fact, it was found that the presence of perfluoroalkyl's leads to a low adhesion of the resist to the mold. However, as expected and mentioned above, these groups also reduced the adhesion of the SSQ to the substrate, leading to bad imprinting performance. A solution to this problem was to use a "coupling" layer of another type of SSQ to enhance the bonding between the perfluorinated resist and the substrate as previously shown.[22] Such coupling layer contains a high amount of photoreactive groups which chemically react with the photocurable moities present in the fluorinated resist improving the bonding of the resist to the substrate. This coupling layer was especially useful when replicating large areas of very small gratings such as the 220nm period on 4" wafer shown in figure 4.6(a) and (b) as well as the highly dense 20nm structures shown in figure 4.6c using the fluorinated SSQ resist.

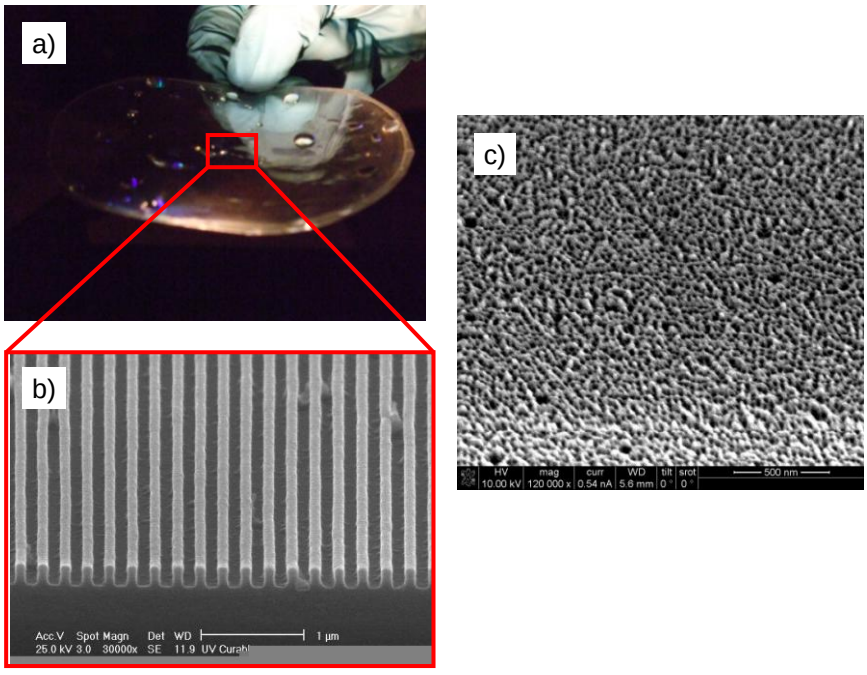

Figure 4.6 (a) Fluorinated SSQ patterned on top of a flexible PET substrate using a 4in SiO_2 hard master (b) SEM picture from the 4in pattern (e) 20nm pore structures pattern on a fluorinated SSQ.

The results shown here were achieved using either flexible fluorinated stamps (ETFE and SSQ)-hard substrate or flexible substrates (PET)–hard molds systems where the demolding is performed through a peeling-off process. The flexibility of the mold (or substrate) itself allows an easy peeling from the mold. However, the same results can not be achieved when using a hard mold–hard substrate system due to the lack of flexibility, which normally presents a more challenging demoulding process.

Besides the excellent performance shown by the developed SSQ's for high yield and high resolution nanopatterning, the high silicon content of these materials provides a great resistance to O_2 plasma etching. This property was exploited for metal line fabrication through lift-off processes using a double-resist layer approach. A 700nm SSQ grating pattern was imprinted on top of a 400nm thick PMMA layer (figure 4.7a). The SSQ pattern was etched with CHF_3 to remove the residual layer (figure 4.8b) followed by O_2 plasma to etch through the PMMA layer (figure 4.7c). Once the O_2 plasma etching was performed, a 70nm thick Cr film was deposited by thermal evaporation. Then, lift-off was done in acetone for 2 min to successfully generate metal lines with high yield as can be see in figure 4.7d.

In addition, this SSQ system not only shows outstanding imprinting capabilities, but can also be employed as an etch mask directly to fabricate silicon structures with high aspect ratio. As can be seen in figure 4.8, imprinted SSQ ($T^{Ph}_{0.40}T^{Methacryloxy}_{0.60}$) patterns (figure 4.8a) were etched with CHF_3 (Figure 4.8b) to remove the residual layer. This was followed by HBr plasma (figure 4.8c) to directly transfer the structures into a silicon substrate. Selectivity's more than 2:1 were easily achieved with this HBr chemistry.

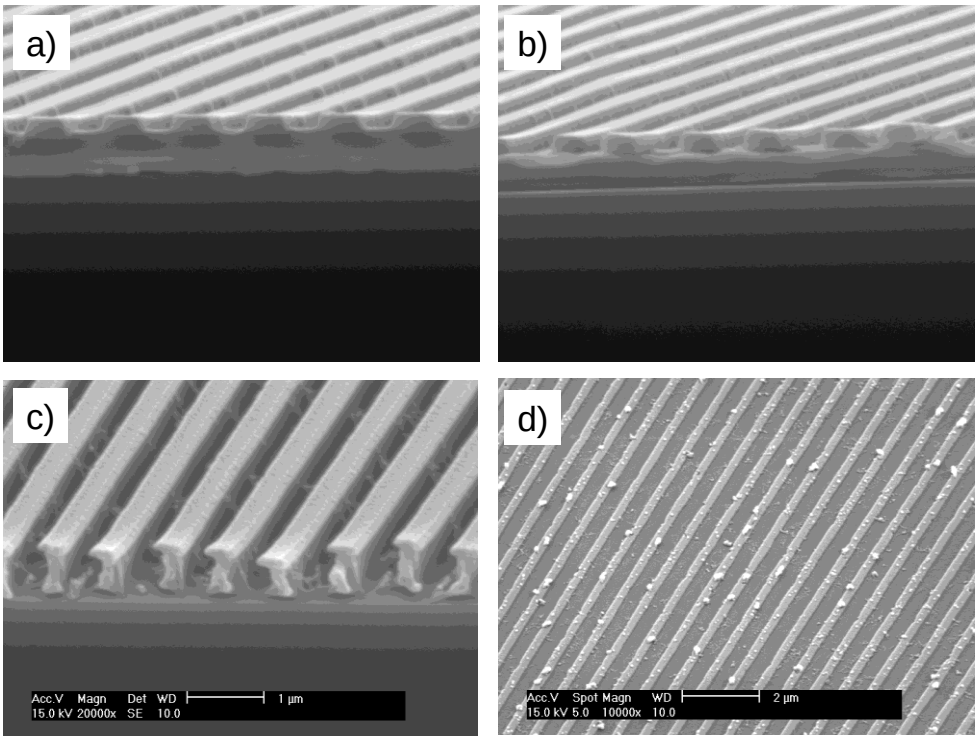

Figure 4.7 (a) SSQ pattern on top of a PMMA layer, (b) SSQ pattern after residual layer was removed with CHF_3 and (c) pattern after PMMA layer etched with O_2 plasma for undercutting (d) Cr lines.

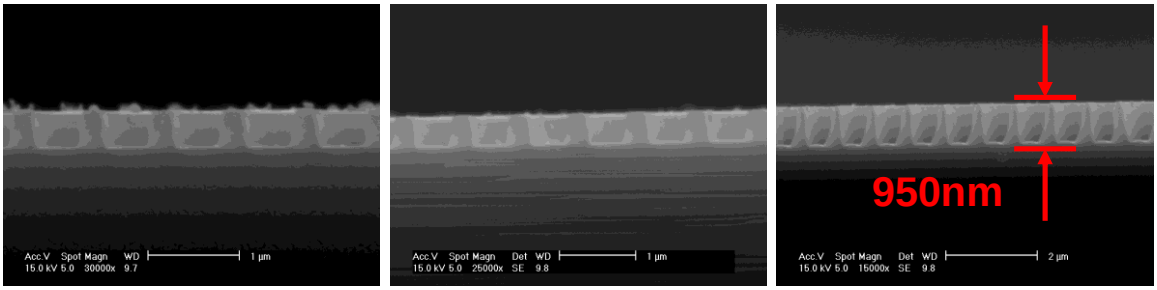

Figure 4.8 (a) 700nm period 350nm height original SSQ pattern, (b) SSQ pattern after residual layer was removed with CHF_3 and (c) 950 nm tall silicon structures etched with HBr.

4.3. Conclusions

A Silsesquioxane resist system with excellent impriting capabilities was sythesized. The appropriate viscosity of the uncured material allows the formation of stable thin films and the easy replication of structures as small as 20nm using low pressure nanoimprinting. An easy mold releasing was achieved due to the low surface

energy material synthesized with fluorofunctionality as well as the outstanding mechanical properties. Finally, the high silicon content of the SSQ material provides high resistance to O_2 plasma etching. The material can be easily etched and due to its high silicon content.

References

[1] CHOU, S. Y.; KRAUSS, P. R.; RENSTROM, P. J. *Appl. Phys. Lett.* **1995**, *21*, 3114-3116.

[2] Chou, S. Y.; Krauss, P. R.; Renstrom, P. J. *Science* **1996**, *5258*, 85-87.

[3] Nie, Z.; Kumacheva, E. *Nat. Mater.* **2008**, *4*, 277-290.

[4] Guo, L. J. *Adv Mater* **2007**, *4*, 495-513.

[5] Kim, E. K.; Stacey, N. A.; Smith, B. J.; Dickey, M. D.; Johnson, S. C.; Trinque, B. C.; Willson, C. G. In *In Vinyl ethers in ultraviolet curable formulations for step and flash imprint lithography;* Journal of Vacuum Science & Technology B; 47th International Conference on Electron Ion and Photon Beam Technology and Nanofabrication; A V S AMER INST PHYSICS: MELVILLE; STE 1 NO 1, 2 HUNTINGTON QUADRANGLE, MELVILLE, NY 11747-4502 USA, 2004; Vol. 22, pp 131-135.

[6] Kim, E. K.; Stewart, M. D.; Wu, K.; Palmieri, F. L.; Dickey, M. D.; Ekerdt, J. G.; Willson, C. G. In *In Vinyl ether formulations for step and flash imprint lithography;* Journal of Vacuum Science & Technology B; 49th International Conference on Electron, Ion, and Photon Beam Technology and Nanofabrication; A V S AMER INST PHYSICS:

MELVILLE; STE 1 NO 1, 2 HUNTINGTON QUADRANGLE, MELVILLE, NY 11747-4502 USA, 2005; Vol. 23, pp 2967-2971.

[7] Baney, R. H.; Itoh, M.; Sakakibara, A.; Suzuki, T. *Chem. Rev.* **1995**, *5,* 1409-1430.

[8] Hui, C. Y.; Jagota, A.; Lin, Y. Y.; Kramer, E. J. *Langmuir* **2002**, *18,* 1394-1407.

[9] Schmid, H.; Michel, B. *Macromolecules* **2000**, *8,* 3042-3049.

[10] Pina-Hernandez, C.; Kim, J. S.; Guo, L. J.; Fu, P. F. *Adv. Mater.* **2007**, *9,* 1222.

[11] Hagberg, E. C.; Malkoch, M.; Ling, Y.; Hawker, C. J.; Carter, K. R. *Nano Lett.* **2007**, *2,* 233-237.

[12] L. Malaquin, C. V. *Alternative Lithography;* 2003; , pp 169.

[13] Malaquin, L.; Carcenac, F.; Vieu, C.; Mauzac, M. *Microelectronic Engineering* **2002**, 379-384.

[14] Schmidt,H. Rinn,G. Nass, R. Sporn,D. *Better Ceramics Through Chemistry;* C. J. Brinker, D. E. Clark, D. R. Ulrich, Ed.; Materials Research Society: Pittsburgh, PA, 1988; pp 743.

[15] Bailey, T.; Choi, B. J.; Colburn, M.; Meissl, M.; Shaya, S.; Ekerdt, J. G.; Sreenivasan, S. V.; Willson, C. G. In *In Step and flash imprint lithography: Template surface treatment and defect analysis;* Journal of Vacuum Science & Technology B; 44th International Conference on Electron Ion and Photon Beam Technology and Nanofabrication (EIPBN); AMER INST PHYSICS: MELVILLE; 2 HUNTINGTON QUADRANGLE, STE 1NO1, MELVILLE, NY 11747-4501 USA, 2000; Vol. 18, pp 3572-3577.

[16] Rolland, J. P.; Van Dam, R. M.; Schorzman, D. A.; Quake, S. R.; DeSimone, J. M. *J. Am. Chem. Soc.* **2004**, *26,* 8349-8349.

[17] Rolland, J. P.; Hagberg, E. C.; Denison, G. M.; Carter, K. R.; De Simone, J. M. *Angewandte Chemie-International Edition* **2004**, *43*, 5796-5799.

[18] Khang, D. Y.; Lee, H. H. *Langmuir* **2004**, *6*, 2445-2448.

[19] Choi, D. G.; Jeong, J. H.; Sim, Y. S.; Lee, E. S.; Kim, W. S.; Bae, B. S. *Langmuir* **2005**, *21*, 9390-9392.

[20] Barbero, D. R.; Saifullah, M. S. M.; Hoffmann, P.; Mathieu, H. J.; Anderson, D.; Jones, G. A. C.; Welland, M. E.; Steiner, U. *Advanced Functional Materials* **2007**, *14*, 2419-2425.

[21] Truong, T. T.; Lin, R. S.; Jeon, S.; Lee, H. H.; Maria, J.; Gaur, A.; Hua, F.; Meinel, I.; Rogers, J. A. *Langmuir* **2007**, *5*, 2898-2905.

[22] Pina-Hernandez, C.; Fu, P.; Guo, L. J. In *In Easy duplication of stamps using UV-cured fluoro-silsesquioxane for nanoimprint lithography;* Journal of Vacuum Science & Technology B; 52nd International Conference on Electron, Ion and Photon Beam Technology and Nanofabrication; A V S AMER INST PHYSICS: MELVILLE; STE 1 NO 1, 2 HUNTINGTON QUADRANGLE, MELVILLE, NY 11747-4502 USA, 2008; Vol. 26, pp 2426-2429.

Chapter 5

Stamps Fabrication using UV-cured Fluoro-Silsesquioxane for Nanoimprint Lithography

5.1 Introduction

An important challenge in NIL for mass manufacturing is the fabrication of molds (also denoted as stamps throughout this text) for high-yield nanoscale replication. The fabrication of SiO_2 molds is a costly and time consuming process. In addition, SiO_2 is a brittle material and so the protruding nanostructures on an SiO_2 mold can be easily broken. Furthermore, due to its high rigidity, an SiO_2 mold cannot be used in applications where high flexibility is required such as roll to roll nanoimprint lithography.[1]

The fabrication of an SiO_2 mold is typically done by a combination of NIL and dry etching processes. An alternative to the SiO_2 is the use of more flexible, cheaper, and easier to process polymeric materials. Intermediate stamps have been previously fabricated by employing low surface energy polymers based on polysiloxanes as well as fluoropolymers by simple embossing or imprinting processes with original SiO_2 masters.[2-6] The low surface energy of such polymers not only eliminates the step of coating an anti-sticking layer on the stamp but also leads to a clean separation of the

master during the mold fabrication.

Poly(dimethysiloxane) (PDMS), a thermoset elastomer, has been widely employed as a stamp for microcontact printing. But the pattern fidelity of PDMS stamps is significantly affected after exposure to organic solvents. Perfluoropolyether (PFPE) based fluoropolymers[2,3,6] were developed to overcome the limitations of PDMS materials. However, PFPE's low modulus is insufficient for the nanoscale replication of high aspect ratio structures. Other fluoropolymers such as Teflon, Dupont AF 2400[4] and ethylene(tetrafluroethylene) (ETFE)[5,7] have also been used as stamps for nanoimprinting. Although they possess low surface energy for easy mold release, high temperatures and pressures are required for their replication from the original master. The very different coefficients of thermal expansion between such polymers and the original SiO_2 master make it difficult to maintain the critical dimension and lead to possible damage to the original master due to excessive thermal stress. In addition, an ETFE mold is not suitable for high temperature NIL applications due to a significant decrease in its modulus above 100°C. Nanoscale patterning has also been achieved with stamps fabricated using sol-gel materials.[8] A disadvantage of the sol-gel process is the difficulty in achieving accurate control and reproducibility of the final chemical structure and material properties.

Recently, silsesquioxane (SSQ) polymers have been used as functional resists due to their low-k properties.[9-12] They have been directly patterned as dielectric materials. In addition, we have also shown that silsesquioxanes, more specifically fluoro-SSQ's [T(Ph)T(Fluoroalkyl)T(Methacryloxy)] possess outstanding properties for applications as nanoimprint resist for nanoscale patterning.[13] A medium viscosity silsesquioxane resin could be easily imprinted and solidified by a brief UV-light exposure. The excellent

mechanical properties (high modulus, toughness) and the low surface energy characteristics of the engineered fluoro-SSQ resins make them a suitable material for NIL stamps. In addition the mechanical properties of SSQ materials can be tailored to achieve high stiffness.

Here, we present the use of fluoro-SSQ materials for simple duplication of SiO_2 masters for nanoimprint lithography. These SSQ-based intermediate stamps replicated from the original master may find applications in high volume production processes using NIL, such as in bit-patterned magnetic disk manufacturing and roll to roll nanoimprint lithography. The low surface energy and the flexibility of the fluoro-SSQ materials allow an easy replication from the master with faithful pattern transfer at room-temperature and with low pressure. A multitude of flexible fluoro-SSQ molds can be easily duplicated from an original SiO_2 master, which helps to maintain an overall low defect density in the NIL process, while preserving the original mold in its pristine state for high volume production.

5.2 Experimental procedure

The silsesquioxane (SSQ) prepolymers used in this study were synthesized through hydrolytic condensation of trialkoxysilanes, $XSiY_3$. Fluoro-SSQ resin is a modification of the phenyl-SSQ or T(Ph)T(Epoxy) NIL resist[11] (structure shown in Fig. 5.1a) by adding the fluoro-functionality. The chemical structure of the synthesized fluoro-SSQ is shown in Figure 5.1b. The function of the various chemical groups in the resin is as follows: the fluoroalkyl group imparts the low surface energy for the fluoro-SSQ; the phenyl groups help to toughen the material; and the methacrylic moieties

harden the initially viscous liquid into a solid material by UV photocuring. To synthesize fluoro-SSQ, 3-(trimethoxysilyl)propyl methacrylate (MPTMS), phenyltrimethoxysilane (PTMS), and trimethoxy(3,3,4,4,5,5,6,6,7,7,8,8,8-tridecafluoro-1-octyl)silane were added to a mixture of solvents at a high temperature under a basic catalyst.

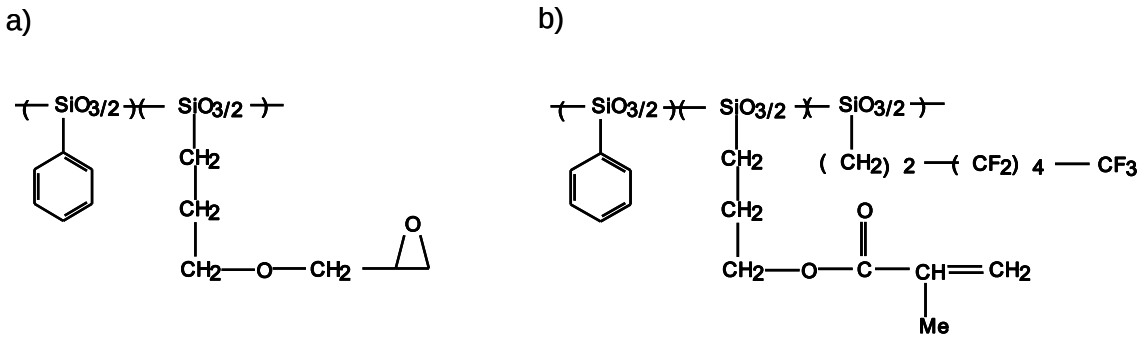

Figure 5.1 Chemical structure of (a) T(Ph)T(Epoxy) resins and (b) fluoro-SSQ resin.

To provide a good mechanical support when making the fluoro-SSQ mold, the fluoro-SSQ prepolymer is applied on either a rigid or a flexible substrate such as glass or polyethylene terephtalate (PET) respectively. But direct application of fluoro-SSQ to such substrates is not possible because fluoro-SSQ's have low surface energy and therefore have poor adhesion to these substrates and tend to stick to SiO_2 masters during the stamp fabrication process. In order to achieve good adhesion between the substrate and the fluoro-SSQ material and ease the separation of this material from the master during the releasing process, an intermediate layer of silsesquioxane materials was employed (Figure 5.2) to fabricate the fluoro-SSQ stamp. This intermediate layer is a higher surface energy T(Ph)T(Epoxy) precursor with methacrylate functionality that acts as an adhesive layer between the fluoro-SSQ and the substrate.

A flexible PET substrate was first treated with O_2 plasma and surface functionalized with a self-assembled monolayer of methacrylate-silane that acts as an adhesion promoter between the substrate and the SSQ prepolymers. The silanization of PET was performed at 70°C for 30min. Next, a 4% T(Ph)T(Methacryloxy) solution in PGMEA was spin coated on top of the surface treated PET substrate to form the intermediate adhesive layer. This layer was pre-cured with UV-light for 20 sec under an air atmosphere. Following this, a 20% fluoro-SSQ solution in PGMEA was spun on top of the adhesive layer to form an active layer for mold replication that has a good release property.

To fabricate a fluoro-SSQ mold, an original SiO_2 master (coated with a fluorosilane monolayer) was placed on top of the fluoro-SSQ layer (Fig. 5.2g) with slight pressure, and UV light was irradiated through the transparent glass or PET substrate for 60sec to cure the fluoro-SSQ. The UV curing was done under a nitrogen atmosphere to avoid oxygen inhibition of the free radical crosslinking. After UV curing, the SiO_2 master was released and the patterns were duplicated in the flexible fluoro-SSQ stamp. Finally, the replicated stamp was exposed to a fluorosilane vapor at 70°C for 50min. The function of this step is to use the fluorosilane molecules to condensate the highly reactive residual silanol groups in the SSQ resin, which would otherwise increase the adhesion with resist during the NIL process.

The fluoro-SSQ stamp was used to imprint PDMS materials[14] and T(Ph)T(Epoxy) (chemical structure shown in Figure 5.1a) through thermal and photocuring processes respectively. For thermal nanoimprinting, a PDMS resist was poured on top of a Si substrate and covered with the fluoro-SSQ stamp. This system was heated at 70°C for 5

min to achieve thermal-curing of the PDMS material. To imprint the T(Ph)T(Epoxy) resin, a 20% solution of T(Ph)T(Epoxy) in PGMEA solvent was spun on top of a silicon substrate. Then, the flexible fluoro-SSQ mold was placed on top, followed by UV exposure for 60sec.

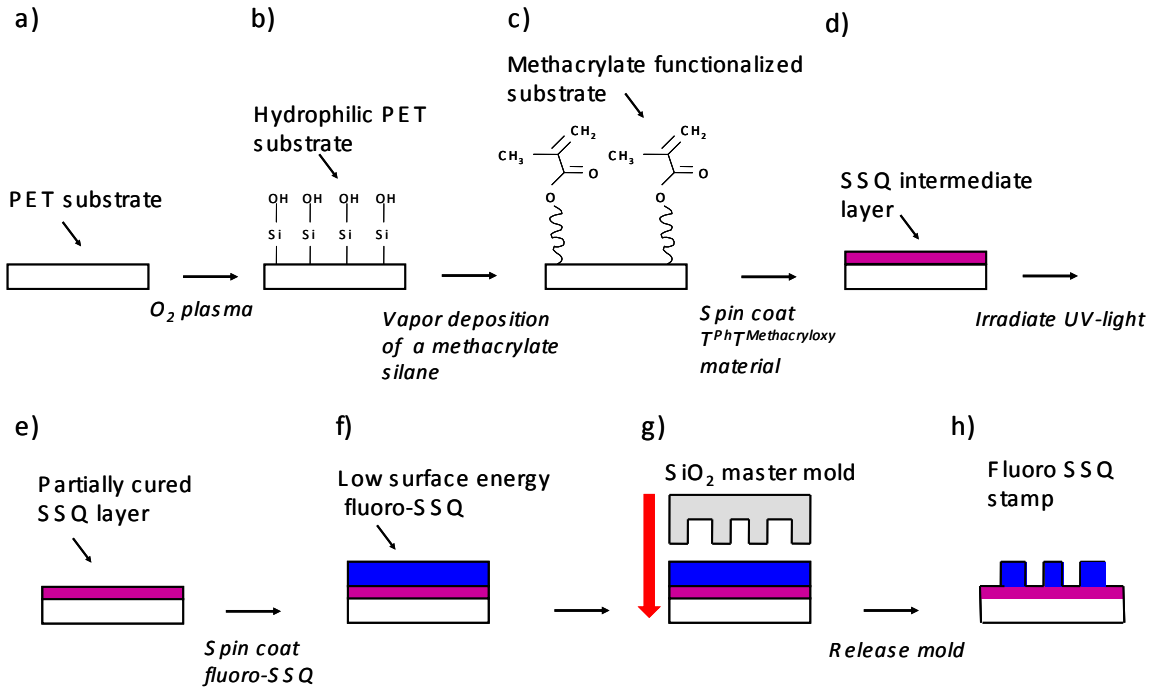

Figure 5.2 Process flow to improve the adhesion between the PET substrate and the fluoro-SSQ material for the fluoro-SSQ stamp fabrication.

5.3 Results

The low surface energy (water contact angle of 108°) of the synthesized fluoro-SSQ resin prevents a sufficient adhesion to the supporting substrates. As described earlier, a monolayer of methacrylate-functional silane and a T(Ph)T(Methacryloxy) intermediate layer was utilized to overcome this issue and to enhance the fluoro-SSQ-substrate adhesion. Similar to the fluoro-SSQ material and the surface treated substrate, the

T(Ph)T(Methacryloxy) intermediate layer contains chemically compatible methacrylate groups to form a strong and continuous covalent network between the supporting substrate and the top fluoro-SSQ layer.

5.3.1 Fluoro-SSQ stamp

The T(Ph)T(Methacryloxy) employed to fabricate the intermediate layer is of medium viscosity (few Pa.s) and should be pre-cured with UV light to achieve enough mechanical integrity and avoid its removal while spin coating the fluoro-SSQ layer. Note that the intermediate layer should only be partially crosslinked during the pre-curing step to assure the presence of sufficient methacylate groups to form a strong network with the fluoro-SSQ layer during the subsequent curing step. As the modulus of the cured fluoro-SSQ material (~1GPa) is sufficient for the replication of nanoscale size structures, and the viscosity of the polymeric precursor is about a few Pa.s, it is expected that the NIL resolution of the new fluoro-SSQ stamp will depend on the feature size on the original master. SEM micrographs of the flexible fluoro-SSQ stamp can be seen in Figure 5.3. 700nm and 220 nm period patterns were easily replicated in fluoro-SSQ on top of a flexible PET substrate.

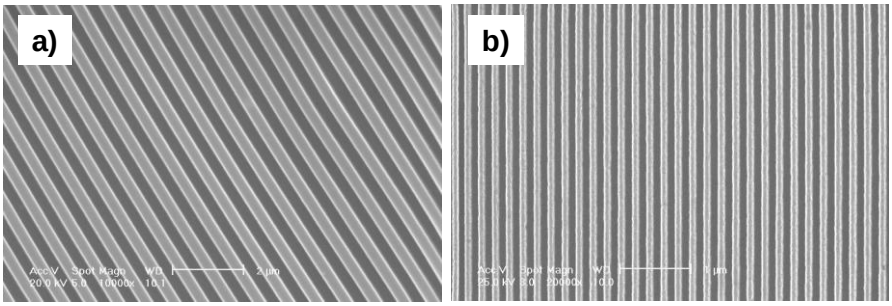

Figure 5.3 SEM pictures of (a) 700nm and (b) 220nm period patterns produced in fluoro-SSQ.

5.3.2 Nanoimprint by using fluoro-SSQ stamp

The SSQ resins contain residual silanol groups (-SiOH) during the synthesis procedure. The silanol groups remain present after the material is UV exposed. Silanol moieties can react with the resist material during the UV curing process, leading to a strong stamp-to-resist adhesion. Therefore an additional heat treatment step was used to remove the silanol groups. Once the flexible fluoro-SSQ stamp was fabricated, it was surface treated by reacting with a fluorosilane vapor at 70°C for 50min. During this surface treatment, the residual silanol groups in the stamp surface are eliminated through a condensation reaction with the fluorosilane molecules.

The surface properties of the fluoro-SSQ material, with a contact angle of 108°, are suitable for high resolution nanopatterning. As a comparison, the water contact angles of PDMS and fluorosilane treated silicon were 105° and 112°, respectively. The flexible fluoro-SSQ stamp was employed to imprint a PDMS resist and a T(Ph)T(Ep) resist. The mold achieved clean separation from the resists and the 700nm and 220nm period dense grating patterns were successfully imprinted in both materials (Figure 5.4). The feature critical dimensions change induced by the fluoro-SSQ stamp is around 5%, which is the percentage the synthesized SSQ materials shrink after UV exposure.

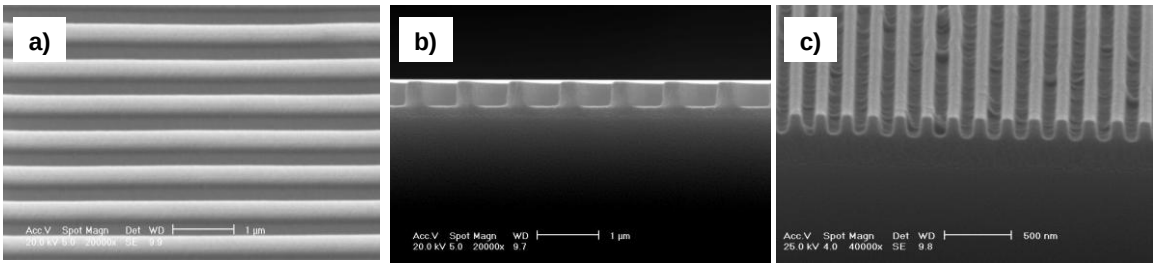

Figure 5.4 SEM pictures of resist patterns imprinted by using the fluoro-SSQ based stamp. (a) 700 nm pitch PDMS grating, (b) 700 nm and (c) 220nm pitch grating patterns in T(Ph)T(Ep) resin.

5.4 Conclusion

A low surface energy fluoro-SSQ on a flexible PET substrate was demonstrated to easily duplicate a NIL master. An intermediate chemically compatible layer was used to enhance the adhesion between the fluoro-SSQ material and the PET substrate. Fluoro-SSQ patterns can be easily replicated with a clean release from the master with a high yield. The fabricated fluoro-SSQ stamps are useful for a high volume nanoimprinting process.

References

[1] S. Ahn, L.J. Guo, *Adv. Mat.* **11**, 2044 (2008).

[2] J.P. Rolland, R.M. Van Dam, D.A. Schorzman, S.R. Quake, J.M DeSimone, J. Am. Chem. Soc. **26**, 8349 (2004).

[3] T.T. Truong, R.S. Lin, S. Jeon, H.H. Lee, J. Maria, A. Gaur, F. Hua, I. Meinel, J. A. Rogers, Langmuir **5**, 2898 (2007).

[4] D.Y. Khang, H.H. Lee, Langmuir **6**, 2445 (2004).

[5] D.R. Barbero, M.S.M. Saifullah, P. Hoffmann, H.J. Mathieu, D. Anderson, G.A.C. Jones, M.E. Welland, U. Steiner, Adv. Funct. Mat. **14**, 2419 (2007).

[6] J.P. Rolland, E.C. Hagberg, G.M. Denison, K.R. Carter, J.M. De Simone, Angewandte Chemie-International Edition **43**, 5796 (2004).

[7] L.J. Guo, Adv. Mater. **4**, 495 (2007).

[8] D.G. Choi, J.H. Jeong, Y.S. Sim, E.S. Lee, W.S. Kim, B.S. Bae, Langmuir **21**, 9390 (2005).

[9] S. Matsui, Y. Igaku, H. Ishigaki, J. Fujita, M. Ishida, Y. Ochiai, H. Namatsu, M. Komuro, J. Vac. Sci. Technol. B **2**, 688 (2003).

[10] G.M. Schmid, M.D. Stewart, J. Wetzel, F. Palmieri, J.J. Hao, Y. Nishimura, K. Jen, E.K. Kim, D.J. Resnick, J.A. Liddle, C.G. Willson, J. Vac. Sci. Technol. B **3**, 1283 (2006).

[11] C. Pina-Hernandez, P.F. Fu, L.J. Guo, Electron Ion and Photo Beam Technology and Nanofabrication (EIPBN) (2007).

[12] H.W. Ro, R.L. Jones, H. Peng, D.R. Hines, H.J. Lee, E.K. Lin, A. Karim, D.Y. Yoon, D.W. Gidley, C.L. Soles, Adv. Mater. **19**, 2919 (2007).

[13] C. Pina-Hernandez, P.F. Fu, L.J. Guo, Submitted.

[14] C. Pina-Hernandez, J.S. Kim, L.J. Guo, P.F. Fu, *Adv. Mater.* **9**, 1222 (2007).

Chapter 6

Improving mold releasing by (1) blending fluoro-based reactive surfactant into T(Ph)T(MA); (2) substrate surface modification

6.1 Introduction

High yield is required for the replication of micro/nano-structures using nanoimprint lithography for large scale industrial applications. Unfortunately high stress is normally involved during the mold releasing process which generates a number of undesirable imperfections for the patterned features. One approach to reduce the defect density is to improve the resist mechanical properties.[1] In the mean time additional requirements must also be met. For example the resist material should properly adhere to the substrate employed so it does not delaminate and sticks to the mold during the releasing process. In addition, the resist must present lower adhesion to the mold to achieve a desired imprinting yield. The above statements can be explained with thermodynamic criteria for mold releasing, which involves surface and cohesion energies.

The work of cohesion ($W_{Cohesion}$) is defined as:

Equation 6.1 $$W_{Cohesion} = 2\gamma_{resist}$$

Where γ_{resist} is the surface energy of the resist.[2]

The work of adhesion ($W_{Adhesion1}$) between the substrate and the resist is defined as:

Equation 6.2 $$W_{Adhesion1} = \gamma_{substrate} + \gamma_{resist} - 2\gamma_{substrate\text{-}resist}$$

Wherein, $\gamma_{substrate}$ is the surface energy of the substrate, and $\gamma_{substrate\text{-}resist}$ is the interfacial energy of the substrate-resist interface.

Similarly the work of adhesion for the mold-resist interface is defined as follows:

Equation 3 $$W_{Adhesion2} = \gamma_{mold} + \gamma_{resist} - 2\gamma_{mold\text{-}resist}$$

Wherein γ_{mold} is the surface energy of the mold

The work of cohesion is only related to the mechanical properties of the material. On the other hand, the work of adhesion is related to the interfaces between the resist with the mold or the substrate, and it can be modified by tailoring any of the material surface. For a successful mold releasing, the work of cohesion must be higher than the work of adhesion between the mold and the resist (Figure 6.1). In addition, the work of adhesion at the substrate-resist interface should be larger than the work of adhesion at the mold-resist interface. Otherwise the danger of resist de-lamination or breaking will likely occur.

In order to decrease the adhesion between the resist and the mold for an ease releasing the surface of the mold can be modified chemically. The formation of a self-assembled monolayer of fluorinated silanes by vapor deposition is perhaps one of the most popular approaches.[3] Other methods, for reducing the surface energy of the mold, include the surface treatments with siloxane oligomers.[4]

Another method to decrease the resist sticking to the mold is by using a low surface energy resist. This can be accomplished by mixing the polymer precursor with surfactant molecules having insoluble heads facing resist-mold interface and tails with high solubility in the monomer precursor.

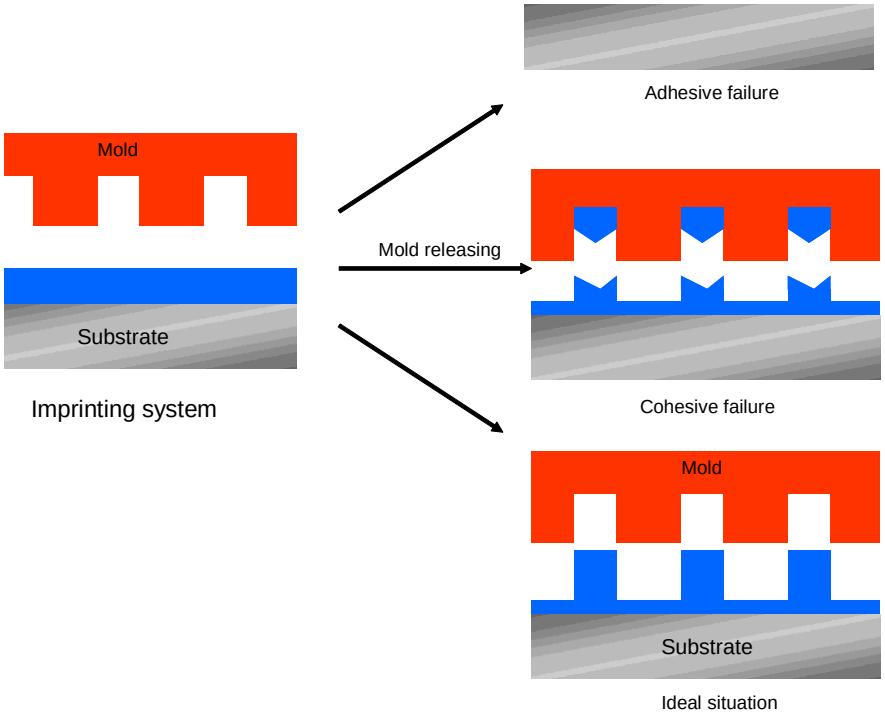

Figure 6.1 Cohesive and adhesion failure upon mold releasing.

Appropriate surfactant molecules are fluoro-surfactants, which contain fluorinated heads. In fact, there are several types of fluorosurfactant molecules commercially available. The fluorinated heads provide a lower surface energy than surfactants with hydrocarbon heads. Some fluorinated surfactants have been previously employed to decrease the resist surface energy with positive results.[5,6]

On the other hand, the substrate-resist adhesion can be enhanced by implanting the substrate surface with reactive chemical groups. The groups then react with the resist to covalently link during the UV-curing process, thus generating strong adhesion between the substrate-resist interfaces.

Here, the imprinting performance was improved with two methods: (a) use reactive fluorinated surfactants to decrease the mold-resist adhesion and (b) implant the substrate with reactive chemical groups improve the substrate-resist adhesion. An important characteristic of the surfactant molecules employed here is the low surface energy (high water contact angle) of the head groups. In addition the surfactant tails are functionalized with chemical groups which can react with the monomeric precursor during the UV-curing imprinting step so a mechanically stable polymeric network can be formed.

6.2 Experimental procedure

The imprinting yield of silsesquioxane materials was improved utilizing two different approaches: 1) decreasing mold sticking by formulating the SSQ precursor with fluoroacrylate molecules and 2) strengthening the adhesion of the resist to the silicon (Si) substrate using covalent bonding. A methacrylate-based phenyl silsesquioxane (SSQ) resin was used for this testing ($T^{Ph}_{0.40}T^{MA}_{0.60}$).

The materials employed as surfactants were two different fluoroacrylates, 2,2,3,3,4,4,4-heptafluorobutyl methacrylate (sigma Aldrich) and *N*-alkyl perfluorooctane-sulfonamidoethyl acrylates (3M); the chemical structure is displayed in figure 6.2. Such surfactants were formulated with the resist material at different weight percentages. The

water contact angles of the cured resist were measured and used as an indication of the surface energy of the resist (Table 6.1).

The silicon substrate was modified by self-assembling a monolayer of 3-methacryloxypropyltrimethoxysilane by vapor deposition at 125ºC during 20min. The methacrylate functionalities can react with the methacrylates from the substrate during the UV curing process to create strong covalent bonds.

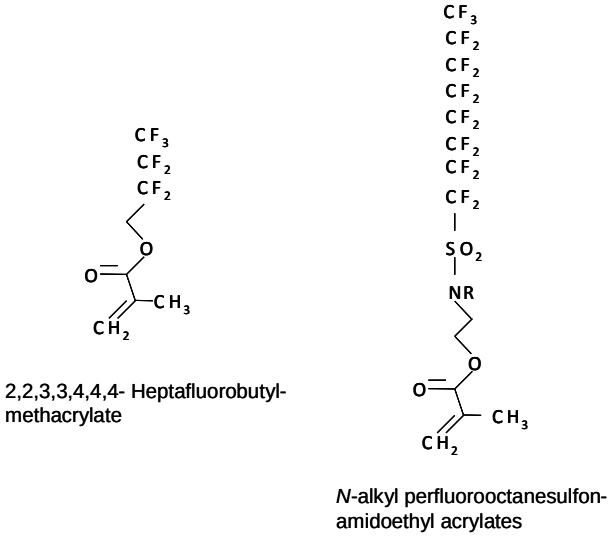

Figure 6.2 Fluorinated-acrylate molecules.

6.3 Results

6.3.1 Blending fluoro-based reactive surfactant into T(Ph)T(MA)

It was found that the thin films of SSQ's formulated with 2,2,3,3,4,4,4-heptafluorobutyl methacrylate showed a large variation in contact angle measurements (water contact angles were used as an indicate of surface energy). It is possible that due to the low polarity of these fluorinated methacylates, they aggregate to form low surface

energy agglomerates in some areas of the thin film, leading to a variation of the surface energy over the surface of the film.

Table 6.1 Water contact angle of methacrylate-SSQ formulated with fluorosurfactants after UV cure.

Surfactant	Content	Water Contact Angle (1)	Water Contact Angle (2)	Water Contact Angle (3)	Average
None	None	71	72	74	72
Heptafluorobutyl methacrylate	0.2%	66	82	106	85
Heptafluorobutyl methacrylate	2.0%	90	100	107	99
Perfluorosulfonamidoacrylates	0.1%	99	102	102	101
Perfluorosulfonamidoacrylates	1.0%	113	114	114	114
Perfluorosulfonamidoacrylates	5.0%	115	115	115	115

On the other hand, the contact angle measurements of the resins formulated with perfluorosulfonamido-acrylates showed constant values over the film surface for the different samples measured. For this molecule, a water contact angle as high as 115deg was measured. Due to their methacrylate moieties, these surfactants become part of the crosslinked network during the crosslinking step, as illustrated in Figure 6.3. In fact, the resist formulated with 1.0% of this acrylate material was imprinted with a 70nm line width fluorinated ETFE mold and showed very weak adhesion to the mold during the releasing step. An imprinting with very few defects was achieved.

The low mold-resist sticking found in these formulations can be related to the surfactant properties of the perfluorosulfonamido-acrylates. These molecules contain fluorinated non-polar heads as well as sulfonamido-acrylate solvent-soluble tails. The insoluble fluorinated heads of these molecules facing up to the surface in the film

reducing its surface energy. At the same time, the organic soluble methacrylate tails form strong covalent bonds with the SSQ resin during the crosslinking process as shown in Figure 6.4.

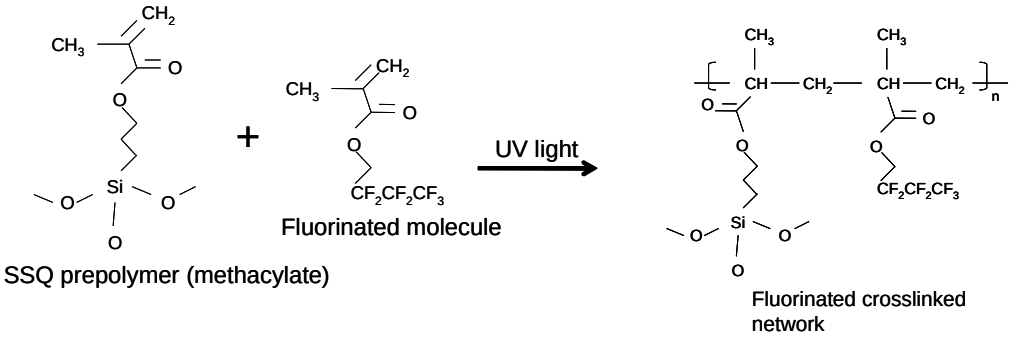

Figure 6.3 Chemical reaction between SSQ prepolymers and fluorinated molecules during the crosslinking process.

When soluble flurosurfactant molecules without methacrylate functionality were tested, poor imprint results were obtained, indicating the importance the functional groups play.

6.3.2 Wafer surface modification with reactive silane

The imprinting of the methacrylate-based PSSQ on top of a bare silicon substrate has a low yield, close to 50%, due to the weak interactions between the non-polar methacrylate groups form the resist and the silicon surface. To increase the substrate-resist adhesion, a vapor deposition with a methacrylate functionalized silane was performed on the silicon substrate and the process was conducted at 80°C for 20min (Figure 6.5).

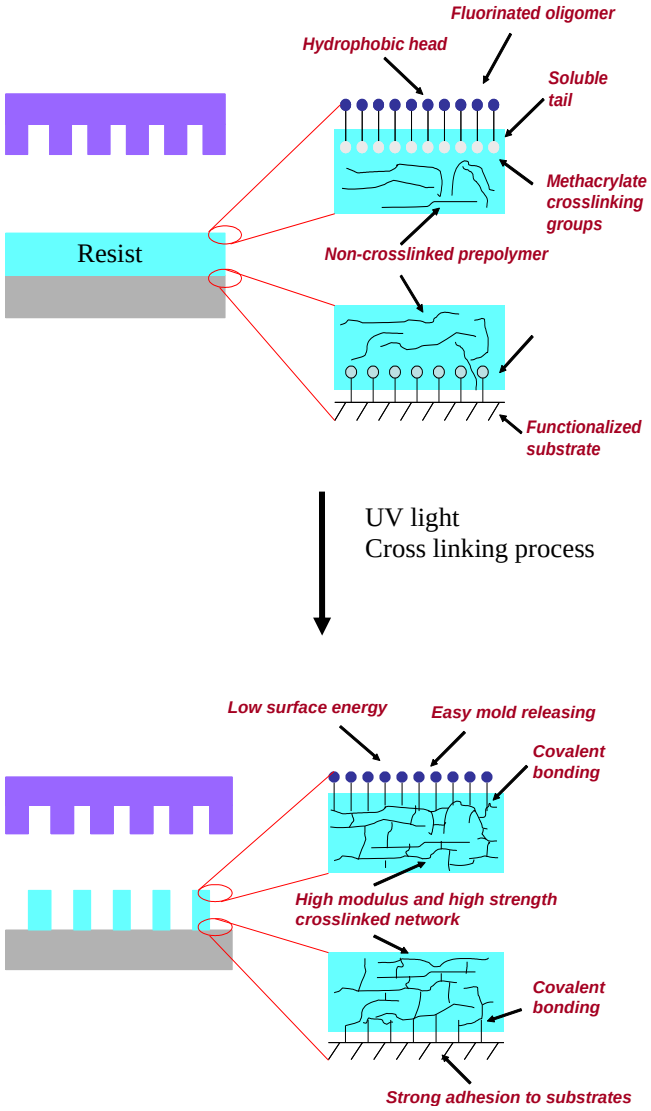

Figure 6.4 Schematics of the imprinting process.

The methacrylate-based PSSQ resin ($T^{Ph}_{040}T^{MA}_{0.60}$) was then spun on top of the methacrylate functionalized silicon surface. The imprinting was performed according to the following sequence: (1) a flexible and transparent mold with a 70nm line/space, either made of ETFE or fluoro-SSQ, was placed and lightly pressed on top the SSQ film under 50psi of pressure; (2) the SSQ resist was then cured under 1-min UV-light radiation.

After the imprint process, the mold was released. Remarkably an imprinting with very few defects was achieved with this approach (Figure 6.6).

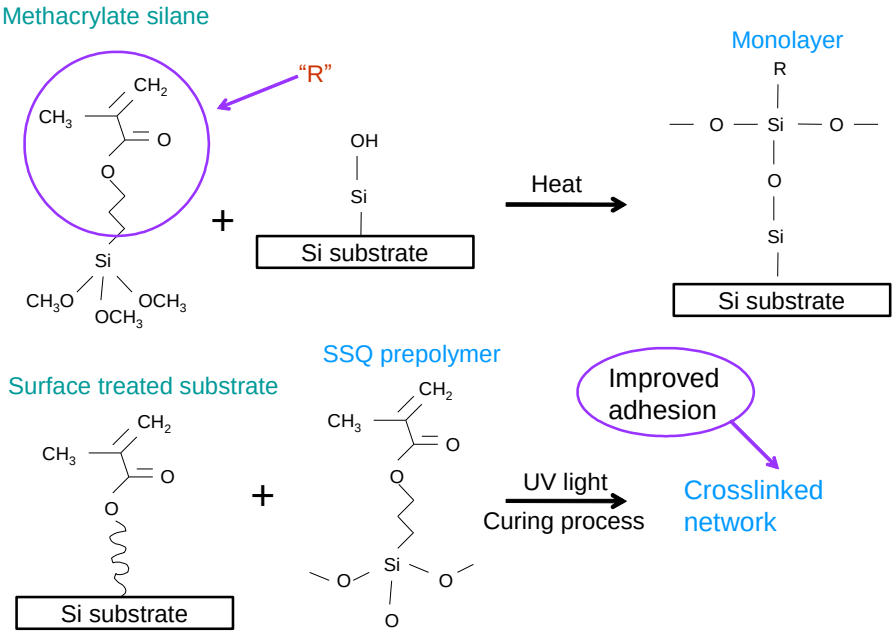

Figure 6.5 Surface treatment of Si substrate with methacrylate silanes.

The silicon substrate was coated by a monolayer of a methacrylate-functionalized silane which has a strong compatibility to the methacrylate based resist (same functional groups). The chemical compatibility helps create a stable resist thin film on the substrate. In addition, the reactive surfaces form strong covalent bonds during the UV curing step which creates a continuous phase between the substrate and the resist.

This approach has also been tested for SSQ resists with epoxy functionalities. However, an appropriate surfactant with epoxy functionalities was not commercially available.

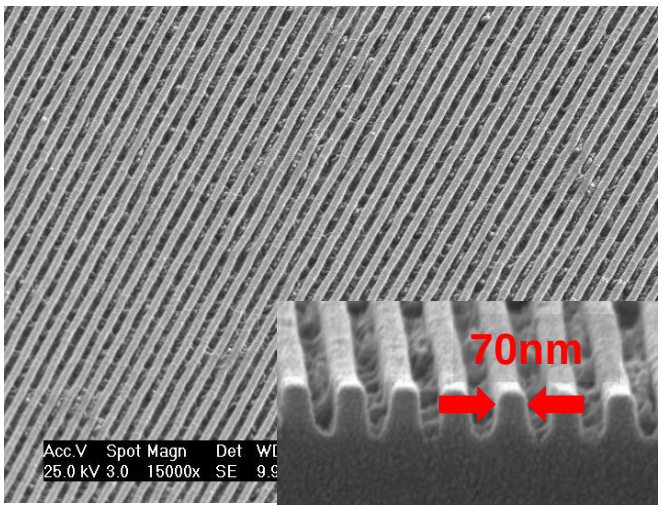

Figure 6.6 SEM of 70nm line width gratings replicated with PSSQ (methacrylate) formulated with 2,2,3,3,4,4,4- Heptafluorobutyl methacrylate.

6.4 Conclusion

An imprinting with very few defects was achieved for a methacrylate-based SSQ resin. Treating the substrate surface with a methacrylate silane greatly increases the substrate-resist adhesion.

On the other hand, the sticking of an SSQ resist with methacrylate moieties to the mold was reduced by formulating the SSQ prepolymer with perfluorosulfonamido-acrylate, a highly fluorinated surfactant. The equivalent fluorosurfactants which could be added onto an epoxy based SSQ resists are not commercially available, and therefore could not be tested for this study.

References

[1] Lee, L. H. *Fundamentals of Adhesion;* Plenum, NY, 1991.

[2] Isrealachvili, J. *Intermolecular and Surface Forces 2nd;* Academic Press: San Diego, 1991.

[3] Bailey, T.; Choi, B. J.; Colburn, M.; Meissl, M.; Shaya, S.; Ekerdt, J. G.; Sreenivasan, S. V.; Willson, C. G. *Journal of Vacuum Science & Technology B*; Vol. 18, pp 3572-3577.

[4] Lee, M. J.; Lee, N. Y.; Lim, J. R.; Kim, J. B.; Kim, M.; Baik, H. K.; Kim, Y. S. *Adv Mater* 2006, *23*, 3115-+.

[5] Bender, M.; Otto, M.; Hadam, B.; Spangenberg, B.; Kurz, H. *Microelectronic Engineering;* 2002; Vol. 61-2, pp 407-413.

[6] Wu, K.; Wang, X.; Kim, E. K.; Willson, C. G.; Ekerdt, J. G. *Langmuir* 2007, *3*, 1166-1170.

Chapter 7

Residual less imprinting of hybrid organic-inorganic silicon based functional materials

7.1 Introduction

Nanoimprint lithography (NIL) has found multiple applications in the replication of simple and complex geometric structures such as gratings, nanopillars and three dimensional stacks of nanostructures.[1,2] However, improvements related to the resist and processing steps such as the elimination of laborious and expensive etching steps must still be addressed. The imprinting of patterns always generates a residual layer between the substrate and the replicated structures with a thickness which depends on the imprinting conditions used. Additional steps such as reactive ion etching (RIE) are to be used for removing this undesirable polymeric layer. This additional processing step leads to a higher cost and longer fabrication times. It also decreases pattern fidelity due to the anisotropic etching which can round off the initially sharp edges as well as to decrease the aspect ratio of the replicated structures. In addition, the conventional polymeric resist materials used for NIL may no be compatible with RIE plasma etching due to the plasmon and heat induced polymer degradation. In order to avoid such processing steps and to speed up the fabrication procedure, the imprinting of structures without any

residual layer is highly desired. A consequence of a residual free patterning can be the introduction of a complete display of new applications such as cell microarrays and selective protein adsorption.[3-5]

The fabrication of patterns with exposed substrate regions has been previously performed with capillary force lithography (CFL).[6] In CFL, the de-wetting of the resist required to obtain an exposed substrate surface depends on the interaction between capillary, hydrostatic pressure and Van der Waals forces between the patterning polymer, the mold and the substrate. In this approach, hydrophilic polymers such as poly(ethylene glycol) (PEG) have been patterned with exposed regions using a soft PDMS stamp. This can be achieved because hydrophobic polymers such as PEG have low affinity to PDMS surfaces (water contact angle: 78º). On the other hand, hydrophobic polymers such as polystyrene present some limitations because they have high affinity to PDMS (similar water contact angles) and generate residual layer if a thick polymer film is used. However, low aspect ratio residual less patterned structures can be formed if an initial thin layer is used. The process has to be performed at temperatures higher than the polymer T_g which can seriously deform the PDMS stamp.

Unfortunately, CFL still faces some other limitations. For instance, PDMS stamps are employed because this material is permeable to the solvents required for the fabrication of patterns with exposed regions. However, PDMS structures deform easily upon applied pressure due to its poor mechanical properties (E = 1.8MPa).[7-9] In addition, this material swells in organic solvents leading to structural deformation. Another disadvantage of CFL is the extremely long processing time required (about 27 hrs); which is prohibitive for real industrial applications.[6]

In addition, the time to achieve residual free imprinting in CFL depends on film thickness and imprinting temperature. Since thin films of few tenths of nanometers require only short times as well as higher temperatures, this techniques is only suitable for structures with a height smaller than 50nm.

Another technique previously used to produce residual less patterns is PRINT (printing in nonwetting templates).[10] In PRINT, only low aspect ratio polymer nanoparticles (PEG) were fabricated for the encapsulation of DNA, proteins and molecules for therapeutics. In this technique, a high surface energy polymer (PEG) is molded with a fluoropolymer[11] using a low surface energy substrate (silicon treated with a fluorosilane). A drawback of this technique is the slow processing times.

In addition, organic nanowires of conjugated polymers (polypirrole) have also been imprinted with a zero residual layer to improve conductivity or polarized luminescence performance.[12] A thin film, 60nm, was used to generate residue free embossing. Unfortunately, the imprinting had to be aided by the presence of solvent (water) to plasticize the polymer and achieve the imprinting. The presence of water can create defects due to bubble formation during the solvent evaporation step. In addition, only very small areas could be imprinted since the original silicon mold was fabricated with e-beam lithography.

The fast residual less patterning of advanced materials has important implications for the future progress of several technological fields such as tissue engineering and optoelectronics. Here we demonstrated the residual less imprinting of silicon based advanced functional materials on hard and flexible substrates in a high throughput modality. Potential applications involve nanofibers, nanoparticles, cell and protein arrays

as well as membranes fabrication. The silicon base polydimethylsiloxane (PDMS) and silsesquioxane (SSQ) materials where easily patterned with exposed substrate surfaces.

The biocompatibility of PDMS combined with the imprinting of residual free patterns can allow the creation of functionalized nanotopologies for protein and cell adhesion with applications in biomedicine and tissue engineering. In addition, the non-residual layer patterning of ceramic precursors such as SSQ materials is a path that can lead to a complete set of new applications such as the fabrication of ceramic membranes with well defined structures (since well controlled and uniform nanopore sizes can be produced) for high temperature separations.

In opposition to CFL, the techniques presented here do not rely on capillary rise of the patterning material but on external pressure and substrate-resist surface interactions to induce the flowing of the patterning material into the mold voids. Importantly is that molds fabricated with materials having low air permeability such as ethylene-tetrafluoroethylene copolymer (ETFE) and SSQ were employed for the patterning process. In addition, in contrast to CFL, the developed approaches are suitable for patterning hydrophobic polymers with no residual layer, so a vast number of new applications can be realized.

Two different approaches were used to fabricate residual free imprinted structures: non-residual layer imprinting on a non-wetting substrate and non-residual layer imprinting on a thermoplastic underlayer.

In the first method, a non-wetting substrate was employed to achieve the imprinting with exposed surfaces; the resist used was a high modulus PDMS previously developed in our group with a water contact angle of 103º.[13,14] The non-wetting

substrate was a silicon substrate coated with a fluorosilane self-assembled monolayer by vapor deposition. Moreover, Ethylene-tetrafluoro-ethylene (ETFE) copolymer was used to fabricate a low surface energy mold (water contact angle of 105º).[15]

Although PDMS prepolymer can easily fill the mold cavities by capillary rise, the weak dispersion forces between the low surface energy fluorinated substrate and the imprinting resist are driving forces to achieve the de-wetting of the PDMS material (PDMS de-wetting generates the exposed substrate surfaces). In addition, the de-wetting is also promoted by the use of high pressures which induce the flowing of the PDMS liquid into the mold-substrate cavities during the imprinting step. The flexibility of the ETFE mold along with the high pressures employed ensures an appropriate mold-substrate conformal contact so large areas can be patterned.

In the second approach, residual free structures were produced by patterning a UV-curable SSQ ($T^{Phenyl}_{0.40}T^{Methacryloxy}_{0.60}$)[16] material on a poly(methyl methacrylate) (PMMA) polymer underlayer surface. A low surface energy and flexible fluoro-SSQ mold was used for this process. The patterning SSQ material (water contact angle 70º) has low affinity to the fluoro-SSQ mold (Water contact angle of 110º) so capillary rise of the patterning material into the mold cavities is hard to achieve. However, if high external pressures (200psi) are used, the low viscosity (~1Pa.s) SSQ material can easily fill the mold cavities.

In addition, an important player to yield the exposed substrate regions is the thickness of the SSQ film (90nm), which needs to be low in relation to the height of the mold cavities (150nm). Thus, when a high external pressure is applied, the SSQ material rises into to the mold cavities; and since there is only a small amount of material

available (due to the relative low resist thickness), the SSQ is easily depleted from the substrate surface generating the exposed regions. This process is also aided by the presence of the thermoplastic PMMA underlayer. PMMA is an inert hydrophobic surface whose weak dispersion forces with the SSQ material promote the de-wetting process of the later material when an external pressure is applied.

7.2 Experimental procedure

7.2.3 Non-residual layer imprinting on a non-wetting substrate

To produce imprinted patterns without residual layer on a non-wetting substrate, a PET or Si substrate was first treated with oxygen plasma during 20 seconds to increase its surface energy by generating polar hydroxyl (-OH) groups on the surface. Then, the substrate was coated with a monolayer of perfluorotrimethoxysilane (PFTMS) applied by vapor deposition at 95ºC during 20min. This process generated a highly hydrophobic surface. A small drop (20 μL) of PDMS precursor (high modulus PDMS previously developed in our group) was placed on top of the surface treated substrate and, a 700 nm SiO_2 period grating mold was used to replicate a pattern (Figure 7.1.a). Heat (80ºC) and pressure (200psi) were applied. The pressure was necessary to spread out the PDMS precursor liquid into the mold cavities and allow the mold and the substrate to make conformal contact. Finally, the mold was released, and a grating of PDMS was fabricated on a flexible/hard substrate.

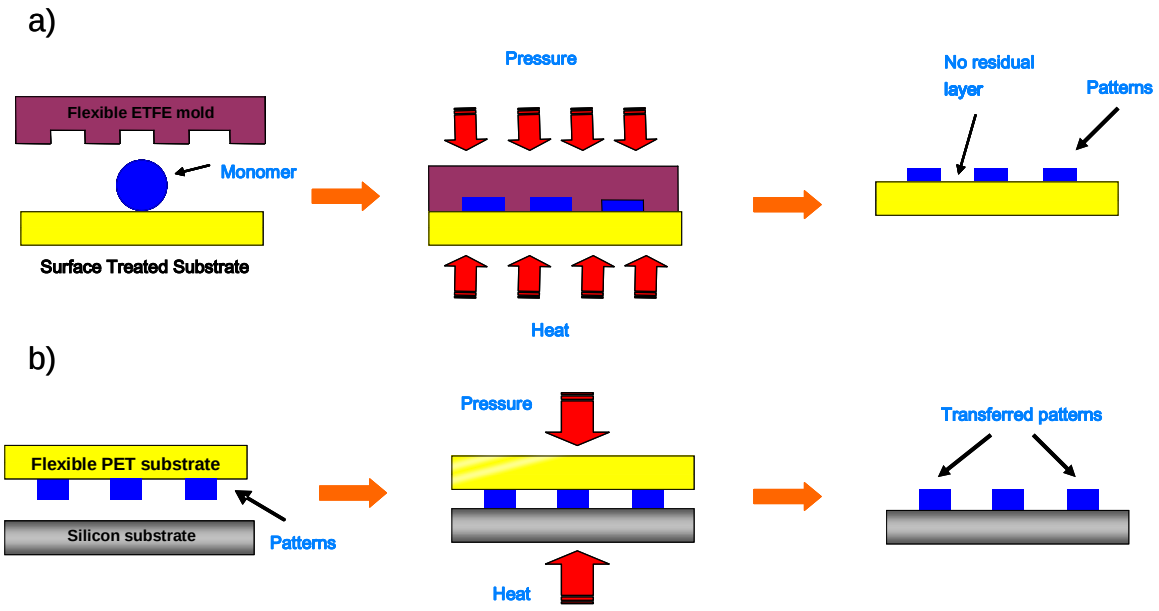

Figure 7.1 (a) Schematics of the imprinting of structures with no residual layer left and, (b) subsequent pattern transfer to a hard substrate.

This grating replicated on the flexible substrate was subsequently transferred to a hard silicon substrate by a reverse imprinting process (Figure 7.1b). This transferring was done to show that these structures can find applications in the fabrication of nanofibers. A temperature of 100ºC and pressure of 200psi was used for this purpose. The temperature and pressure allow a better conformal contact between the structures and the receiving substrate to successfully transfer the structures.

7.2.2 Non-residual layer imprinting on a thermoplastic underlayer

The procedure for imprinting a pattern with an exposed substrate surface on a thermoplastic poly(methylmethacrylate) (PMMA) layer is presented here. A high molecular weight PMMA (950K) layer was spun on top of a silicon substrate, followed by the spin coating of a 4% SSQ ($T^{Ph}_{0.40}T^{Methacryloxy}_{0.60}$) solution in PGMEA, to form a

90nm thin film. The SSQ film was pressed against a flexible and transparent fluoro-SSQ, 220nm period nanopillar, under 200psi of pressure. The SSQ thin film was then cured by UV-broadband irradiation for 40 seconds using a Nanonex imprinter tool. The mold was then released and a lift-off step was performed to remove the PMMA layer so a nanohole array with uniform size distribution (figure 7.2) was obtained.

The initial thickness of the SSQ film is an important factor to considerate. Such layer must be thinner than the height of the nanopillars mold in order to achieve the imprinting of structures with no residual layer. If a residual layer was left, an undesirable and time consuming extra etching step would be required to remove it.

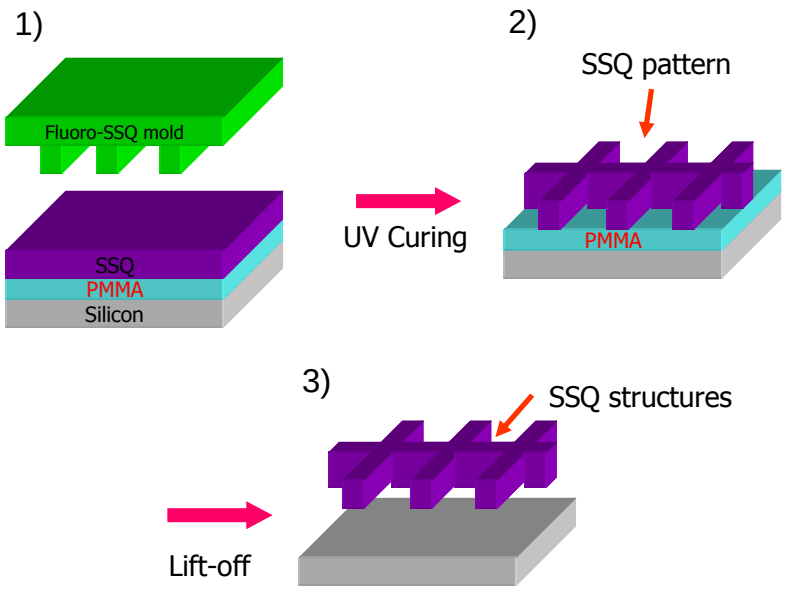

Figure 7.2 Steps followed to fabricate a nanohole array.

7.3 Results and discussion

7.3.1 Non-residual layer imprinting on a non-wetting substrate

To demonstrate residual-free imprinting using modified PDMS (Figure 7.3), a 700nm period pattern could be replicated on top of a PET substrate and a Si wafer by using the surface treatment described in the previous section. The whole process did not involve any RIE step. As long as its surface energy is low, the substrate material should not be a limitation as we have demonstrated non residual layer fabrication by using both hard and flexible substrates. The resist material does not wet the substrate due to the low surface energy induced by the silane treatment. This would eliminate the possibility of generating any residual layer because the resist tends to flow towards the mold cavities, instead of wetting the substrate surface, during the imprinting process.

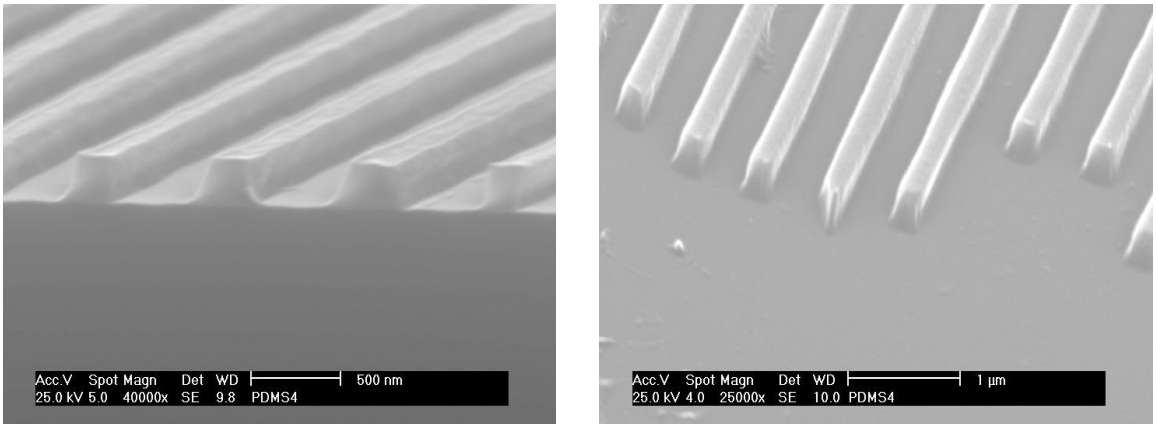

Figure 7.3 Non-residual layer gratings generated on a Si substrate.

This non-residual layer imprinting method also depends on the surface energy of the mold used. The ideal surface will allow the monomer precursor to spread out while applying pressure, allowing the recessed features from the mold and the surface substrate to make conformal contact.

It is important to point out that the spreading time of the monomeric resist will depend on the magnitude of the applied pressure as well as the viscosity of the monomer precursor. The viscosity of the PDMS formulation employed here is quite low (few centistokes) so its spreading is fast. However, the spreading of materials with a high viscosity, such as thermoplastic polymers above their melt temperatures, will be much more difficult.

Similarly, structures imprinted on a PET substrate were transferred to a hard silicon substrate (Figure 7.4a). In general moderate temperature (100°C) and high pressure were employed for this transfer. This technique can be extended for making up multilevel stacks of the polymer nanostructures, by repeating the pattern transfer process. This strategy is similar to the reverse nanoimprint technique reported previously.[1] The approach described here offers a great simplification and allows a faster and cheaper fabrication process, since it completely eliminates the RIE process required for the traditional fabrication steps.

On the other hand, currently only a small percentage (<5%) of the pattern was transferred to the hard substrate due to the difficulty in achieving good mechanical contact between the non-flexible and flat Si substrate and the replicated PDMS lines on the PET substrate. A more flexible substrate will allow much improved yield by providing a better conformal contact. This process can also be useful to fabricate

polymeric nanofibers with controlled cross-sectional dimensions as shown in Figures 7.4(b) and (c). The stamping without residual layers on plastic substrate can be regarded as nanofibers if the structures can be harvested. Nanofibers have found applications in various areas, such as scaffolds for tissue engineering, composite materials reinforcement, sensors, filtration media, and catalysts, and in the micro- and nano-optoelectronic fields.

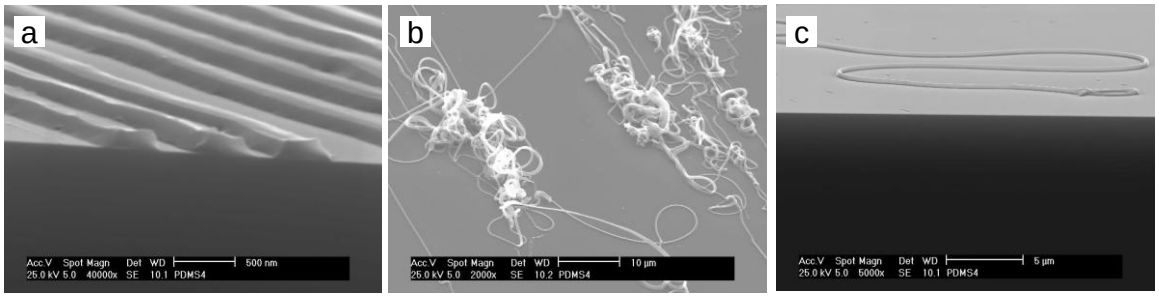

Figure 7.4 Nanofibers transferred form a flexible substrate to a hard Si substrate, (a) an array of nanofibera bundle of nanofibers, (b) a bundle of nanofibers (c) a single nanofiber.

There are several techniques for processing nanofibers such as phase separation, self-assembly, template synthesis and electrospinning. Electrospinning is probably the most preferred method. It is a simple, flexible and versatile process that is able to make one-by-one very long single nanofibers. In this technique, an electric field is applied to draw a polymer melt or polymer solution from the tip of a capillary to a collector. The dimensions of the nanofiberss can be varied and controlled.

Several challenges still remain in this field. Due to limitations in processing, practical applications of polymer nanofibers are rather limited so far. The processing and collecting of uniaxially aligned continuous nanofibers has not been achieved yet. Obtaining defect-free and uniform diameter nanofibers is difficult. Finally, the throughput of the nanofibers manufacturing should be improved.

The fabrication technique presented here offers the advantage of producing highly aligned fibers with a high throughput. It is also possible to obtain fibers with uniform and controllable dimensions.

7.3.2 Non-residual layer imprinting on a thermoplastic underlayer

A SEM of the SSQ hole-structure imprinted on top of a silicon substrate is presented in Figure 7.5(a); the height of the structures is about 150nm. It can be noticed in the same figure that no residual layer is left. The same types of structures were imprinted on top of a PMMA layer which was previously spin cast on a silicon substrate. In Figure 7.5(b) the SSQ structures along with a thick PMMA underlayer on top of the silicon substrate are presente.

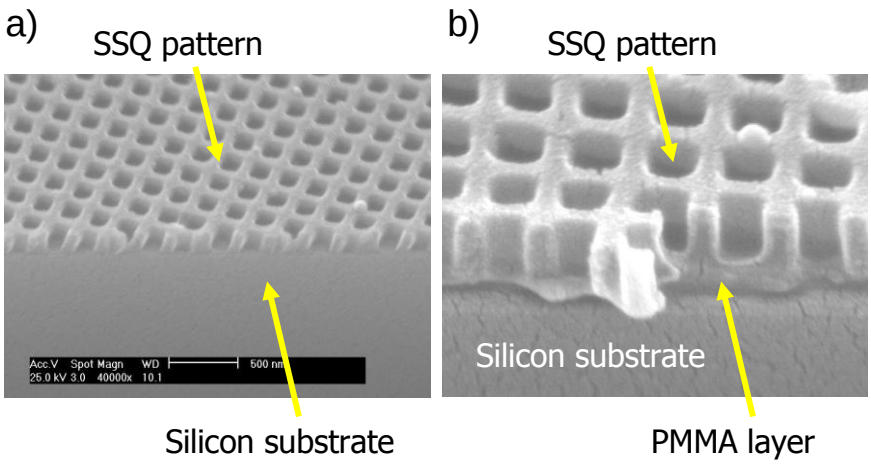

Figure 7.5 Nanohole array fabricated on a SSQ resist.

Once the nanohole array was imprinted, a lift-off with acetone was performed to remove the PMMA underlayer. Then, the fabricated SSQ pattern was mechanically disturbed using a glass microfiber mat to break and twist some parts of the pattern so the

back side of the membrane can be examined with a SEM instrument. Figure 7.6 shows some parts of the holes array structures, including the top and bottom sides, and some membrane pieces on top of others. This approach can be applied using other types of polymeric substrates and achieve the same type of results. The only requirement is that the polymeric substrate must be easily dissolved by a solvent cleaning step and that it does not interact chemically with the SSQ precursor to avoid forming an unremovable crosslinked inter-phase.

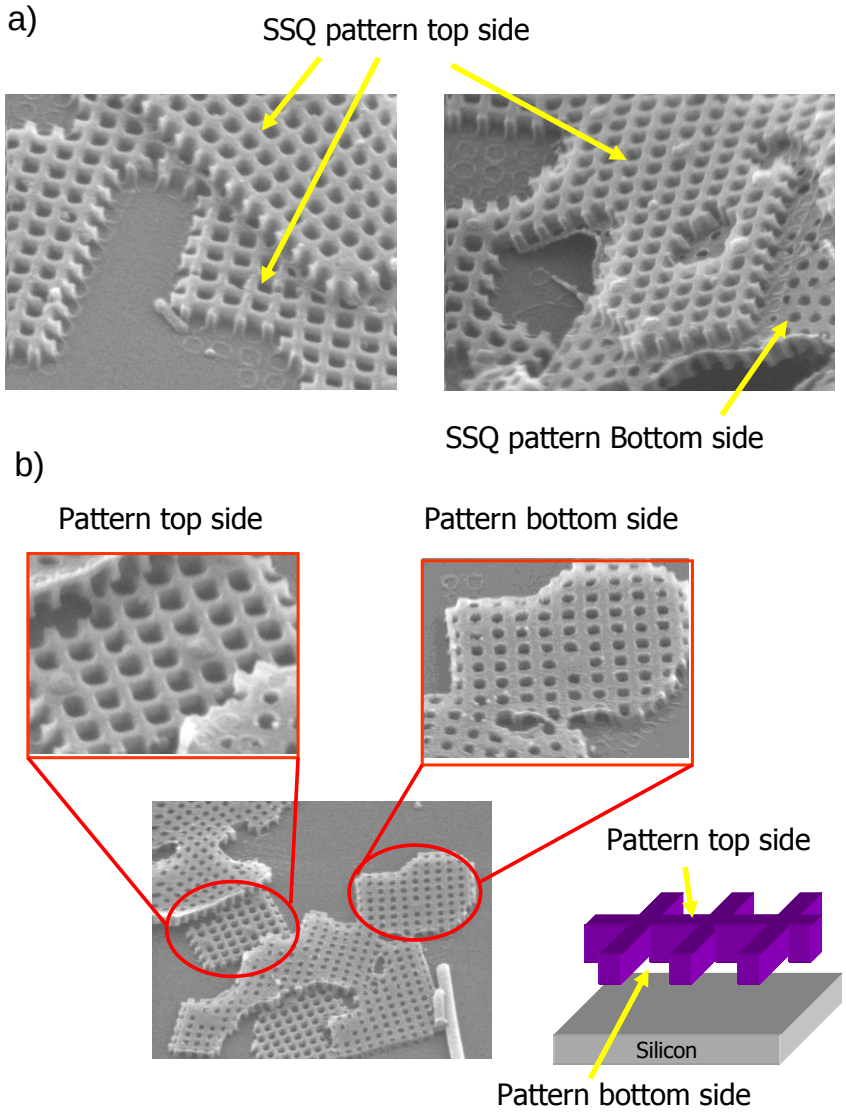

Figure 7.6 Top side and bottom side views of an imprinted nanohole array.

Remarkably a microfiber from the mat is observed below a piece of the SSQ pattern and through the holes array. This evidence clearly conveys that the imprinted structures are residual layer free.

The residual layer free nanohole array SSQ pattern can be used as a membrane with well defined structures. The size and uniformity of the pores can be easily controlled by using the appropriate imprinting template. In addition, the pattern can be thermally process to generate a functional ceramic membrane due to the thermal conversion of SSQ networks into SiO_2 under appropriate process conditions.

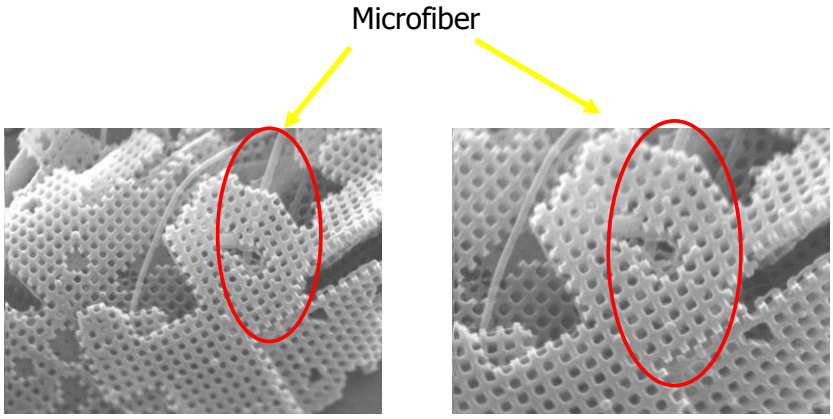

Figure 7.7 Microfiber seen through a nanohole array.

7.4 Conclusions

Structures with no residual layer were imprinted on top of both a flexible and hard substrates. Hydrophobic and chemical resistant high modulus PDMS and SSQ ($T^{Phenyl}_{0.40}T^{Methacryloxy}_{0.60}$) materials were imprinted with exposed substrate surface. Two different processing methodologies were introduced. Residual free PDMS material was patterned on a non-wetting substrate. The low affinity between PDMS and the low surface energy substrate provided the driving force to achieve the PDMS dewetting. In

addition, SSQ material with no residual layer was patterned on thermoplastic polymeric layers. In this case, the high external pressures and the low SSQQ film thickness used allow the patterning without residual layer. Multilayer and 3D structures can be achieved by repeating the pattern transfer process without the involvement of any RIE process. This stamping of structures without residual layers can be used to produce size controlled nanofibers from a variety of polymer materials, once the imprinted polymer nanogratings are properly harvested. In addition, membranes with uniform pore size and well controlled porosity can also be fabricated.

References

[1] Bao, L. R.; Cheng, X.; Huang, X. D.; Guo, L. J.; Pang, S. W.; Yee, A. F. In *In Nanoimprinting over topography and multilayer three-dimensional printing;* Journal of Vacuum Science & Technology B; 46th International Conference on Electron, Ion, and Photon Beam Technology and Nanofabrication (EIPBN); A V S AMER INST PHYSICS: MELVILLE; STE 1 NO 1, 2 HUNTINGTON QUADRANGLE,, MELVILLE, NY 11747-4502 USA, 2002; Vol. 20, pp 2881-2886.

[2] Guo, L. J. *Adv Mater* **2007**, *4*, 495-513.

[3] Chen, C. S.; Mrksich, M.; Huang, S.; Whitesides, G. M.; Ingber, D. E. *Science* **1997**, *5317*, 1425-1428.

[4] Beebe, D. J.; Moore, J. S.; Bauer, J. M.; Yu, Q.; Liu, R. H.; Devadoss, C.; Jo, B. H. *Nature* **2000**, *6778*, 588-+.

[5] Falconnet, D.; Pasqui, D.; Park, S.; Eckert, R.; Schift, H.; Gobrecht, J.; Barbucci, R.; Textor, M. *Nano Letters* **2004**, *10*, 1909-1914.

[6] Suh, K. Y.; Lee, H. H. *Adv. Funct. Mater.* **2002**, *6-7,* 405-413.

[7] Delamarche, E.; Schmid, H.; Michel, B.; Biebuyck, H. *Adv Mater* **1997**, *9,* 741-746.

[8] Bietsch, A.; Michel, B. *J. Appl. Phys.* **2000**, *7,* 4310-4318.

[9] Hui, C. Y.; Jagota, A.; Lin, Y. Y.; Kramer, E. J. *Langmuir* **2002**, *18,* 1394-1407.

[10] Rolland, J. P.; Maynor, B. W.; Euliss, L. E.; Exner, A. E.; Denison, G. M.; DeSimone, J. M. *J. Am. Chem. Soc.* **2005**, *28,* 10096-10100.

[11] Rolland, J. P.; Van Dam, R. M.; Schorzman, D. A.; Quake, S. R.; DeSimone, J. M. *J. Am. Chem. Soc.* **2004**, *26,* 8349-8349.

[12] Hu, Z.; Muls, B.; Gence, L.; Serban, D. A.; Hofkens, J.; Melinte, S.; Nysten, B.; Demoustier-Champagne, S.; Jonas, A. M. *Nano Lett.* **2007**, *12,* 3639-3644.

[13] Pina-Hernandez, C.; Kim, J. S.; Guo, L. J.; Fu, P. F., *Adv Mater* **2007**, *9,* 1222.

[14] Pina-Hernandez, C.; Kim, J.; Fu, P.; Guo, L. J. In *In Nonresidual layer imprinting and new replication capabilities demonstrated for fast thermal curable polydimethysiloxanes;* Journal of Vacuum Science & Technology B; 51st International Conference on Electron, Ion, and Photon Beam Technology and Nanofabrication; A V S AMER INST PHYSICS: MELVILLE; STE 1 NO 1, 2 HUNTINGTON QUADRANGLE, MELVILLE, NY 11747-4502 USA, 2007; Vol. 25, pp 2402-2406.

[15] Barbero, D. R.; Saifullah, M. S. M.; Hoffmann, P.; Mathieu, H. J.; Anderson, D.; Jones, G. A. C.; Welland, M. E.; Steiner, U. *Advanced Functional Materials* **2007**, *14,* 2419-2425.

[16] Pina-Hernandez, C.; Fu, P. F.; Guo, L. J. *Electron Ion and Photo Beam Technology and Nanofabrication (EIPBN)* **2007**.

Chapter 8

The fabrication of nano-patterns by precisely controlled dimensional shrinking

8.1 Introduction

The fabrication of nanostructures is critical in the semiconductor industry for building devices with high processing speed and memory capacity.[1] The manufacturing of integrated circuits requires the creation of features with small sizes for the 32nm node process with a precise control. Photolithography is the standard technology employed in the semiconductor industry for fabricating sub-micrometric structures. However, as the SI industry maintains the current scaling trend, photolithography is approaching its physical limits.[2] Thus, large amounts of resources are spent to develop new lithography's with capabilities suitable to overcome the barriers photolithography is encountering.[3]

However, the newly developed lithographic techniques still present several limitations. One of the apparent alternatives to replace photolithography is extreme ultraviolet (EUV) lithography. Nevertheless, the patterning with EUV must be performed

under vacuum conditions which reduces throughput and makes it an expensive approach.[4] Another nanofabrication technology with the potential to replace photolithography is electron beam lithography (EBL), which presents extremely high resolution (5nm). However, since EBL is a serial writing approach its throughput is also low.[5] Other approaches capable of high resolution, down to the atomic scale, such as scanning tunneling microscopy (STM), are also extremely slow to be implemented in real industrial settings.[6]

Bottom up approaches such as block copolymer self assembly have the potential to fabricate structures with really high resolution; but only small areas with high defect density can be readily patterned. In addition, this approach is only appropriate to create features with simple geometries such as circular and lamellar shape structures.

Less expensive and high throughput contact techniques have been developed such as NIL[7] and SFIL[8] with molecular scale resolutions (2nm). In contact approaches, the nanofeatures from a mold surface are transferred into a thin polymeric film by using pressure and heat or UV light. A disadvantage of contact technologies is the need of original master molds which are fabricated by the aforementioned processes.

A combination of a top down, high throughput patterning technology with a high resolution bottom-up approach has the potential to overcome the challenges normally encountered on the precise fabrication and accurate control of small size nanostructures. For instance, decreasing the separation distance among patterned microstructures can allow the fabrication of nanofeatures in a high throughput fashion with the use of inexpensive equipment. The fabricated nanopatterns can then be directly transferred into

underlying substrates for subsequent fabrication steps or employed as cheap stamps to directly replicate nanosize structures.

Previously, a "molecular ruler" was introduced to modify the size of metallic structures originally fabricated with electron beam lithography; metallic structures smaller than 20nm were created[9]. Since this technique relies on layer-by-layer deposition[10] of mercaptoalkanoic acids, it is a laborious and time consuming process; for instance, only a 2nm size modification can be achieved after each layer deposition step. The molecular ruler approach has been combined with several top down techniques to create small size structures[11-15].Other similar approaches include the growing of polymeric brushes on different types of patterned polymers by atom transfer radical polymerization (ATRP) to control the size of imprinted structures. Unfortunately, the complete process can take from 4 to 16 hours depending on the type of monomer used to generate the polymer brushes[16-18]. In addition, the chemistry and size of patterned structures was modified using thiol-based anchoring molecules but an accurate control of the grown film could not be achieved.[19]

In this context, we propose novel strategies for the precisely controlled fabrication of nanostructures smaller than 20nm by post-imprinting modification of patterned films on multifunctional silsesquioxane (SSQ) materials. Nanosize structures can be easily created with a combination of a high throughput contact imprinting technology and the temperature controlled construction of crosslinking layers. The fundamental principle of this method consists of adding an extra-layer of material on top of an imprinted pattern, as presented in Figure 8.1, to increase the structure dimensions and reduce the separation

distance among them. In this manner, structures of nanoscale dimensions can be created by starting from imprinted patterns with originally large sizes.

A great benefit of this method is the possibility to further process the created nanostructures by several means such as reactive ion etching; which due to the exceptional etching properties of the patterning silsesquioxane materials can allow the fabrication of small nanostructures in silicon or silicon dioxide layers.

In addition, since SSQ's have shown outstanding characteristics as stamps for nanoimprinting, the produced patterns with reduced dimensions can be easily transferred into other types of polymer films. In this fashion, NIL stamps for actual nanoscale replication can be engineered without the need to rely on other more expensive and low throughput techniques.

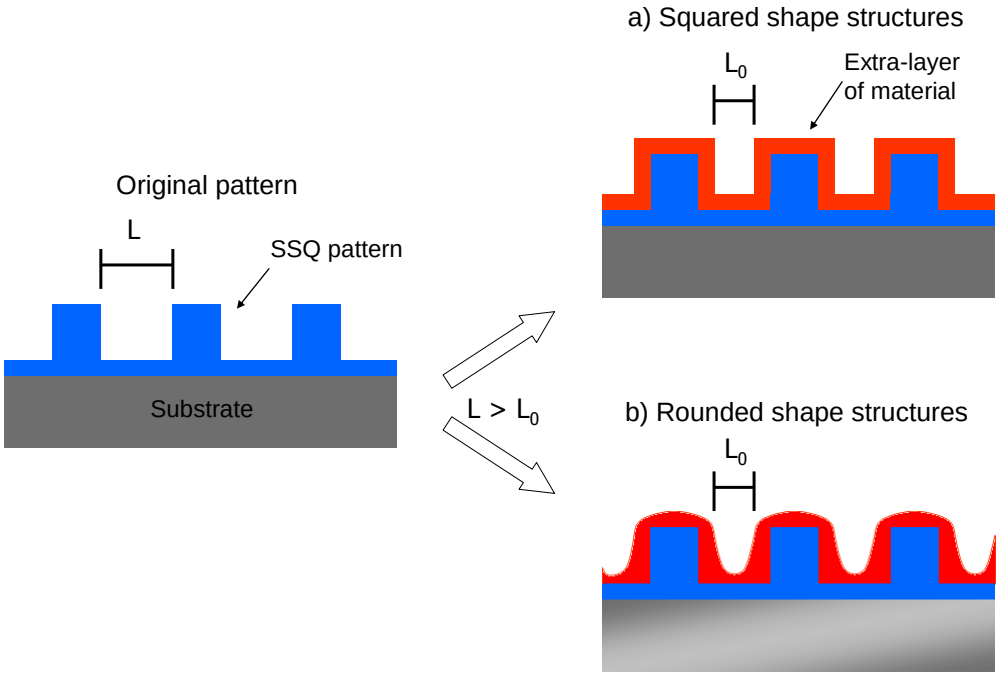

Figure 8.1 The decrease in gap size can be achieved adding an extra layer of material to increase size of structures; the structure shape is also controlled.

The nanostructures with sizes smaller than originally patterned were created using three different approaches. The first technique involves the alternated deposition of silylamine and epoxysilicone crosslinked layers on top of imprinted SSQ [T(Ph)T(MA)] layers. Several crosslinked layers can be coated so any desired size can be achieved. In a second method, structure size reductions were achieved by UV-curing of methacrylate oligomer [T(Ph)T(MA)] layers which thickness is controlled by a top film which UV-curing is inhibited by the presence of oxygen. Finally, in a third approach, small size structures were obtained by the crosslinking of a prepolymer (epoxysilicone) layer induced by the thermal diffusion of photoacid generator (PAG) from the inside of an imprinted SSQ [T(Ph)T(Epoxy)] pattern.

In the first process, temperature controlled crosslinked layers were created around imprinted features using the successive deposition of silylamine and epoxysilicone molecules, as illustrated in Figure 8.2; in this manner, the feature dimensions can be modified by decreasing the gap size among them. A functional silsesquioxane (SSQ) NIL resist was used for this process. The SSQ resists employed is a multifunctional material [T(Ph)T(MA)] that contains methyl methacrylate groups for photocuring and phenyl groups for mechanical stability.

The importance of using SSQ patterns is the presence of reactive silanol groups on their surface which act as coupling sites to bind the silylamine and epoxysilicone crosslinked films used to modify the structure size. The silanol groups are generated during the synthesis of the SSQ polymer precursors so the resist material does not require any further modification or formulation to create the reactive sites. In addition, as silanols are highly reactive, they can react with a number of functional groups.

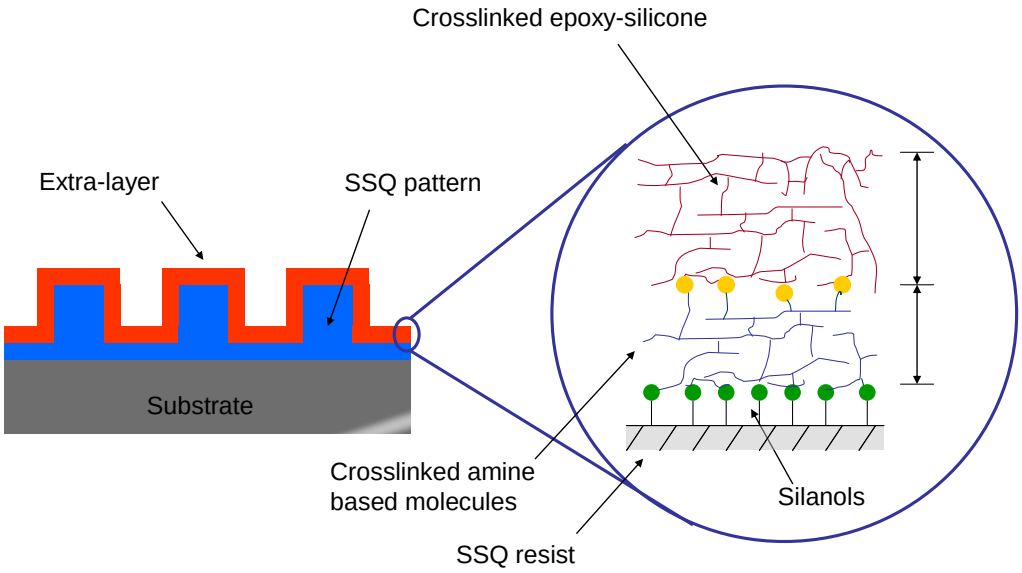

Figure 8.2 Growing of crosslinked layers for trench width reduction.

The proposed approach presents the advantage that the thickness of the crosslinked extra-layer can not only be accurately controlled in one single process but a series of sequential coating steps can be performed to achieve much larger dimensions. N-methyl-aza-trimethylsilacyclopentane and N-aminoethyl-aza-trimethylsilacyclopentane were the silylamines (shown in Fig. 8.3) coupled to the SSQ [T(Ph)T(MA)] pattern. During the crosslinking reaction, the silanol groups from the SSQ pattern surface react with the silicon atom from the silylamine molecule, opening up the cyclopentane to generate reactive primary and secondary amines. The newly generated amine groups can react with other silicon atoms from additional silylamine molecules and create a crosslinked layer. This crosslinked layer contains a high amount of amine groups which can react with a second type of molecules, (epoxypropoxypropyl)-terminated polydimethylsiloxane (epoxysilicone) (Mw 900-1100g/mol, viscosity 20-35 cst), to

generate a second crosslinked layer. Importantly is that this sequential process can be repeated several times to modify the pattern size to any desired dimensions.

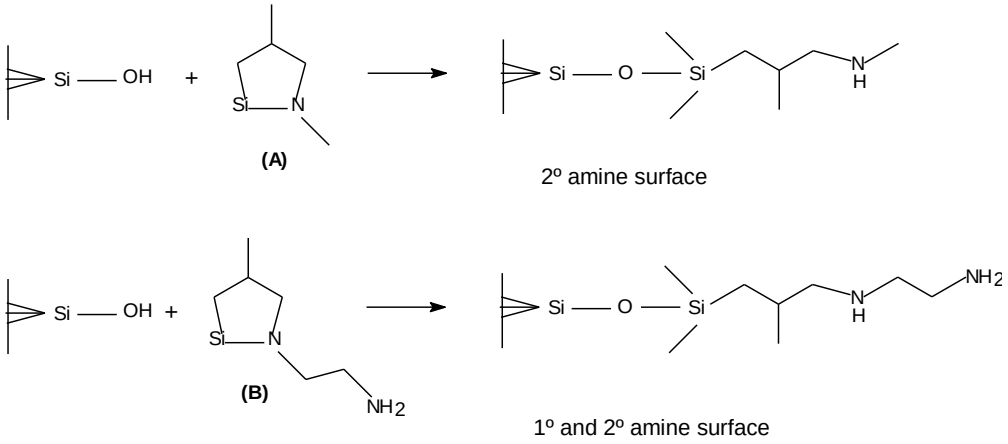

Figure 8.3 Molecules capable of forming an amine rich layer on a surface with silanol groups.

A second strategy consists of UV-curing a monomer precursor layer on top of a patterned film [T(Ph)T(Epoxy)] to reduce the trench width among the imprinted structures; similarly to the way it was presented in the previous approach. The UV-curable precursor is a methyl methacrylate based SSQ [T(Ph)T(MA)] material which crosslinks through a free radical process. The photo curing is performed on a normal air atmosphere. Under these processing conditions, two layers of the monomer precursor are formed on top of the patterned structures. The top layer is oxygen rich so it does not cure after UV-irradiation due to the free radical process being inhibited by the presence of oxygen. On the other hand, the bottom layer fully cures due to the low oxygen concentration in that region (figure 8.4). Thus, the oxygen poor layer can be UV-cured so the pattern size can be modified. The top uncured oxygen rich layer can be removed by a solvent aided cleaning step. The thickness of both layers can be controlled using different

conditions such as UV exposure time, UV intensity and initial total (thickness of original spin cast layer) thickness. Furthermore, the shape can be modified using this approach to obtain rounded shape structures as presented in Figure 8.1.

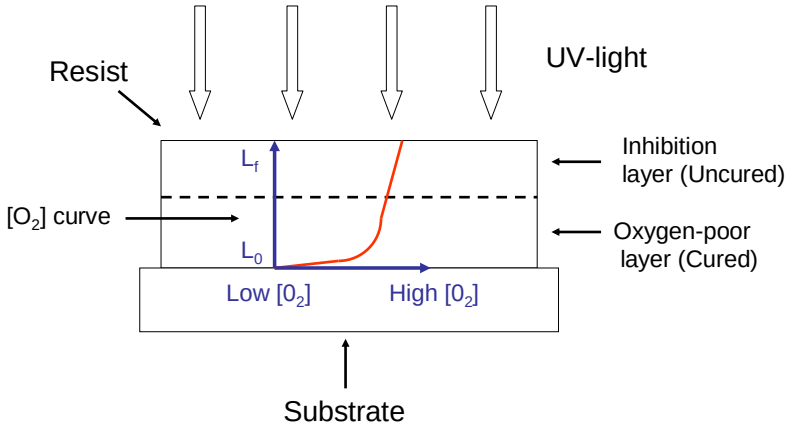

Figure 8.4 Schematic showing the change of oxygen concentration as a function of film depth.

Finally, in a third method, the separation distance among structures is reduced by the thermally induced diffusion of photoacid generator (PAG) from the imprinted pattern [T(Ph)T(Epoxy)] which initiates the crosslinking of a thin (epoxypropoxypropyl)-terminated polydimethylsiloxane (epoxysilicone) oligomer layer. The PAG is originally present in the pattern because this chemical initiates the crosslinking of the resist materials during the imprinting process. Then, during the structure size modification step, the PAG diffuses out from the pattern due to the thermal process. Besides inducing the diffusion of the PAG, the applied heat provides the energy required to initiate the crosslinking of the monomer (an epoxysilicone material) used to modify the pattern dimensions (figure 8.5). The thickness of the crosslinked layer can be controlled using

different temperatures and times; at higher temperature, the amount of PAG diffused out from the SSQ pattern is larger so a thicker second layer is formed.

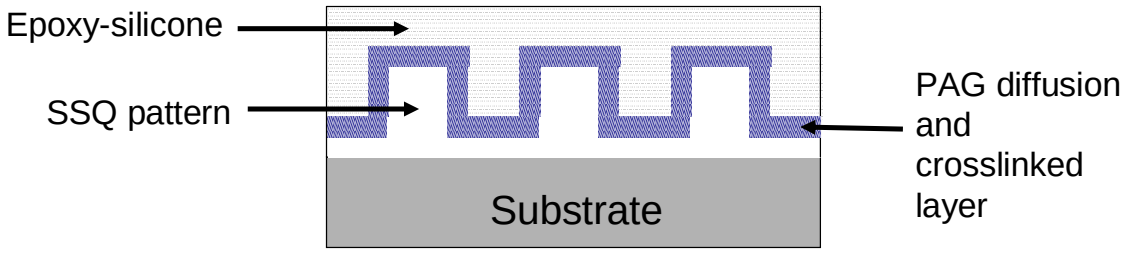

Figure 8.5 Schematics showing a reduction in gap structure utilizing the diffusion of PAG.

8.2. Experimental procedure

8.2.1 Deposition of crosslinked layers for nanoscale structure fabrication

This approach benefits from the presence of silanol groups on the surface of the cured SSQ patterns ($T^{Ph}_{0.40}T^{Methacryloxy}_{0.60}$) which act as binding sites. Silanols are functionalities which react chemically with a number of compounds. A layer of crosslinked silylamine material can be grown on top of a silanol rich surface to accurately control the separation distance among imprinted structures. More importantly, the growing layers accurately follow the patterns surface contour so sharp definitions can be achieved with structures having squared or close to 90 deg. corners.

A crosslinked layer of silylamine molecule with amine groups, as those shown in figure 8.3, was deposited on top of an SSQ ($T^{Ph}_{0.20}T^{Methacryloxy}_{0.80}$) pattern though vapor deposition (20min at different temperatures, from 50 to 95ºC). This layer yields the coupling between the SSQ surface and a second layer of material (epoxysilicone

prepolymer). Two silyl amines, N-methyl-aza-trimethylsilacyclopentane and N-aminoethyl-aza-trimethylsilacyclopentane, were initially tested but the later gave better results due to its higher content of amine groups.

The surface modified SSQ pattern was then immersed in the epoxysilicone prepolymer liquid and heat was applied. The system can be heated at different temperatures from 100ºC to 140ºC at different times. The amine groups from the crosslinked silylamine layer induce the ring opening of the epoxypropoxy groups to anchor the epoxysilicone molecules and initiate the crosslinking of this layer. Both crosslinked layers on top of the SSQ pattern surface have the effect of reducing the gap size. The experimental procedure is described in figure 8.6.

8.2.2 Structure size control by photocuring a polymer precursor (oxygen inhibition control)

Microstructure dimensions were modified using a thin layer of SSQ with methyl methacrylate ($T^{Ph}_{0.40}T^{Methacryloxy}_{0.60}$) groups for crosslinking. The SSQ was dissolved in PGMEA and spin casted on top of a polymer pattern, in this case an SSQ ($T^{Ph}_{0.20}T^{Epoxy}_{0.80}$) network itself. Then, UV light was irradiated for several seconds, depending on the desired thickness, to cure the bottom oxygen poor layer. Finally, the top uncured SSQ layer with high oxygen content is removed with acetone to modify the size of the micropatterns. This method possesses the advantage that the original pattern can be fabricated with any type of resist material for NIL as no specific functionalities are needed on the imprinted surface.

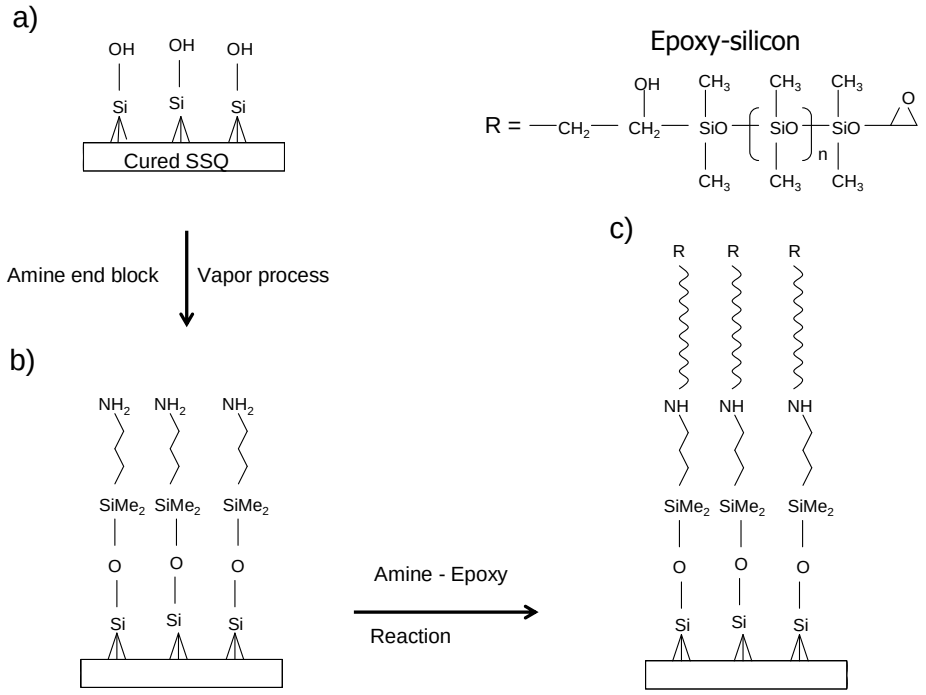

Figure 8.6 Schematic showing the steps followed to grow molecular layers on top of SSQ surfaces (Note the drawing in fig. b and c are linear molecules for an easy visualization but in reality, they represent crosslinked networks).

8.2.3 Trench width reduction induced by thermal diffusion of photoacid generator

The experimental procedure followed to modify the gap size or patterned films by thermal diffusion of photoacid generator is shown in figure 8.7. First, a layer of epoxysilicone prepolymer is dispensed on top of a SSQ pattern; the SSQ ($T^{Ph}_{0.20}T^{Epoxy}_{0.80}$) pattern which was originally imprinted using UV-curing contains PAG inside. (epoxypropoxypropyl)-terminated polydimethylsiloxane (Mw of 900-1100g/mol) prepolymer (epoxysilicone) is then dispensed on top of the pattern either by pouring or spin cast. The sample is baked at high temperatures (120 to 150°C) for different times to allow the diffusion of PAG out from the SSQ ($T^{Ph}_{0.20}T^{Epoxy}_{0.80}$) pattern and promote the epoxysilicone crosslinking. Finally, the sample is washed with acetone to remove the non-reacted polymeric precursors.

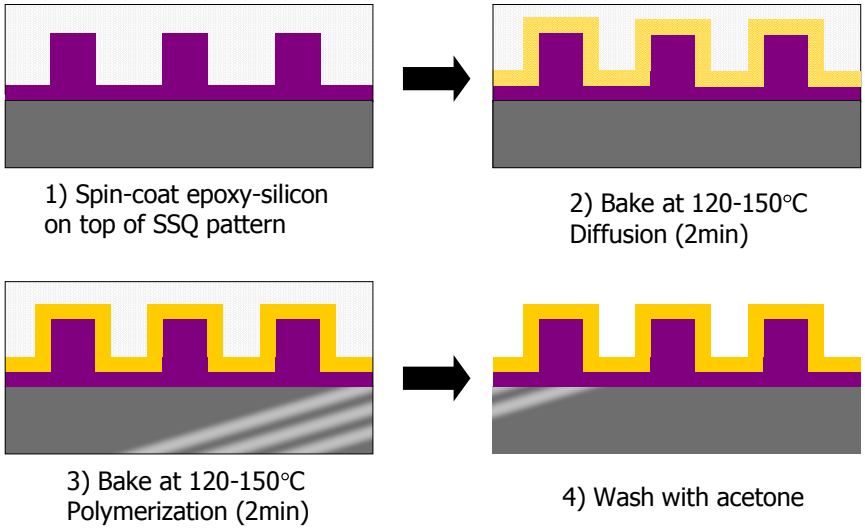

Figure 8.7 Steps to achieve gap size reduction with the PAG diffusion approach.

8.3. Results

8.3.1 Deposition of crosslinked layers for nanoscale structure fabrication

The thickness of the silylamine film can be accurately controlled from few nanometers (5nm) up to 28nm depending on the temperature used (figure 8.8). The large thickness increment seen when using 95ºC (28nm) is an indication that a crosslinked layer of silylilamine is being formed (The thickness of crosslinked layers deposited on top of flat SSQ films was measured with ellipsometry).

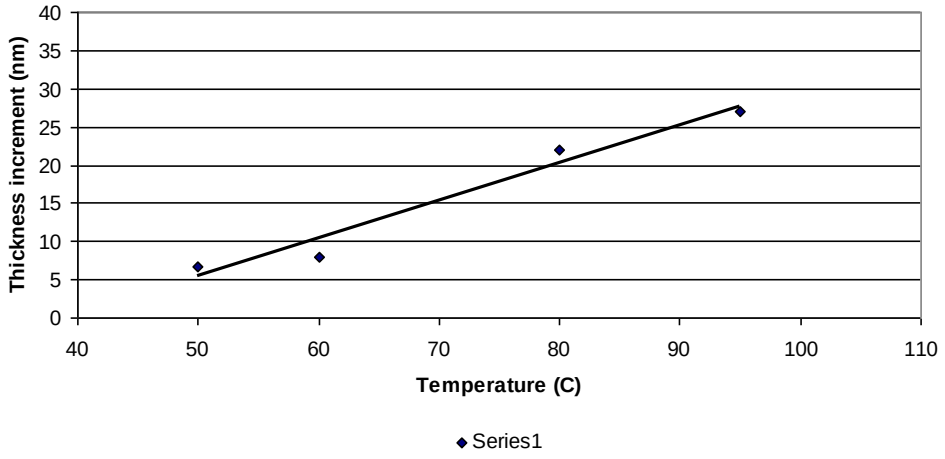

Figure 8.8 Plot presenting the thickness increment of aminosilane coating with temperature.

On the other hand, the thickness of the epoxysilicone film (also measured by ellipsometry), showed a lower increment, up to 5nm, depending on temperatures and coating times employed, as presented in figure 8.9. This small variation in size is an advantage if a gentle thickness control is wanted. Not a substantial difference in thickness is observed when using different temperatures (100 ºC and 140ºC).

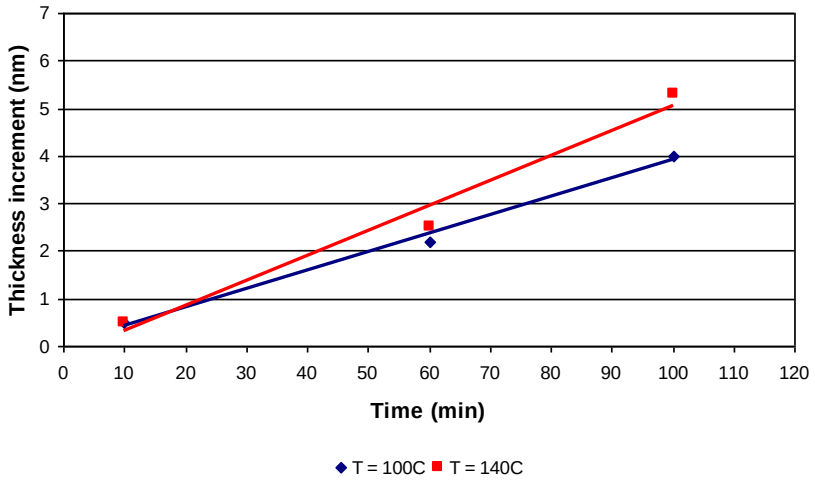

Figure 8.9 Plot presenting the thickness increment of epoxysilicone coating with time at different temperature.

Importantly, the deposition of the silylamine and epoxysilicone layers can be performed in alternated series of multiple coating steps so any desired size can be achieved.

Next, patterns with reduced trench width are presented in figure 8.10. A control sample, 220nm period pattern with a 70nm trench size is shown is shown in figure 8.10a. It can be seen in figure 8.10b that a 10nm gap size reduction was achieved after growing one layer silylamine and epoxysilicone films on top of imprinted SSQ gratings. Finally, a 30nm gap size reduction can be observed in figure 10c, in which three coating steps were applied. These results clearly show the trench size reduction is consistent with the number of coating steps performed.

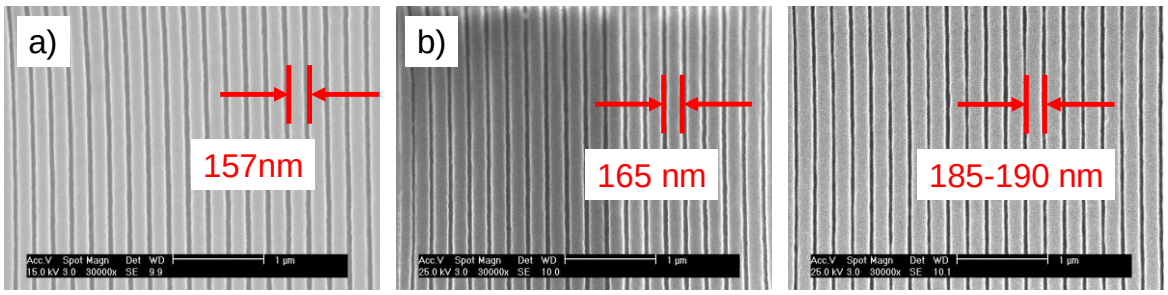

Figure 8.10 SEM's of a a) control sample, b) a sample where the trenches size was reduced 8 nm and with one layer and c) a sample where the size was reduced 30nm with three layers.

Interesting is the fact that the growing layers follow the shape contour of the patterned structures as observed in the SEM's presented in figure 8.11. Therefore, the modified patterns are able to conserve the original profile. It is also important to notice how the trench size decreases according to the number of layers coated. The original pattern (figure 8.11a) had trench widths of 60nm, but after three layers were coated, a small trench with a 20nm size was readily obtained (figure 8.11d). Some small size beads

seen on top of the modified SSQ patterns correspond to crosslinked epoxysilicone which was not completely removed by acetone during the cleaning step. They can be cleaned by an additional cleaning process.

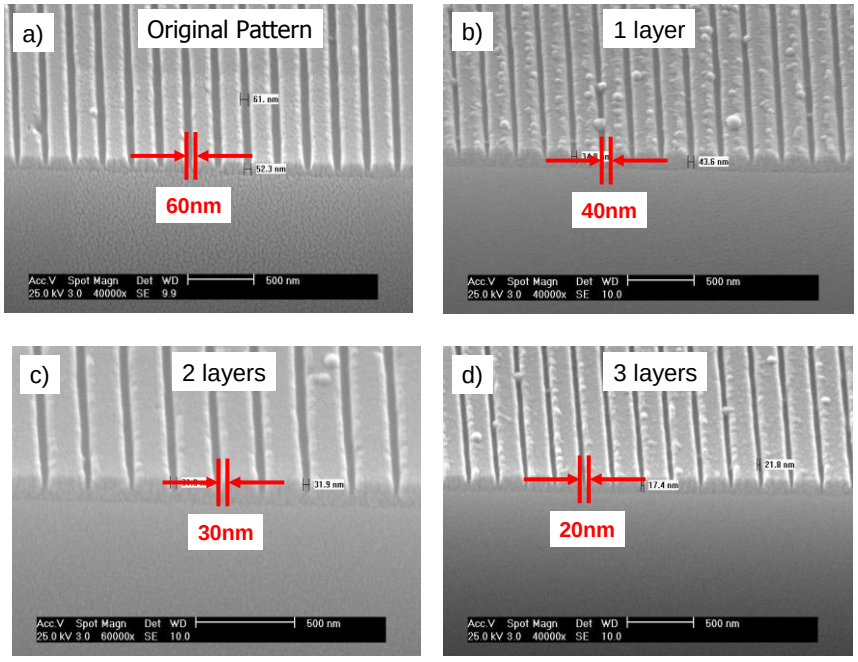

Figure 8.11 SEM's showing cross sections of an a) original sample, b) a sample with one layer coated c) a sample two layers coated and d) a sample with three layers coated; 220nm period pattern.

The crosslinked layers are deposited on top of the patterns using a dip coating (for the epoxysilicone) and vapor deposition approaches. Therefore, this approach seems not to have physical size limitations and structures with any desired dimensions can be constructed. As long as the epoxysilicone molecules used have a low molecular weight they can penetrate inside the pattern trenches. The same applies for the silylamine molecules which are able to easily travel inside the pattern pitch due to their small size and the lack of intermolecular forces in the vapor phase.

8.3.2 Structure size control by photocuring a polymer precursor (oxygen inhibition control)

Different structure dimensions can be obtained by varying the height of the spun methyl methacrylate polymer precursor (SSQ). It can be seen in figure 8.12 how the thickness of the cured layer (oxygen-poor layer) depends on the height (x axis) of the initial spin cast film as. In addition, it was found that a cured layer thickness threshold occurs at an initial layer height of 200nm which is due to the larger adsorption of the irradiated UV light by the methactylate SSQ precursor (to obtain these values, thin films were prepared on silicon substrates and their thickness was measured with ellipsometry).

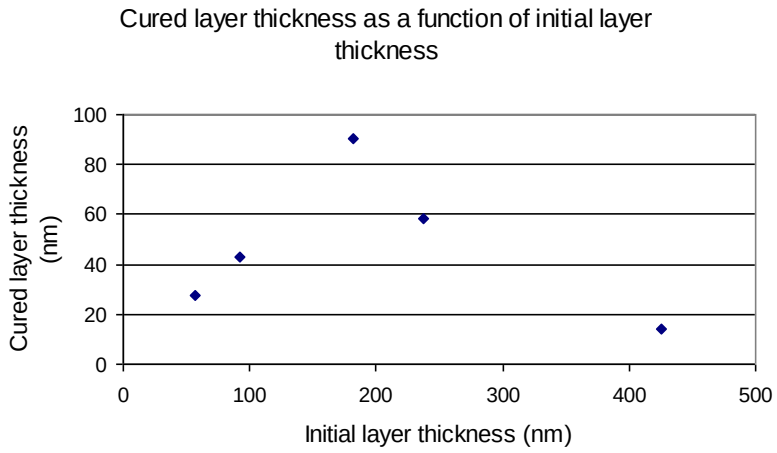

Figure 8.12 Plot showing the thickness of the cured layer as a function of total initial layer.

A reduction in gap size of about 30-50nm was achieved when an initial 90nm thick film of methactylate SSQ precursor was spun (figure 8.13a). More impressively, when an 180nm methacrylate spun layer was used, a size reduction of about 130-170nm was possible (figure 8.13c). Control SSQ patterns with 700nm period grating and 300nm width trenches were used for these tests.

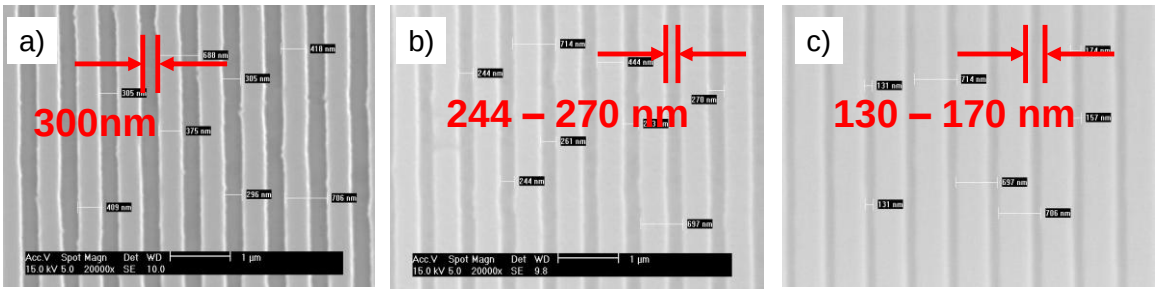

Figure 8.13 SEM's showing the decrease in gap size for different initial film thickness; a) control sample, b) 90 nm and c)180nm.

It is important to mention that this approach generates structures with rounded shapes as it is shown in figure 8.14. Here, the control sample was modified using an 180nm methacrylate precursor film cured during 20 sec. The rounded structures mightn find applications in the fabrication of low waveguides with low roughness.

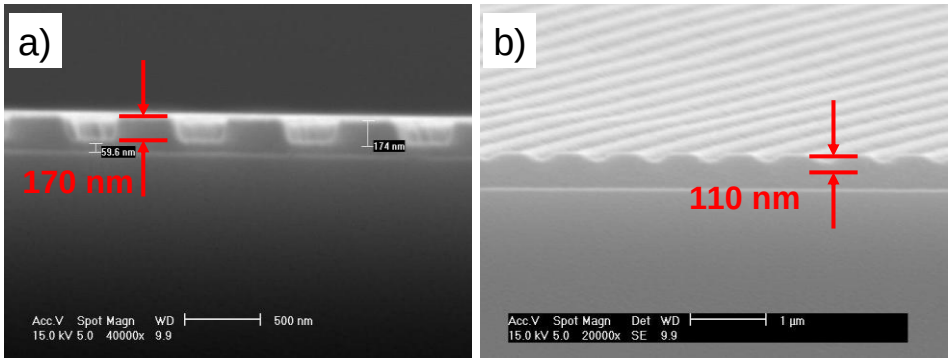

Figure 8.14 Cross sections of a) control sample, b) gap reduced sample generated from a layer with a initial thickness of 180nm.

No chemical interaction or bonding is required between the pattern and the conformal layer for the size modification process so this method has the potential to be applied on a variety of patterned materials. A good wetting of the methacrylate precursor on the patterned surface is one of the few requirements for a precise thickness control. Moreover, the pattern must not be soluble on the solvent the methacrylate precursor is normally dissolved to create the thin layer by spin cast.

8.3.3 Trench width reduction induced by thermal diffusion of photoacid generator

The thickness of the crosslinked epoxysilicone layer depends on the baking time and temperature used as shown in table 1 and figure 8.15 (Ellipsometry was also employed to measure the thickness increment of epoxysilicone films on top of Si substrates). Higher temperatures and times increase the distance PAG molecules diffuse out from the SSQ pattern creating a larger reactive film around the imprinted structures which leads to a thicker crosslinked epoxysilicone layer.

Table 8.1. Variation in thickness for different temperatures and time reactions.

Variation thickness (nm)			Time (min)
100°C	120°C	150°C	
		17.6	5
19.5	30.9	33.3	15
20.6	24.1	31.1	30
24.7	37.3	54.3	80

Patterned SSQ materials previously photocured by the cationic crosslinking of epoxypropoxy groups (700nm period and 300nm width trenches) (figure 8.16a) were used to evaluate the effectiveness of this technique. As expected, after baking the patterns at 120°C and 150°C, a trench size reduction from 300nm to about 200nm was achieved as (figures 8.16b and c).

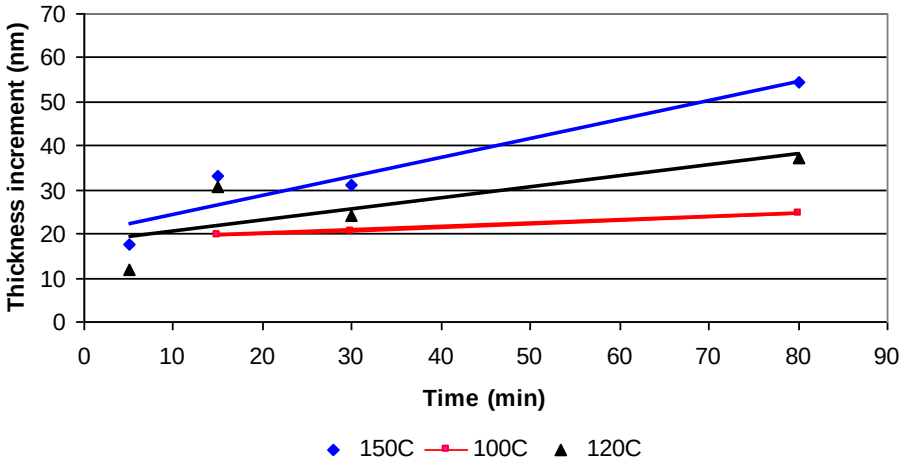

Figure 8.15 Plot of thickness increment with time for different temperatures an times.

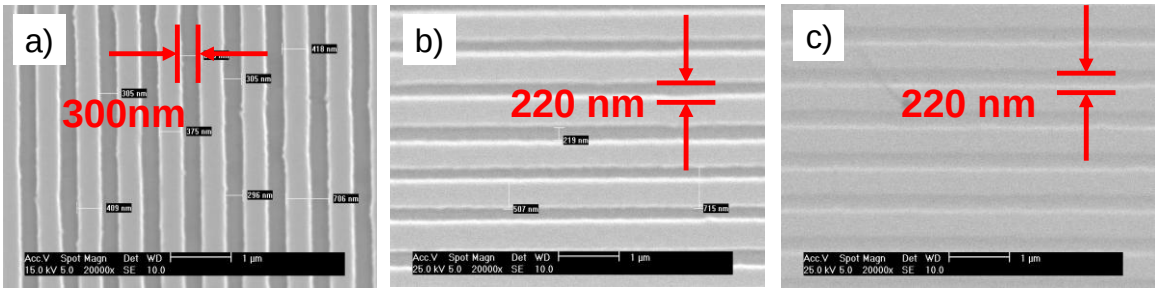

Figure 8.16 SEM's presenting the decrease in gap size through the diffusion of PAG for different temperatures; a) control sample, b) 120°C and c)150°C.

The cross section views for a control pattern and for a sample baked at 120°C are presented in figure 8.17. Here, the gap size decreased 80nm while the height was reduced only 40nm. The pattern rounding observed in figure 8.17b is due to a larger PAG diffusion occurring from in the inner corners of the structures.

Since the thickness of the diffusive layer around the patterns depends on the baking times and temperatures, this approach is useful to create structures of whichever dimension are required without foreseeable physical or technical limitation as normally encountered with lithograpy.

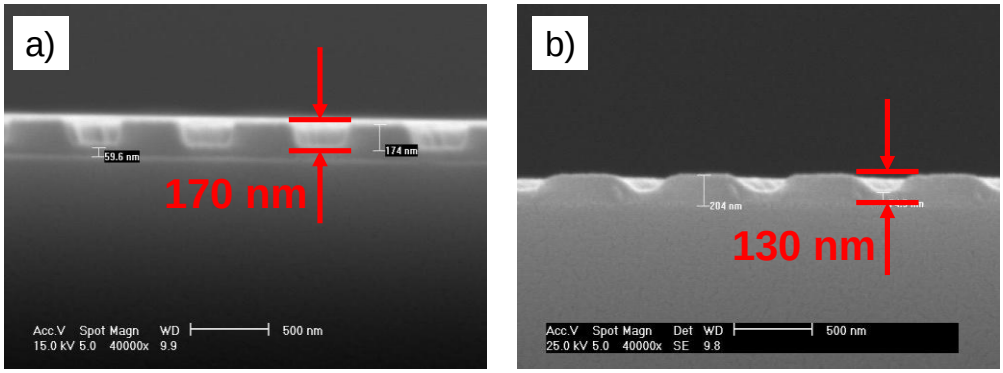

Figure 8.17 SEM's showing cross sectional views of a) control sample, b) a sample where the gap was reduced by baking at 120°C.

8.4 Conclusions

In summary, structures as small as 20nm were created with a combination of a fast top down imprinting approach and a high resolution bottom up layer deposition technique. In addition, several approaches to modify the structure dimensions of patterned films by a post-imprinting modification were developed. The gap width was accurately controlled and reduced from several hundreds to only few nanometers. Multifunctional SSQ NIL resists with capabilities beyond an easy patterning were employed. These techniques can be employed for several applications such as the engineering of membranes with nanopore structures for molecular separations, the generation of NIL molds with ultrasmall sizes (which fabrication is normally problematic with regular lithographic techniques) and the direct fabrication of structures on silicon based materials for the next-generation CMOS devices.

References

[1] Russell, T. P. *Science* **2002**, *5583,* 964-967.

[2] Peercy, P. S. *Nature* **2000**, *6799*, 1023-1026.

[3] Ito, T.; Okazaki, S. *Nature* **2000**, *6799*, 1027-1031.

[4] Wua, B.; Kumar, A. *J. Vac. Sci. Technol. B* **2007**, *6*, 1743-1761.

[5] Naulleau, P. P.; Anderson, C. N.; Chiu, J.; Denham, P.; George, S.; Goldberg, K. A.; Goldstein, M.; Hoef, B.; Hudyma, R.; Jones, G.; Koh, C.; La Fontaine, B.; Ma, A.; Montgomery, W.; Niakoula, D.; Park, J.; Wallow, T.; Wurm, S. Microelectronic Engineering; 2009; Vol. 86, pp 448-455.

[6] Wouters, D.; Schubert, U. S. *Angew. Chem. -Int. Edit.* **2004**, *19*, 2480-2495.

[7] Chou, S. Y.; Krauss, P. R.; Renstrom, P. J. *Science* **1996**, *5258*, 85-87.

[8] Bailey, T.; Choi, B. J.; Colburn, M.; Meissl, M.; Shaya, S.; Ekerdt, J. G.; Sreenivasan, S. V.; Willson, C. G. In *In Step and flash imprint lithography: Template surface treatment and defect analysis;* Journal of Vacuum Science & Technology B; 44th International Conference on Electron Ion and Photon Beam Technology and Nanofabrication (EIPBN); AMER INST PHYSICS: MELVILLE; 2 HUNTINGTON QUADRANGLE, STE 1NO1, MELVILLE, NY 11747-4501 USA, 2000; Vol. 18, pp 3572-3577.

[9] Hatzor, A.; Weiss, P. S. *Science* **2001**, *5506*, 1019-1020.

[10] Evans, S. D.; Ulman, A.; Goppertberarducci, K. E.; Gerenser, L. J. *J. Am. Chem. Soc.* **1991**, *15*, 5866-5868.

[11] Anderson, M. E.; Mihok, M.; Tanaka, H.; Tan, L. P.; Horn, M. W.; McCarty, G. S.; Weiss, P. S. *Adv Mater* **2006**, *8*, 1020-+.

[12] Anderson, M. E.; Srinivasan, C.; Hohman, J. N.; Carter, E. M.; Horn, M. W.; Weiss, P. S. *Adv Mater* **2006**, *24*, 3258-+.

[13] Fujikawa, S.; Takaki, R.; Kunitake, T. *Langmuir* **2006**, *21*, 9057-9061.

[14] Srinivasan, C.; Anderson, M. E.; Carter, E. M.; Hohman, J. N.; Bharadwaja, S. S. N.; Trolier-McKinstry, S.; Weiss, P. S.; Horn, M. W. *Journal of Vacuum Science & Technology B;* 2006; Vol. 24, pp 3200-3204.

[15] Srinivasan, C.; Hohman, J. N.; Anderson, M. E.; Weiss, P. S.; Horn, M. W. *Journal of Vacuum Science & Technology B;* 2007; Vol. 25, pp 1985-1988.

[16] von Werne, T. A.; Germack, D. S.; Hagberg, E. C.; Sheares, V. V.; Hawker, C. J.; Carter, K. R. *J. Am. Chem. Soc.* **2003**, *13*, 3831-3838.

[17] Jhaveri, S. B.; Beinhoff, M.; Hawker, C. J.; Carter, K. R.; Sogah, D. Y. *ACS Nano* **2008**, *4*, 719-727.

[18] Koutsioubas, A. G.; Vanakaras, A. G. *Langmuir* **2008**, *23*, 13717-13722.

[19] Khire, V. S.; Yi, Y.; Clark, N. A.; Bowman, C. N. *Adv Mater* **2008**, *17*, 3308-+.

Chapter 9

Conclusions and future research

9.1 Conclusions

Nanoimprint lithography (NIL) is a simple and inexpensive patterning technique for nanoscale fabrication. In contrast to other next generation lithography's which are usually quite slow and only useful for small fabrication areas (from few microns to few millimiters), NIL is capable of producing large areas nanoscale patterns in a matter of seconds. In addition, a vast variety of materials can be patterned by using NIL so the possibilities for useful applications are immense. An important component for the success of nanoimprinting and its transfer from research to industrial settings will be the development of the appropriate materials that are suitable as the resist or patterned material.

In general, the contribution of this dissertation is the engineering of thermally and UV curable precursor polymers suitable as nanoimprint lithography resists and applications. In addition, new patterning approaches, derived from nanomprinting were developed for a variety of purposes.

Most specifically, silicon containing polymer precursors were explored as NIL resist and stamp applications. Fast thermally curable polydimethylsiloxane (PDMS) resist

for high throughput processing, required in real industrial applications, were engineered. It was found that the formulated PDMS presented higher modulus than the commercially sylgard 184 and had appropriate properties for imprinting of 70nm nanostructures and below. The PDMS based material developed also has good etching properties due to its high silicon content. In addition, it could be imprinted in a very short period of time (10sec).

On the other hand, several combinations of silicone resins with D, T and Q units were synthesized. The best imprinting results were obtained with materials containing T and /or Q units. The higher degree of crosslinking of polymers having these units leads to a higher modulus material preventing lateral structure from collapsing. However a too high content of Q units can lead to some breaking of the patterned structures.

In addition, silsesquioxane (SSQ) resists (silicone resins with T units) suitable for high resolution (<20nm) high yield nanopatterning (4" wafers were easily replicated) were engineered. High aspect ratio nanoscale period patterns (100nm) were successfully replicated. The developed materials capabilities are beyond an easy patterning but transfer into substrates such as silicon and SiO_2 by using dry etching was achieved due to their high resistance to O_2 plasma and compatibility to Si and SiO_2 etching chemistries.

The silicon resins presented here have low molecular weight which provides the suitable viscosity appropriate for nanoscale imprinting. In addition, they present a low degree of shrinkage upon curing which is needed to preserve the size scale of the replicated structures.

The synthesized silsesquioxanes contained either epoxy or methacrylate functionalities. SSQ's methacrylate groups cure through a free radical crosslinking,

which is inhibited by the presence of oxygen. As a result the photocuring of methacrylate containing SSQ's is performed under nitrogen. On the other hand, epoxy group crosslink through a cationic process which presents the advantage that is not inhibited by oxygen.

SSQ's including phenyl and methyl groups were also synthesized and tested. It was found that materials with the bulky phenyl groups generate better imprinting results while the SSQ's with methyl functionalities are brittle so produce broken patterns.

SSQ's with different molar ratios of phenyl groups were tested. The materials with a molar ratio close to 50% of phenyl groups gave the better result. However, materials containing more than 50% of phenyls groups gave solids in the uncured state so they were not used for NIL experiment.

A UV + thermal imprinting was developed to imprint high aspect ratio structures with high resolution. Besides the traditional crosslinking provided by the photocuring of epoxy groups, the silanol groups in the multifunctional SSQ resist are a key component of this process. The heating step caused the crosslinking of the silanol groups so a higher modulus material can be created to withstand the harsh conditions present in nanoimprinting processing.

The synthesized materials can also be used as low surface energy, UV transparent, flexible polymer stamps. Besides mechanical integrity, these polymers contain fluorinated groups which allow an easy demolding process with low defect density.

A double layer resist system for high resolution and high yield nanoimprinting of SSQ materials was developed. The bottom layer contains the appropriate chemical groups for a strong adhesion to the substrate while the top layer possesses releasing fluorinated functionalities which present low adhesion to the mold.

In addition, two different processes to create patterns with no residual layers by using the synthesized and formulated resists were developed. The residual-less patterns were easily imprinting using hydrophobic polymers in a short period of time. The developed approaches can have a variety of applications for the fabrication of nanoparticles, nanofibers, array for cellular engineering and fabrication of nanosize pore membranes.

Furthermore, the engineered silsesquioxane systems are multifunctional materials which can be used patterned and used in subsequent processing steps. For example, a methodology was engineered to reduce the trench of imprinted patterns and create nanostructures with much smaller sizes than originally replicated by using the multifunctional SSQ materials.

Finally, several types of fluorosurfactants were mixed with the synthesized SSQ resists to decrease mold-resist sticking, improve mold releasing and obtain patterns with a low amount of defects. It was found that fluorosurfactants with functional groups which can react and form strong covalent bonds with the resist during the crosslinking process give the best results. A fluorosurfactant with methacrylate groups was used together with a SSQ resist containing methacrylate groups. An imprinting yield close to 100% and an easy mold releasing were achieved.

9.2 Future research

Several applications have been developed in different research groups by using NIL in the past years. However, a vast array of applications can still be searched and a wide variety of improvements can be performed into the already developed systems.

9.2.1 Synthesis of fluorosurfactants for easy mold releasing

Further investigations can be done to synthesize an appropriate fluorosurfactant molecules with both high solubility in this type of epoxy SSQ's as well as functional groups which can react with the resist during the UV-curing step to form a stiff covalent network.

9.2.2 Silsesquioxanes of interlayer dielectric

On the other hand, the unique properties of the developed silsesquioxane resists can make them suitable for interlayer dielectric applications. They can be heated at high temperatures and preserve the desired properties. It can be important to test these materials for applications as low dielectric layers. Porogenes can be added to further reduce the material dielectric constant.

9.2.3 Direct fabrication of hard and soft molds from silsesquioxane patterns

A resist which can be directly converted into a high modulus ceramic mold by a heat treatment so high temperature processing materials such as metals can be directly imprinted is desirable. The resist can be patterned as a polymer and converted into SiO_2. Silsesquioxanes are appropriate precursors for SiO_2. An important challenge is to reduce the resist shrinking caused by the thermal treatment which can be up to 50% with the materials currently used.

Furthermore, the trench width reduction strategies can be explored to create soft and hard stamps with sizes smaller than regularly possible with other nanofabrication techniques. A high yield and high throughput fashion can be readily achieved.

9.2.4 Nanofibers fabrication

On the other hand, the residual less approaches developed can be easily employed to create three dimensional scaffolds of degradable polymers such as PEG for tissue engineering. In addition, these strategies are suitable processes to fabricate fibers of controlled size using almost any type of material.

9.2.5 Membrane fabrication

Membrane science and technology has attracted increased interest in academic research and industrial fields in recent years. In fact, a number of novel advanced functional materials, polymeric and ceramic, are being developed for membrane technology. In addition there is a strong motivation for both improving separation processes and developing new potential applications. A membrane with a uniform pore size is required. In addition, an approach to control the size and morphology of porosity is desired. Some drawbacks are low membrane lifetime, generally low selectivity and concentration polarization.

A variety of materials for membrane fabrication can be chosen according to processing requirements, chemical and thermal stability as well as low fouling. Many types of membranes are made of polymers but inorganic materials such as ceramics and metals are also employed.

Hydrophobic and hydrophilic polymers can be used. An advantage of hydrophilic polymers such as crosslinked SSQ is that they present reduced fouling. On the other hand, inorganic materials present superior chemical and thermal stability relative to polymeric materials, they are easier to clean and have high modulus.

Although there are several approaches for membrane fabrication a template approach such as nanoimprint lithography can have the advantage of producing structures with controlled size and morphology. Furthermore, this technology is a potential high throughput and high yield process.

It is important to mention that membranes with regular pore size, very narrow pore size distribution and small thickness are required and can be readily fabricated with NIL.

Nanoimprinting combined with trench width reduction and residual less patterning can be a powerful tool to create membranes for novel applications such as catalytic membrane reactors.